Adsorption Studies of Rhodamine B and Pb^{2+} Ions Using Poly (lactic acid)/Activated Carbon Composite Beads Form Prepared by Phase Inversion Method

Memoon Sattar

A Thesis Submitted in Fulfillment of the Requirements for the Degree of Doctor of Philosophy in Chemistry
Prince of Songkla University
2017

Adsorption Studies of Rhodamine B and Pb^{2+} Ions Using Poly (lactic acid)/Activated Carbon Composite Beads Form Prepared by Phase Inversion Method

Memoon Sattar

A Thesis Submitted in Fulfillment of the Requirements for the Degree of Doctor of Philosophy in Chemistry
Prince of Songkla University
2017

Thesis Title Adsorption Studies of Rhodamine B and Pb^{2+} Ions Using Poly (lactic acid) / Activated Carbon Composite Beads Form Prepared by Phase Inversion Method

Author Miss Memoon Sattar

Major Program Chemistry

Major Advisor

.....
(Asst. Prof. Dr. Orawan Sirichote)

Examining Committee :

.....Chairperson
(Asst. Prof. Dr. Usa Onthong)

.....Committee
(Asst. Prof. Dr. Orawan Sirichote)

Co-advisor

.....
(Asst. Prof. Dr. Watchanida Chinpa)

.....Committee
(Asst. Prof. Dr. Watchanida Chinpa)

.....Committee
(Dr. Laemthong Chuenchom)

The Graduate School, Prince of Songkla University, has approved this thesis as fulfillment of the requirements for the Doctor of Philosophy Degree in Chemistry

.....
(Assoc. Prof. Dr. Teerapol Srichana)
Dean of Graduate School

This is to certify that the work here submitted is the result of the candidate's own investigations. Due acknowledgement has been made of any assistance received.

.....Signature
(Asst. Prof. Dr. Orawan Sirichote)
Major Advisor

.....Signature
(Miss Memoon Sattar)
Candidate

I hereby certify that this work has not been accepted in substance for any degree, and is not being currently submitted in candidature for any degree.

.....Signature
(Miss Memoon Sattar)
Candidate

ชื่อวิทยานิพนธ์ การศึกษาการดูดซับสีย้อมโรดามีนบี และโลหะตะกั่วด้วยตัวดูดซับเชิงประกอบทรงกลมจากพอลิแลคติกแอซิด/ถ่านกัมมันต์ ที่เตรียมโดยวิธีการแยกเฟส
ผู้เขียน นางสาวเมมุน ซัตตาร์
สาขาวิชา เคมีเชิงฟิสิกส์
ปีการศึกษา 2559

บทคัดย่อ

การเตรียมตัวดูดซับเชิงประกอบทรงกลมจากพอลิแลคติกแอซิด (PLA) และผงถ่านกัมมันต์ (AC) โดยวิธีการแยกเฟส เพื่อใช้ในการดูดซับสารพิษจากสารละลายสีย้อมโรดามีนบี และโลหะตะกั่ว โดยเม็ด PLA/AC ที่เตรียมได้ มีความสะดวกต่อการใช้งานมากกว่าผงถ่านกัมมันต์ AC, ประสิทธิภาพการดูดซับสูง, ไม่เป็นพิษ, เป็นมิตรกับสิ่งแวดล้อม และราคาถูก โดยในงานวิจัยนี้ได้ทำการศึกษาลักษณะเฉพาะทางกายภาพของตัวดูดซับเม็ด PLA/AC ที่เตรียมได้ โดยใช้กล้องจุลทรรศน์อิเล็กตรอนแบบส่องกราด (SEM), การวิเคราะห์การองค์ประกอบของธาตุ C, H, N และ O, การหาพื้นที่ผิวจำเพาะและการกระจายตัวของรูพรุน และการหาประจุที่ผิวเป็นศูนย์ (pH_{pzc}) อีกทั้งได้นำตัวดูดซับที่เตรียมได้ไปศึกษา การดูดซับสารละลายสีย้อมโรดามีนบี และโลหะตะกั่ว โดยจากผลการทดลองพบว่ารูปแบบการดูดซับของตัวดูดซับเม็ด PLA/AC สอดคล้องกับรูปแบบการดูดซับของแลงเมียร์ โดยปริมาณการดูดซับสีย้อมโรดามีนบี และ โลหะตะกั่วสูงสุด คือ 149.57 และ 202.81 มิลลิกรัมต่อกรัม ตามลำดับ อีกทั้งยังได้ศึกษาจลนศาสตร์ทางเคมีพบว่า การดูดซับสารละลายสีย้อมโรดามีนบีและโลหะตะกั่วบนเม็ด PLA/AC สอดคล้องกับจลนศาสตร์การดูดซับอันดับสองเทียม และจากผลการทดลองทั้งหมดแสดงให้เห็นว่าเม็ด PLA/AC ที่เตรียมได้ มีประสิทธิภาพในการดูดซับสารละลายสีย้อมโรดามีนบี และโลหะตะกั่ว เม็ด PLA/AC ที่เตรียมได้ จึงเป็นอีกหนึ่งทางเลือกสำหรับการกำจัดสารพิษของสารละลายสีย้อมและโลหะหนักที่จากแหล่งน้ำเสียต่างๆได้

Thesis Title	Adsorption Studies of Rhodamine B and Pb^{2+} Ions Using Poly (lactic acid)/Activated Carbon Composite Beads Form Prepared by Phase Inversion Method
Author	Miss Memoon Sattar
Major Program	Chemistry
Academic Year	2016

ABSTRACT

The preparation of porous materials using biodegradable materials has attracted much attention in the field of environmental pollution control. A non-toxic, user-friendly and inexpensive adsorbent bead was prepared from poly (lactic acid) (PLA) and activated carbon (AC) using phase inversion technique. The porous structure of the PLA/AC 5% wt. bead was characterized by scanning electron microscopy (SEM), elemental composition (C, H, N, O) analysis, surface area and pore size distribution (BET analysis), fourier-transform infrared spectrophotometry (FT-IR) and point of zero charge measurements (pH_{pzc}). The removal of the Rhodamine B and Pb^{2+} ions were studied by batch equilibration method. They were found that the adsorption was the best fit by the Langmuir adsorption isotherm. The values of maximum adsorption capacity were 149.57 and 202.81 mg g^{-1} for Rhodamine B and Pb^{2+} ions, respectively. The kinetic adsorption studies of Rhodamine B and Pb^{2+} ions can be successfully described by the pseudo-second-order kinetic model. The results indicated that the PLA/AC 5% wt. beads will provide an alternative granular adsorbent for the removal of pollutant cationic dyes and heavy metal from wastewater.

ACKNOWLEDGEMENTS

First and foremost, praises and thanks to the God (Allah) for blessing and helping me throughout my research work to complete the research successfully. I would also like to thank some people who were important part of my Ph.D.

I would like to express the deepest appreciation to my major advisor**,** **Asst. Prof. Dr. Orawan Sirichote**, my co-advisor, **Asst. Prof. Dr. Watchanida Chinpa**, for their understanding, guidance, patience and encouragement throughout my studies. For me, they are the best teachers and made me feel like a close relative.

I also would like to express the deepest appreciation to my best co-worker, **Fareeda Hayeeye**. She is my best friend who not only helped, advised and encouraged me but also gave me happiness throughout my studies.

I would like to thank **Dr. Laemthong Chuenchom** for advising me to look at research and my work in different ways.

I would like to thank the committee of this thesis for their valuable time, especially, **Asst. Prof. Dr**. **Usa Onthong** from Thaksin University, Patthalung campus.

I would like to thank all the lecturers, my colleagues and officers of the Department of Chemistry, Faculty of Science, Prince of Songkla University for their teachings and knowledge and the staff of Department of Chemistry, Faculty of Science, Prince of Songkla University, as well who assisted me with some technical aspects.

I am grateful to the PSU Ph.D. Scholarship and Faculty of Science Research Fund Year 2015 for supporting. Moreover, I greatly appreciated the Graduate School and the Department of Chemistry, Faculty of Science, Prince of Songkla University Hat Yai campus,

I am extremely grateful to my family and my friends for their support, prayers, care and encouragement which helped me through this study and my life.

Memoon Sattar

CONTENTS

CONTENTS (Continued)

LIST OF TABLES

LIST OF TABLES

LIST OF FIGURES

LIST OF FIGURES

LIST OF ABBREVIATIONS

AC	Activated carbon
PLA	Poly(lactic acid)
PLA/AC bead	Poly(lactic acid)/ Activated carbon composite bead form
q_e	The amount of solute adsorbed per unit weight of PLA/AC (mg g^{-1})
q_m	The amount of maximum adsorption capacity (mg g^{-1})
C_e	The equilibrium solute concentration conditions (mg L^{-1})
b	The Langmuir constant
K_F and n	The Freundlich constant
k_1	The rate constant of pseudo-first order model
k_2	The rate constant of pseudo-second order model
t	Time
ΔH°	Enthalpy
ΔS°	Entropy
ΔG°	Gibb's free energy
K_c	The ratio of C_A and C_e
R	The universal gas constant
T	The absolute temperature (K)

CHAPTER 1

INTRODUCTION

1.1 Introduction

Wastewater streams especially from textile and printing industries contain dyes and heavy metal ions. For heavy metals are compelling quantities from a variety of applications of electroplating and metal surface treatment processes.

Dyes and heavy metal ions are represent important groups of pollutants from industrial wastewater especially a weaving factory. The World Bank estimates that 17 – 20% of industrial water pollution comes from textile dyeing and finishing treatment given to fabric (Kant, 2012). The water consumption of a weaving factory having a production of about 8000 kg of fabric per day is about 1.6 million liters. This is consumed 16% in dyeing and 8% in printing. Wastewater from dyeing will be discharged into the river about 15 - 20% of the total wastewater flow (Wasif, et al., 1996 and Vijaraghavan, et al., 1999). Mills discharge millions of gallons of this effluent as hazardous toxic waste, full of color and organic chemicals from dyeing.

Dye is one of the major constituents of the wastewater discharged in many industries including dying, textile, leather, paint and plastic industry (Garg, et al., 2004). Almost every industrial process involves a solution of a dye and heavy metal in water, in which many materials are dipped or washed. After a batch of products, it's cheaper to dump the used water – dye effluent – than to clean and re-use the water in the factory so dye factories across the world are dumping millions of tons of dye effluent into rivers (Crini, et al., 2006 and Ashly, et al., 2014). One of the most basic dyes was used in industries is Rhodamine B. It is frequently found in industrial wastewater and a carcinogenic affecting to aquatic life and ecosystem.

In addition, most of heavy metal ions are also non-degradable and contaminated continuously in the environment. Heavy metal ions; Pb^{2+} ions which flow into and throughout ecosystems are serious and on-going problem to

environment and very harmful to human and animal health (Tiwari, et al. 2013). A low concentration of Pb^{2+} ions 0.006 mg L^{-1} in blood can damage the fatal brain and cause diseases of kidneys, circulatory system including nervous system (Chuah, et al., 2005).

Therefore, it is also important to treat Rhodamine B and Pb^{2+} ions from industrial wastewater prior to its discharge to the environment.

There are various methods for removing them in industry wastewater treatment such as ultrafiltration (Majewska-Nowak, et al., 1989), coagulation-flocculation (Prashant, 2012), precipitation (Yüzera, et al., 2008), electroplating (Fabíola, et al., 2016), evaporation (Zeng, et al., 2008), ion exchange (Ho, et al., 2011 and Li, et al., 2014), membrane processes (Lina, et al., 2007) and adsorption (Dogan, et al., 2007; Suna, et al., (2010) and Bansode, et al., 2003).

Many of these processes when applied to dilute systems with dye and heavy metals ion concentrations of less than 100 mg L^{-1} are less effective or cost restrictive (Jose, et al., 1999 and Arivoli, et al., 2008). Thus, technology for the removal of trace amounts of Rhodamine B and Pb^{2+} ions from diluted aqueous solutions attends to a growing interest.

Adsorption is one of the effective technologies for removing the high concentration of Rhodamine B and Pb^{2+} ions by powder activated carbon (AC powder). It is the most effective adsorbent for adsorption process due to AC powder has very high surface area, high porosity porous and high the adsorption capacities (Sirichote, et al., 2008). There have been several reports that various materials are used for preparation of AC powder. These include AC powder prepared from the walnut shell (Sumanjit, et al., 2008), bagasse pith (Hamdi, et al. 2008), tamarind fruit shells (Edwin, et al., 2008), orange peel (Velmurugana, et al., 2011) and pericarp of rubber fruit (Hayeeye, et al., 2014). They can be used for removing Rhodamine B. Besides, there have been many researches on Pb^{2+} ions adsorption by AC which was prepared from coconut shell (Jyotsna, et al., 2004 and Sharaf El-Deen, et al., 2016),

Annona squamosa (custard apple) fruit shell (Sivakumar, et al., 2013), date stones (Jamal, et al., 2013) and walnut wood (Ghaedi, et al., 2015).

However, AC powder is limited to practical use (Ninan, et al., 2014). Thus, studies on the adsorption of Rhodamine B and Pb^{2+} ions by granular AC have been also reported in the literature. Granular AC prepared from various materials such as walnut shell (Kima, et al., 2001), pecan shell (Bansode, et al., 2003), coconut shell (Jyotsna, et al., 2005), peanut shells (Wilson, et al., 2006), red mud (Zhua, et al., 2007), cherry stones (Jaramillo, et al., 2009), phosphoric acid treated parthenium carbon(PWC) (Hem, et al., 2009), oil palm empty fruit brunch activated carbon walnut shell (Manase, 2012), black tea leaves pecan shell (Mohammad, et al., 2012) and cationic surfactant (Hexadecyltrimethylammonium chloride) modified bentonite clay (Anirudhan, et al., 2015) have been studied. However, the maximum adsorption capacity of granular AC is usually lower than that of AC powder.

Therefore, in this thesis had tried to modify AC powder handier by combining poly (lactic acid) (PLA) with AC powder in a bead form for as a new adsorbent (PLA/AC beads). The PLA/AC composite beads were prepared by phase inversion method and used for adsorption studies of Rhodamine B and Pb^{2+} ions from aqueous solutions. PLA is biodegradable, environment-friendly, thermoplastic aliphatic polyester which is ease of bead formation, its the chemical structure is shown in Figure 1.

1.2 Preliminary knowledge and theoretical sections.

1.2.1 Wastewater treatment process

Wastewater treatment process is a procedure used to convert waste water which is not required or suitable for usage. Wastewater will be returned to the water cycle with least environmental problems or reused. The wastewater pollution with chemical contaminants is one of the most important environmental problems. There are many methods widely used for removing pollutants from industrial

wastewater treatment process such as ultrafiltration, coagulation-flocculation, precipitation, electroplating, evaporation and ion exchange.

Evaporation is the process of the solvent which typically water is vaporised from the concentrated solution. Product of this process is contains solute in solid form from the initial concentrated solution. Procedure could also be applied naturally in solar for evaporation, or through the use of commercially available evaporation instrumentation (Dind, et al., 1978)

Coagulation-flocculation can be divided into 2 distinct procedures that ought to be applied consecutively. The first one termed coagulation, is that the method whereby destabilization of a given colloidal suspension or solution is going down. The process of coagulation is to overcome the factors that make the stability of a given system. It is achieved with the use of applicable chemicals, usually aluminium or iron salts, the supposed coagulant agents. The second sub-process, termed flocculation, refers to the induction of destabilized particles so as to come along, to form contact and thereby, to make massive agglomerates, which can be separated easier usually through gravity subsiding. Coagulation typically completes during a very short period of time, whereas flocculation happens usually over a range of 20 to 45 min. It is a typical applies, particularly in many countries, the improvement of particles aggregation during the second step by the addition of organic polyelectrolytes, the supposed flocculent aids or simply flocculant (Semerjian, et al. 2003).

Precipitation is chemical procedure in which undesirable soluble metallic ions and bound anions are removed from water or wastewater by conversion to the insoluble particle which could be a normally used metals, phosphorus, and hardness. At equilibrium the insoluble particles precipitate that can be simply removed from waste water. Chemical precipitant is usually followed by a solids separation operation which will include coagulation, sedimentation or filtration to remove of the precipitates. The method is often preceded by chemical reduction so as to change the characteristics of the metal ions to a form that can be precipitated (Liao, et al., 1993).

Ion exchange can be utilized in waste treatment plants to exchange one ion for another for the aim of demineralization. There are primarily two kinds of ion exchange systems, one that is using the anion resins and another is that the cation exchange resins. The materials are often more broken down to individual grouping depending on it is a strong base cation, weak acid cation, strong base anion, or weak base anion. Despite which kind of exchangers, the resins can very sensitive to fouling caused by presence of organic matter within the untreated water. Therefore it is imperative that before the inflowing undergoes the treatment procedure, another separate section is required to remove most of the suspended solids. Then the soluble organics also in order that it will loads towards the ion exchange unit (Dobrevsky, et al., 1997).

In addition, various wastewater treatment processes including above processes are applied in three stages of wastewater process; primary, secondary and tertiary treatments.

Primary wastewater treatment is intended to remove organic and inorganic solids by the physical processes of sedimentation and flotation. Approximately 25 - 50% of the incoming biochemical oxygen demand (BODs), 50-70% of the total suspended solids (SS), and 65% of the oil and grease are removed throughout primary treatment. Some organic nitrogen, organic phosphorus, and heavy metals related to solids also are removed throughout primary sedimentation, however colloidal and dissolved constituents are not affected (Ramalho, et al., 1983)

Secondary treatment is historically applied to the liquid portion of waste when primary treatment has removed solids and floating material. Secondary treatment is that the portion of a waste material treatment sequence removing dissolved and colloidal compounds measured as biochemical oxygen demand (BOD). Secondary treatment is usually performed by indigenous, aquatic microorganisms during a managed aerobic habitat. Bacteria and protozoa consume biodegradable soluble organic contaminants (e.g. sugars, fats, and organic short-chain carbon molecules from human waste, food waste, soaps and detergent) whereas reproducing to form cells of biological solids. Biological oxidation processes are sensitive to

temperature and, between 0 °C and 40 °C, the rate of biological reactions increase with temperature. Most surface aerated vessels operate at between 4 °C and 32 °C (Ramalho, et al., 1983).

Tertiary treatment is a final treatment stage to increase the waste water quality to the required level. This advanced treatment is accomplished by a variety of ways like coagulation sedimentation; filtration, reverse osmosis, and increasing secondary biological treatment to any stabilize oxygen-demanding substances or remove nutrients. In varied mixtures, these processes are able to do any degree of pollution control desired. As wastewater is pure to higher and better degrees by such advanced treatment processes, the treated wastewater can be reused for urban, landscape, and agricultural irrigation, industrial cooling and process, recreational uses and water recharge, and even indirect and direct augmentation of drinking water. (Ramalho, et al., 1983).

At present, many researches are interesting in tertiary treatment combined biological-physical treatment and innovative physicochemical processes as advanced wastewater treatments.

Combined biological-physical treatment is differentiated from tertiary treatment that in tertiary treatment any unit processes are added after conventional biological treatment, while in combined treatment, biological and physicochemical treatments are mixed (Sutton, 1994).

Innovative physico-chemical processes for treating industrial wastewater containing heavy metals usually involve technologies for reduction of toxicity so as to fulfill technology-based treatment standards. The innovative physicochemical was used for wastewater treatment such as; membrane filtration, electrodialysis, photocatalysis and adsorption on new adsorbents.

Membrane filtration has received extensive attention for the treatment of inorganic effluent, since it is capable of removing not only suspended solid and organic compounds, but also inorganic contaminants like heavy metals. Depending on

the scale of the particle that may be preserved, varied kinds of membrane filtration like ultrafiltration, nanofiltration and reverse osmosis are often utilized for significant metal removal from wastewater.

Electrodialysis is a membrane separation during which ionized species within the solution are passed through an ion exchange membrane by applying an electrical potential. The membranes are thin sheets of plastic materials with either anionic or cationic characteristics. Then a solution containing ionic species passes through the cell compartments, the anions migrate toward the anode and also the cations toward the cathode, crossing the anion exchange and cation-exchange membranes.

Photocatalytic method in aqueous suspension of semiconductor has received significant attention in sight of alternative energy conversion. This photocatalytic method was achieved for fast and efficient destruction of environmental pollutants. Upon illumination of semiconductor–electrolyte interface with light energy larger than the semiconductor band gap, electron–hole pairs are formed within the conductivity and also the valence band of the semiconductor, severally. These charge carriers that migrate to the semiconductor surface are capable of reducing or oxidizing species in solution having appropriate oxidation-reduction potential. Varied semiconductors are used such as TiO_2, ZnO, CeO_2 and CdS. As usually observed, the most effective photocatalytic performances with maximum quantum yields are always obtained with titanium oxide (Amy, et al. 1995).

Adsorption on new adsorbents has become one among the alternative treatment techniques for wastewater treatment. Basically, adsorption could be a mass transfer method by that a substance is transferred from the liquid phase to the surface of a solid, and becomes bound by physical and/or chemical interactions. Varied cheap adsorbents, derived from agricultural waste, industrial by-product, natural material, or modified biopolymers, are recently developed and applied for the removal pollutants contaminated wastewater. In general, there are 3 main steps concerned in waste sorption onto solid sorbent material: (i) the transport of the waste from the bulk

solution to the sorbent material surface; (ii) adsorption on the particle surface; and (iii) transport to the sorbent particle. Technical relevancy and cost-effectiveness are the key factors that play major roles within the selection of the most appropriate adsorbent to treat wastewater (Barakat, 2011).

. Therefore, the aim of this research is to prepare the new adsorbent for Rhodanine B and Pb^{2+} ions adsorption as an innovative physicochemical wastewater treatment.

1.2.2 Adsorbent

Adsorbent is a material which has the ability to cause molecules of gases, liquids or solids to adhere to its internal surfaces without changing the adsorbent physically or chemically. In wastewater treatment, an adsorption by activated carbon (AC) possessing has high ability to attract and to hold particles.

Activated carbon (AC) is a kind of carbon that has been method to make it extremely porous and therefore to have a very large surface area obtainable for adsorption process. Only one gram of activated carbon has surface area in more than 500 m^2, as determined by nitrogen adsorption isotherm. Adequate activation for useful applications could come entirely from the high surface area, although additional chemical treatment usually enhances the adsorbing properties of the material.

AC primarily consists of elementary carbon in graphite alike structure. It is often made by heat treatment, or “activation”, of raw materials such as wood, coal, peat and coconut shell. Throughout the activation method, the distinctive internal pore structure is made, and it is this pore structure that provides the outstanding adsorption properties of AC.

AC is advanced products that are troublesome to classify on the basis of their behaviors, surface characteristics and preparation ways. However, some broad classification is made for general purpose based on their physical characteristics (Chuenchom, 2004).

One of the most important adsorbent materials is AC because of their highly developed porosity, large surface area ranging from 500 to 3000 m^2 g^{-1}, various characteristics of surface chemistry, and high degree of surface reactivity. Agricultural by-products also are considered as very important source material for the production of AC as they are renewable and inexpensive materials.

AC is produced by two steps as carbonization and activation. The carbonization step is to complement the carbon content and to make an initial porosity and also the activation process, helps in enhancing the pore structure that activated carbon is different from coal because of activated carbon has very high surface area. Therefore, activated carbon are often used to absorb the radioactive material in gaseous, liquid and well therefore activated carbon has been used widely within the adsorption process. Past activation refers to the development of the adsorption properties of carbon. It is often made by one of the following processes:

(1) Physical activation: The precursor is developed into activated carbons using gases. This can be typically done by using one or a combination of the following processes:

Carbonization: material with carbon content is pyrolyzed at temperatures within the range 600–900 °C, in absence of air (usually in inert atmosphere with gases like argon or nitrogen)

Activation: raw material or carbonized material is exposed to oxidizing atmospheres (carbon dioxide, oxygen, or steam) at temperatures higher than 250 °C, typically within the temperature range of 600–1200 °C.

(2) Chemical activation: Prior to carbonization, the raw material is impregnated with certain chemicals. The chemical is typically an acid, strong base, or a salt (phosphoric acid, potassium hydroxide, sodium hydroxide, calcium chloride, and zinc chloride 25%). Then, the raw material is carbonized at lower temperatures (450–900 °C). Chemical activation is preferred over physical activation owing to the lower temperatures and shorter time needed for activating material.

(http://en.wikipedia.org/wiki/activated carbon).

Porosity: definition

Based on the experience of adsorption chemistry, total porosity is classified into three groups. The origins and structure of porosities are detailed upon below. IUPAC classifies porosities as follows: Micropores dimension is less than 2 nm, mesopores dimension is between 2 and 50 nm and macropores is dimension greater than 50 nm.

It has also been useful to classify micropores more into ultra- (< 0.5 nm width) and super- (1.0 – 2.0 nm) micropores, these definitions being relevant when considering adsorption behavior. Micropores are considered as being concerning the size of adsorbate molecules and accommodate one, two or maybe three molecules. Mesoporosity is wider than micropores. Macroporosity has very little interest for the surface chemist. They are transport pores to the inside of particles and are considered as external surface. Some AC contains all of these sizes of porosity related to the botanical composition of the material. The pore size distribution is very necessary for the practical application, the best fit depends on the compounds of interest, the matrix (gas, liquid) and treatment condition. The specified pore structure of an AC product is attained by combining the proper raw material and activation conditions (Chuenchom, 2004).

Classification of AC

Activated carbons are complex products which are difficult to classify on the basis of their behavior, surface characteristics and other fundamental criteria. However, some broad classification is made for general purpose based on their size, preparation methods, and industrial applications.

Powdered activated carbon (PAC) is made in particular form as powders with an average diameter between 0.15 and 0.25 mm. Thus they present a large surface to volume ratio with a small diffusion distance. PAC is made up of crushed or ground carbon particles, 95–100% of which will pass through a designated

mesh sieve or sieve. Granular activated carbon is defined as the activated carbon being retained on a 50 mesh sieve (0.297 mm) and PAC material as finer material which ASTM classifies particle sizes corresponding to an 80 mesh sieve (0.177 mm). PAC is generally added directly to other process units, such as raw water intakes, rapid mix basins, clarifiers, and gravity filters.

Extruded activated carbon (EAC) combines PAC with a binder, which are fused together and extruded into a cylindrical shaped activated carbon block with diameters from 0.8 to 130 mm. These are mainly used for gas phase applications because of their low pressure drop, high mechanical strength and low dust content.

Bead activated carbon (BAC) is made from petroleum pitch and supplied in diameters from approximately 0.35 to 0.80 mm. Similar to EAC; it is also noted for its low pressure drop, high mechanical strength and low dust content, but with a smaller grain size. Its spherical shape makes it preferred for fluidized bed applications such as water filtration.

Impregnated carbon Porous carbons containing several types of inorganic impregnant such as iodine, silver, cation such as Al, Mn, Zn, Fe, Li, Ca have also been prepared for specific application in air pollution control especially in museums and galleries. Due to antimicrobial/antiseptic properties, silver loaded activated carbon is used as an adsorbent for purifications of domestic water. Drinking water can be obtained from natural water by treating the natural water with a mixture of activated carbon and flocculating agent $Al(OH)_3$. Impregnated carbons are also used for the adsorption of H_2S and thiols (mercaptans). Adsorption rates for H_2S as high as 50% by weight have been reported.

Polymers coated carbon is a process by which a porous carbon can be coated with a biocompatible polymer to give a smooth and permeable coat without blocking the pores. The resulting carbon is useful for hemoperfusion. Hemoperfusion

is a treatment technique in which large volumes of the patient's blood are passed over an adsorbent substance in order to remove toxic substances from the blood.

Granular activated carbon (GAC) is an irregular shaped particle with sizes ranging from 0.2 to 5 mm which has a relatively larger particle size and smaller external surface compared to powdered activated carbon. GAC are used for water treatment, deodorization and separation of components of flow system. This type is used in both liquid and gas phase applications. So, the aim of this research to prepare the new effective granular adsorbent.
(http://en.wikipedia.org/wiki/activated carbon)

Utilities of granular activated carbon (GAC)

The main types of activated carbon employed in water treatment applications are granular carbon (GAC). The two most common options for locating a GAC treatment unit in water treatment plants are: (1) post-filtration adsorption, where the GAC unit is located after the conventional filtration process (post-filter contactors or adsorbers); and (2) filtration-adsorption, in which some or all of the filter media in a granular media filter is replaced with GAC. In post-filtration applications, the GAC contactor receives the highest quality water and, thus, has as its only objective the removal of dissolved inorganics and organic compounds. The effective of GAC adsorbent is related to the maximum adsorption capacity of GAC.

In this research the effective GAC had been prepared by the combination of powder activated carbon with biodegradable polymer in bead form.

1.2.3 Biodegradable polymer

Biodegradable polymer is the polymer which is decomposed under aerobic or anaerobic conditions, as a result of the action of microorganism/enzymes. The materials develop it like starch, cellulose, and polyesters. Aliphatic polyesters are the most commonly used polymers of this type. In this research the biodegradable polymer, poly(lactic acid) (PLA) was selected for preparing a new granular adsorbent.

Poly(lactic acid) (PLA) is one of the biodegradable and biobased thermoplastic aliphatic polyester derived from renewable and degradable resources such as corn starch, chips or starch and rice, which can help alleviate the energy crisis as well as reduce the dependence on fossil fuels of our society. The name "polylactic acid" does not comply with IUPAC standard nomenclature, and is potentially ambiguous or confusing, because PLA is not a polyacid (polyelectrolyte), but rather polyester (Cram 101 Textbook reviews). High molecular weight of PLA is a colorless, glossy, rigid thermoplastic material with properties similar to polystyrene. The two isomers of lactic acid can produce four distinct materials: poly(D-lactic acid) (PDLA), a crystalline material with a regular chain structure; poly(L-lactic acid) (PLLA), which is hemicrystalline, and likewise with a regular chain structure; poly(D,L-lactic acid) (PDLLA) which is amorphous; and meso-PLA, obtained by the polymerization of meso-lactide. PDLA, PLLA and PDLLA are soluble in common solvents including benzene, chloroform, dioxane. PLA has a degradation half-life in the environment ranging from 6 months to 2 years, depending on the size and shape of the article, its isomer ratio, and the temperature (Garlotta et al., 2001 and Lin, et al., 2012). PLA can be processed by film casting, extrusion, blow molding, and fiber spinning due to its greater thermal process ability in comparison to other biomaterials such as poly(ethylene glycol) (PEG), poly(hydroxyalkanoates) (PHAs), and poly(ε-caprolactone) (PCL) (Rhim et al., 2006). These thermal properties contribute to the application of PLA in fields of industry such as textiles and food packaging. PLA production is a popular for using due to cost-efficient, non-petroleum plastic production. The huge benefit of PLA as a bioplastic is its versatility and the fact that it naturally degrades when exposed to the environment. PLA is a synthetic polymer that lactic acid and lactide are two main monomers of PLA. The chemical structure of PLA is shown in Figure 1. The most common route to PLA is the ring-opening polymerization of lactide with various metal catalysts (Martin, et al. 2001).

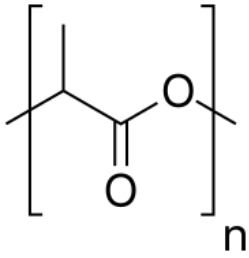

Figure 1 The chemical structure of PLA.

Properties of PLA

IUPAC name: 2-hydroxypropanoic acid

Common names: Poly (lactic acid)

Molecular formula: $(C_3H_6O_2)_n$

Density: 1.21 – 1.43 $g \cdot cm^{-3}$

Appearance: white

Melting point: 150 to 160 °C

Solubility in water: Insoluble in water

In this research AC-powder are compacted into bead form by mixing with poly(latic acid) (PLA). PLA was selected to use as polymer matrix because of its ease of bead formation by phase inversion method.

1.2.4 Phase inversion technique

Phase inversion is a process of controlled polymer transformation from a liquid phase to solid phase. There are four basic techniques used to create phase inversion membranes: precipitation from vapor phase, precipitation by controlled evaporation, thermally induced phase separation, and immersion precipitation. The majority of phase inversion membranes are prepared by immersion precipitation.

Phase inversion occurs by the following steps: a homogeneous polymer solution is thermodynamically unstable due to the exchange of solvent (in polymer solution) and non-solvent (in coagulant bath). Consequently, the system

separates into two phases: polymer-rich phase and polymer-poor phase. Polymer-poor phase becomes pores distributed in the polymer-rich phase solidified after phase separation (Mulder, 2000) In this thesis the PLA/AC beads was prepared from phase inversion then these beads were used to adsorb dyes and heavy metals.

1.2.5 Dyes

The first human-made (synthetic) organic dye, mauveine was discovered by William Henry Perkin in 1856. Many thousands of synthetic dyes have since been prepared. Synthetic dyes quickly replaced the traditional natural dyes. They cost less, they offered a vast range of new colors, and they imparted better properties to the dyed materials. Dyes are classified according to their solubility and chemical properties.

Classification of dyes

Acid dyes are water-soluble anionic dyes that are applied to fibers such as silk, wool, nylon and modified acrylic fibers using neutral to acid dye baths. Attachment to the fiber is attributed, at least partly, to salt formation between anionic groups in the dyes and cationic groups in the fiber. Acid dyes are not substantive to cellulose fibers. Most synthetic food colors fall in this category.

Basic dyes are water-soluble cationic dyes that are mainly applied to acrylic fibers, but sometimes they are used for wool and silk. Usually acetic acid is added to the dye bath to help the uptake of the dye onto the fiber. Basic dyes are also used in the coloration of paper.

Direct dyes are normally carried out in a neutral or slightly alkaline dyebath, at or near boiling point, with the addition of either sodium chloride (NaCl) or sodium sulfate (Na_2SO_4). Direct dyes are used on cotton, paper, leather, wool, silk and nylon. They are also used as pH indicators and as biological stains.

Mordant dyes require a mordant, which improves the fastness of the dye against water, light and perspiration. The choice of mordant is very important as different mordants can change the final color significantly. Most natural dyes are mordant dyes and there is therefore a large literature base describing dyeing techniques. The most important mordant dyes are the synthetic mordant dyes, or chrome dyes, used for wool; these comprise some 30% of dyes used for wool, and are especially useful for black and navy shades. The mordant, potassium dichromate, is applied as an after-treatment. It is important to note that many mordants, particularly those in the heavy metal category, can be hazardous to health and extreme care must be taken in using them.

Vat dyes are essentially insoluble in water and incapable of dyeing fibers directly. However, reduction in alkaline liquor produces the water soluble alkali metal salt of the dye, which is in the leuco form, has an affinity for the textile fiber. Subsequent oxidation reforms the original insoluble dye. Indigo is the original vat dye which is used as the color of denim.

Reactive dyes utilize a chromophore attached to a substituent that is capable of directly reacting with the fibre substrate. The covalent bonds that attach reactive dye to natural fibers make them among the most permanent of dyes. "Cold" reactive dyes, such as Procion MX, Cibacron F, and Drimarene K, are very easy to use because the dye can be applied at room temperature. Reactive dyes are by far the best choice for dyeing cotton and other cellulose fibers at home or in the art studio.

Disperse dyes were originally developed for the dyeing of cellulose acetate, and are water insoluble. The dyes are finely ground in the presence of a dispersing agent and sold as a paste, or spray-dried and sold as a powder. Their main use is to dye polyester but they can also be used to dye nylon, cellulose triacetate, and acrylic fibres. In some cases, a dyeing temperature of 130 °C is required, and a pressurized dyebath is used. The very fine particle size gives a large surface area that

aids dissolution to allow uptake by the fibre. The dyeing rate can be significantly influenced by the choice of dispersing agent used during the grinding.

Azoic dyes are a technique in which an insoluble azo dye is produced directly onto or within the fiber. This is achieved by treating a fiber with both diazoic and coupling components. With suitable adjustment of dyebath conditions the two components react to produce the required insoluble azo dye. This technique of dyeing is unique, in that the final color is controlled by the choice of the diazoic and coupling components. This method of dyeing cotton is declining in importance due to the toxic nature of the chemicals used.

Sulfur dyes are inexpensive dyes used to dye cotton with dark colors. Dyeing is effected by heating the fabric in a solution of an organic compound, typically a nitrophenol derivative, and sulfide or polysulfide. The organic compound reacts with the sulfide source to form dark colors that adhere to the fabric. Sulfur Black 1, the largest selling dye by volume, does not have a well-defined chemical structure (http://en.wikipedia.org/wiki/dye).

Rhodamine

Rhodamine is a family of related chemical compounds, fluorone dyes. Examples are Rhodamine 6G and Rhodamine B. They are used as a dye and as a dye laser gain medium. It is typically used as a tracer dye among water to determine the speed and direction of flow and transport. Rhodamine dyes fluoresce and can therefore be detected simply and inexpensively with instruments referred to as fluorometers. Rhodamine is employed extensively in biotechnology applications such as fluorescence microscopy, flow cytometry; fluorescence correlation spectroscopy and Enzyme-linked immunosorbent assay (ELISA). Rhodamine is generally toxic, and is soluble in water, methyl alcohol and ethyl alcohol. Its structure is shown in Figure 2 (Snare, 1982).

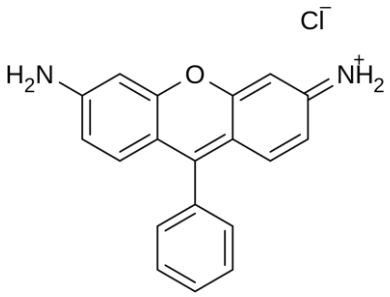

Figure 2 The structure of Rhodamine

The structures of Rhodamine 6G and Rhodamine B in aqueous solution are displayed below in Figure 3 (a) and (b), respectively.

(a)

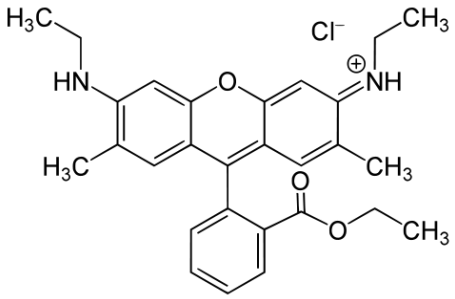

(b)

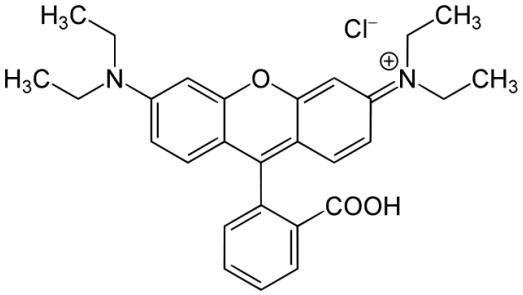

Figure 3 Structure of Rhodamine 6G (a) and Rhodamine B (b)

Discharges of Rhodamine B in natural waters can cause environmental degradation. In California, Rhodamine B is suspected to be carcinogenic; therefore products containing it must present a warning on the label (Ashly, et al., 2014). Rhodamine B was selected as a representative of the common cationic dyes in effluents from textile and food industries, from wastewater. The properties of Rhodamine B are displayed below.

Properties of Rhodamine B

IUPAC name: [9-(2-carboxyphenyl)-6-diethylamino-3-xanthenylidene]-diethylammonium chloride

Other names: Rhodamine 610, C.I. Pigment Violet 1, Basic Violet 10, C.I. 45170

Molecular formula: $C_{28}H_{31}ClN_2O_3$

Molar mass: 479.02 g mol^{-1}

Appearance: red to violet

Melting point: 210 - 211 °C (Decomposes)

Classification of dye: basic dye

Rhodamine B is often used as a tracer dye within water to determine the rate and direction of flow and transport. Rhodamine B is used in biology as a staining fluorescent dye, sometimes in combination with auramine O, as the auramine-rhodamine stain to demonstrate acid-fast organisms, notably Mycobacterium. Solubility in water is ~50 g L^{-1}. However, the solubility in acetic acid solution (30 vol. %) is ~400 g L^{-1}. Chlorinated tap water decomposes Rhodamine B. Rhodamine B solutions adsorb to plastics and should be kept in glass.

Rhodamine B is being tested for use as a biomarker in oral rabies vaccines for wildlife, such as raccoons, to identify animals that have eaten vaccine bait.

1.2.6 Heavy metal ion

A toxic heavy metal is any relatively dense metal or metalloid that is noted for its potential toxicity, especially in environmental contexts (Srivastava, et al., 2010). The term has particular application to cadmium, mercury, lead and arsenic, (Brathwaite, et al., 1985) all of which appear in the World Health Organisation's (WHO) list of 10 chemicals of major public concern. Other examples include manganese, chromium, cobalt, nickel, copper, zinc, selenium, silver, antimony and thallium (National Organization for Rare Disorders, 2015).

Wastewater streams from many activities in agriculture and industries such as chemical industry, mining and metal processing contain heavy metals such as lead, copper and cadmium. They are generally toxic to environment and human health. For example, lead and its compounds even at low concentration are poisonous to animals and humans. A lead concentration 0.006 mg L^{-1} in blood can damage the fetal brain, cause diseases of kidneys, circulatory system, and nervous system (Barakat, 2011). And copper concentrations 4 – 6 mg L^{-1} cause to gastrointestinal symptoms such as nausea, abdominal pain, diarrhea, and vomiting occur. The World Health Organization recommended a maximum acceptable concentration of Pb(II) in drinking water of 1.5 mg L^{-1}(Rao, 1992). Therefore, it is necessary to treat lead and copper-containg wastewater prior to its discharge to the environment (Bánfalvi, 2011 and World Health Organization, 2005)

Lead (II) nitrate ($Pb(NO_3)_2$)

Lead (II) nitrate is an inorganic compound. It normally occurs as a colourless crystal or white powder and, unlike most other lead (II) salts, is soluble in water. Lead(II) nitrate is the only common soluble lead compound. It readily dissolves in water to present a clear, colourless solution (Ferris, et al., 1959). As an ionic substance, the dissolution of lead (II) nitrate involves dissociation into its constituent ions. $Pb(NO_3)_2\ (s) \rightarrow Pb^{2+}\ (aq) + 2\ NO^{-3}\ (aq)$

Properties of Lead (II) nitrate

IUPAC name: Lead (II) nitrate
Other names: Lead nitrate, Lead dinitrate, Plumbous nitrate
Molecular formula: $Pb(NO_3)_2$
Molar mass: 331.2 g mol^{-1}
Appearance: White colourless crystals
Melting point: 270 °C (Decomposes)

Lead (II) nitrate is an oxidizing agent which is toxic and classified as most likely carcinogenic to humans. Consequently, it must be handled and stored with the suitable safety precautions to prevent inhalation, uptake and skin contact. Because of its risky nature, the restricted applications of lead (II) nitrate are under constant scrutiny. They have been linked to renal cancer and brain tumour in experimental animals and to renal cancer, brain cancer and lung cancer in humans thus, the removal of lead from aqueous solutions is important for human and aquatic life (World Health Organization, 2006 and Ferris, 1959).

Removing dyes and heavy metal from large volumes of water are often technically costly. There is a developing method that ought to be not only efficient and economical, however also simply to be enforced. Adsorption has been found to be an efficient and economic methodology with high potential for removing of dyes and heavy metals from wastewater. Moreover, adsorption has attracted interest especially from low-cost, eco-friendly and abundantly available material capable to remove important quantities of dyes and heavy metal ions from industrial wastewater. (Khaled, et al. 2015)

1.2.7 Adsorption

Adsorption is the adhesion of atoms, ions, or molecules from a gas, liquid, or dissolved solid to a surface. This process creates a film of the adsorbate on the surface of the adsorbent which is different to absorption process, in which a fluid (the absorbate) is dissolved by or permeates a liquid or solid (the absorbent), respectively. Adsorption is a surface-based process while absorption involves the whole volume of the material. The term sorption encompasses both processes, while desorption is the reverse of it. Adsorption is a surface phenomenon.

Similar to surface tension, adsorption is a consequence of surface energy. In a bulk material, all the bonding requirements (they are ionic, covalent, or metallic) of the constituent atoms of the material are filled by other atoms in the material. However, atoms on the surface of the adsorbent are not wholly surrounded by other adsorbent atoms and therefore can attract adsorbates. The exact nature of the bonding depends on the details of the species involved, but the adsorption process is generally classified as physisorption (characteristic of weak van der Waals forces) or chemisorption (characteristic of covalent bonding). It may also occur due to electrostatic attraction

Adsorption is present in many natural, physical, biological, and chemical systems, and is widely used in industrial applications such as heterogeneous catalysts activated charcoal, capturing and using waste heat to provide cold water for air conditioning and other process requirements, synthetic resins, increase storage capacity of carbide-derived carbons, and water purification. Adsorption, ion exchange, and chromatography are sorption processes in which certain adsorbents are selectively transferred from the fluid phase to the surface of insoluble, rigid particles suspended in a vessel or packed in a column (Ferrari, et al. 2010).

Moreover, this method is usually used to adsorb toxins within the environment specifically. The wastewater treatment plant of industries such as food, dyes, textiles, paper and plastic is use adsorption method that includes a highly effective wastewater treatment. The adsorption is a method wherever molecules from

the gas phase or from solution bind in a condensed layer on a solid or liquid surface. The molecules that bind to the surface are known as the adsorbate whereas the substance that holds the adsorbate is called the adsorbent. The method when the molecules bind is called adsorption. Removal of the molecules from the surface is called desorption. There are two differing kinds of adsorption:

[1] Chemisorption (or chemical adsorption) is a kind of adsorption which involves a chemical reaction between the surface and the adsorbate. In the majority of chemisorption processes, adsorbate–adsorbent bonds are significantly weaker than those in typical chemical compounds. New chemical bonds are generated at the adsorbant surface. Chemisorption usually forms bonding with energy of 1–10 eV. In contrast with chemisorption is physisorption, which leaves the chemical species of the adsorbate and surface intact. It is conventionally accepted that the energetic threshold separating the binding energy of "physisorption" from that of "chemisorption" is about 0.5 eV per adsorbed species. Due to specificity, the nature of chemisorption can greatly differ, depending on the chemical identity and the surface structure (Milan, 2014).

[2] Physisorption (or physical adsorption), is a process in which the electronic structure of the atom or molecule is barely perturbed upon adsorption. The fundamental interacting force of physisorption is caused by van der Waals force. Even though the interaction energy is very weak (~10–100 meV), physisorption plays an important role in nature. Van der Waals forces originate from the interactions between induced, permanent or transient electric dipoles (Milan, 2014).

In comparison with chemisorption, in which the electronic structure of bonding atoms or molecules is changed and covalent or ionic bonds form, physisorption, generally speaking, can only be observed in the environment of low temperature (thermal energy at room temperature ~26 meV) and the absence of the relatively strong chemisorptions. In practice, the categorisation of a particular adsorption as physisorption or chemisorption depends principally on the binding energy of the adsorbate to the substrate (Bond, 1987).

Chemisorption and physisorption are usually distinguishable from each other without any great difficulty. Table A summarizes the main criteria.

Table A Criteria for distinguishing between chemisorption and physisorption. (Bond, 1987)

Criteria	**Chemisorption**	**Physisorption**
Heat of adsorption (ΔH_{ads})	> 40 kJ mol^{-1} usually around 600-700 kJ mol^{-1}	0 – 40 kJ mol^{-1}
Force of attraction	Chemical bond forces	Van der Waals forces
Chemical change of adsorptive	Formation of a surface compound	None
Activation energy, E_a	Usually small	Zero
Increasing temperature	Irreversible	Reversible
Specific	It is highly specific	It is not very specific

The adsorption characteristics in solution phase between the adsorbent and adsorbate were explained by the adsorption isotherm models normally. Several models are often accustomed describe adsorption data. The two most often used for dilute solutions are the Langmuir and Freundlich isotherms (Chuenchom, 2004).

Factors affecting adsorption:

The extent of adsorption depends upon the following factors: nature of adsorbate and adsorbent, the surface area of adsorbent, activation of adsorbent and experimental conditions such as pH, contact time and temperature etc.

Adsorption isotherm

Adsorption is usually described through isotherms, that is, the amount of adsorbate (X) on the surface of adsorbent with mass m as a function of its pressure (if gas) or concentration (if liquid) at constant temperature. The quantity adsorbed is

nearly always normalized by the mass of the adsorbent to allow comparison of different materials (Foo, et al., 2010).

Basic adsorption isotherm

In the process of adsorption, adsorbate gets adsorbed on adsorbent. The adsorption and desorption processes can be written as the following equation:

$$\text{Adsorbate} + \text{Adsorbent} \underset{\text{Desorption}}{\overset{\text{Adsorption}}{\rightleftharpoons}} \text{Adsorption}$$

According to Le Chatelier principle, the direction of equilibrium would shift in that direction where the stress can be relieved. In case of application of excess of pressure to the equilibrium system, the equilibrium will shift in the direction where the number of molecules decreases. Since number of molecules decreases in forward direction, with the increases in pressure, forward direction of equilibrium will be favored.

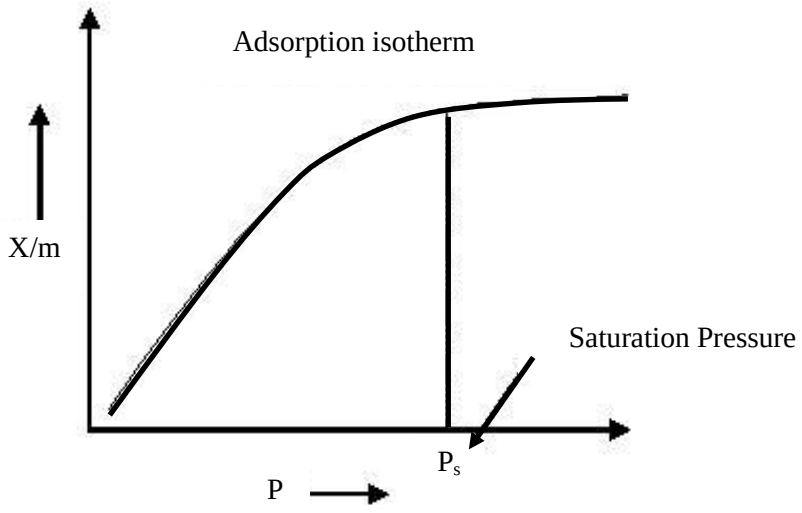

Figure 4 The plot of basic adsorption isotherm.

From the graph (Figure 4), we can predict that after saturation pressure P_s, adsorption does not occur anymore. This can be explained by the fact that there are limited numbers of vacancies on the surface of the adsorbent. At high pressure a stage is reached when all the sites are occupied and further increases in pressure does not cause any difference in adsorption process. At high pressure, adsorption is independent of pressure.

Surface area

For the determination of surface area the solid samples are pretreated by applying some combination of heat, vacuum and flowing gas to remove the adsorbed contaminants acquired (typically water and carbon-dioxide) from atmospheric exposure. The solid is then cooled, under vacuum, usually to cryogenic temperature (77 K -195 C). An adsorptive (typically nitrogen) is dosed to the solid in controlled increments. After each dose of adsorptive, the pressure is allowed to equilibrate and the quantity adsorbed is calculated. The quantity adsorbed at each pressure (and temperature) defined an adsorption isotherm, from which the quantity of gas required to form a monolayer over the external surface of the solid is determined. With the area covered by each adsorbed gas molecule known, the surface area can be calculated.

BET analysis which is the method of Brunauer, Emmet, and Teller provides precise specific surface area evaluation of materials by nitrogen multilayer adsorption measured as a function of relative pressure using a fully automated analyzer. The technique encompasses external area and pore area evaluations to determine the total specific surface area in $m^2\ g^{-1}$ yielding important information in studying the effects of surface porosity and particle size in many applications (Brunauer, et al. 1938)

Some of activated carbon strongly adsorbs many gases and has an adsorption cross section of 0.162 nm^2 for nitrogen adsorption at liquid nitrogen temperature (77 K). BET theory can be applied to estimate the specific surface area of

activated carbon from experimental data, demonstrating a large specific surface area, even around 3000 $m^2 g^{-1}$ (https://en.wikipedia.org/wiki/BET_theory).

BJH, the method of Barrett, Joyner, and Halenda is a procedure for calculating pore size distributions from experimental isotherms using the Kelvin model of pore filling. It applies only to the mesopore and small macropore size range (Barrett, et al. 1951).

Type of adsorption isotherm

The adsorption isotherm is used to compare the adsorption capacity of adsorbents for given substances. It is noted that there are two adsorption categories: physical and chemical adsorption. In the case of physical adsorption, the interactions between the adsorbate and the adsorbent are electrostatic (Tien, 1994 and Khalfaoui, et al. 2002). Chemical adsorption involves specific forces, such as those that are operative in the formation of chemical bonds. Three phenomena may be involved in physical adsorption: monomolecular and multimolecular adsorption and condensation in pores or capillaries. So the interpretation of adsorption studies can be complicated. Brunauer and his co-workers (Tien, 1994) have classified physical adsorption isotherms into five characteristic types as shown in Figure 5 (Khalfaoui, et al. 2003).

Five different types of adsorption isotherm were classified by Brunauer and his co-workers (Brunauer, et al. 1940).

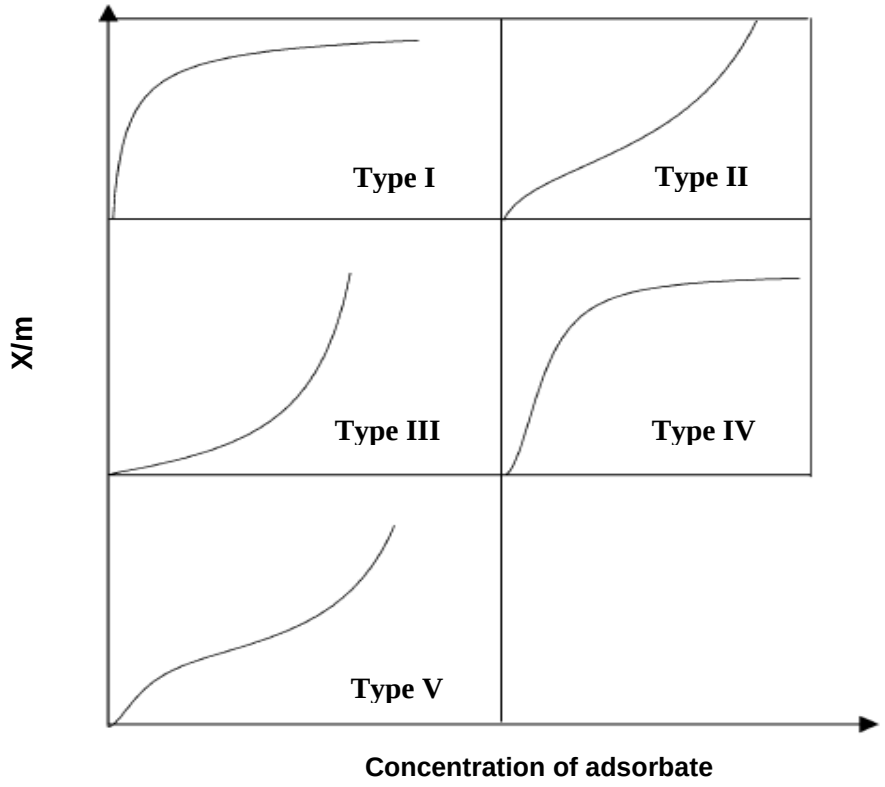

Figure 5 The five types of adsorption isotherm in the classification of Brunauer, Emett, and Teller (Tien, 1994).

Type I adsorption isotherm

The above graph depicts monolayer adsorption. This graph can be easily explained using Langmuir adsorption isotherm. Examples of type I adsorption are adsorption of nitrogen (N_2) or hydrogen (H) on charcoal.

Type II adsorption isotherm

The graph shows large deviation from Langmuir model of adsorption. Examples of type II adsorption are nitrogen gas (N_2) adsorbed on iron (Fe) catalyst and nitrogen gas (N_2) adsorbed on silica gel.

Type III adsorption isotherm

Type III adsorption isotherm also shows large deviation from Langmuir model. This isotherm explains the formation of multilayer. There is no flattish portion in the curve which indicates that monolayer formation is missing. Example of type III adsorption isotherm is iodine (I_2) on silica gel.

Type IV adsorption isotherm

At lower pressure region of graph is quite similar to type II. This explains formation of monolayer followed by multilayer. The saturation level reaches at a pressure below the saturation vapor pressure. This can be explained on the basis of a possibility of gasses getting condensed in the tiny capillary pores of adsorbent at pressure below the saturation pressure (P_s) of the gas. Examples of type IV adsorption isotherm are of adsorption of benzene on iron oxide (Fe_2O_3) and adsorption of benzene on silica gel.

Type V adsorption isotherm

Example of type V adsorption isotherm is adsorption of water (vapors) on charcoal. Type IV and V adsorption isotherms show phenomenon of capillary condensation of gas (http://www.chemistrylearning.com/adsorption-isotherm/).

In the IUPAC recommendations there are six physical adsorption isotherm types instead of the BDDT five groups, as shown in Figure 6 (Sing, et al. 1985, Balbuena, et al. 1992 and Kaneko, et al. 1994).

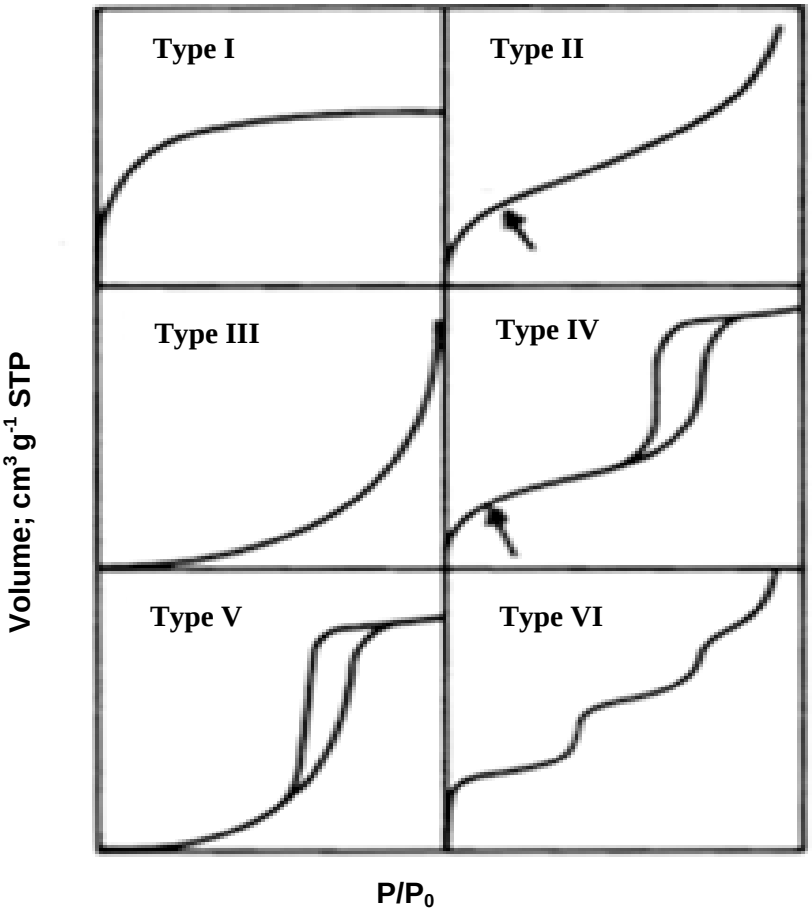

Figure 6 The IUPAC classification of six types of adsorption isotherm (Sing, et al. 1985).

Type I adsorption isotherm corresponds to the so-called Langmuir isotherm. In the case of physical adsorption, the type I isotherm has a high volume of micropores where molecules are adsorbed by micropore filling which has been actively studied in adsorption science.

Type II adsorption isotherm is the most familiar. The multilayer adsorption theory by Brunauer, Emmett, and Teller was originally developed for this type of adsorption, Hence, this isotherm is indicative of the multilayer adsorption process, suggesting the presence of nonporous or macroporous surfaces. Although the adsorption isotherm near P/P_0,= 1 gives important information on macropores, such

an analysis is not practical for accurate measurement. This is because serious condensation on the apparatus walls begins near the saturated vapor pressure.

Type III adsorption isotherm arises from nonporous or macroporous surfaces which interact very weakly with the adsorbent molecules.

Type IV adsorption isotherm gives useful information on the mesopore structure through its hysteresis loop, that is, nonoverlapping of the adsorption and desorption branches. In the mesopores, molecules form a liquid-like adsorbed phase having a meniscus of which curvature is associated with the Kelvin equation, providing the pore size distribution.

Type V adsorption isotherm is closed to the type IV isotherm instead of very weak adsorbent-adsorbate interaction.

Type VI adsorption isotherm is the stepped adsorption isotherm which comes from phase transition of the adsorbed molecular layer or adsorption on the different faces of crystalline solids.

In the following description, mainly type I and IV isotherms will appear in relation to the micropore and mesopore analyses, respectively (Kaneko, et al. 1994).

Langmuir adsorption isotherm

Irving Langmuir was the first to derive a scientifically based adsorption isotherm in 1918 (Langmuir, 1918). The model applies to gases adsorbed on solid surfaces. It was a semi-empirical isotherm with a kinetic basis which was derived based on statistical thermodynamics. It is the most common isotherm equation to use due to its simplicity and its ability to fit a variety of adsorption data. It is based on four assumptions:

1. The surface of the adsorbent is uniform, that is, all the adsorption sites are equivalent.

2. The surface is energetically homogeneous and adsorbed molecules do not interact.
3. There are no phase transitions.
4. At the maximum adsorption, only a monolayer is formed: molecules of adsorbate do not deposit on other, already adsorbed, molecules of adsorbate, only on the free surface of the adsorbent.

These four assumptions are seldom all true: there are always imperfections on the surface, adsorbed molecules are not necessarily inert, and the mechanism is clearly not the same for the very first molecules to adsorb to a surface as for the last. The fourth condition is the most troublesome, as frequently more molecules will adsorb to the monolayer; this problem is addressed by the BET isotherm for relatively flat (non-microporous) surfaces. The Langmuir isotherm is nonetheless the first choice for most models of adsorption, and has many applications in surface kinetics and thermodynamics (Czepirski, et al. 2000).

The non-linear Langmuir equation is as the following form

$$q_e = \frac{q_m b C_e}{1 + b C_e} \qquad \text{(Non –Linear form)} \qquad (1)$$

where q_e represents the amount of solute adsorbed per unit weight of adsorbent (mg g^{-1}); q_m is the amount maximum sorption capacity corresponding to complete monolayer coverage of the surface, also called the monolayer capacity (mg g^{-1}); C_e is the equilibrium solute concentration conditions (mg L^{-1}); and b is an equilibrium constant related to the energy of sorption (Reddad, et al., 2002).

Equation (1) is usually linearlized by inversion to obtain the following form

$$\frac{C_e}{q_e} = \frac{1}{q_m b} + \frac{C_e}{q_m} \qquad \text{(Linear form)} \qquad (2)$$

Many researchers have usually used equation (2) to analyze batch equilibrium data by plotting C_e/q_e versus C_e, which yields a linear if data conform to the Langmuir isotherm (Zhengang et al, 2009).

Limitation of Langmuir adsorption equation

1. The adsorbed gas has to behave ideally in the vapor phase. This condition can be fulfilled at low pressure condition only. Thus Langmuir equation is valid under low pressure only.

2. Langmuir equation assumes that adsorption is monolayer. But, monolayer formation is possible only under low pressure condition. Under high pressure condition the assumption breaks down as gas molecules attract more and more molecules towards each other. BET theory proposed by Bruanuer, Emmert and Teller explained more realistic multilayer adsorption process.

3. Another assumption was that all the sites on the solid surface are equal in size and shape and have equal affinity for adsorbate molecules i.e. the surface of solid if homogeneous. But we all know that in real solid surface are heterogeneous.

4. Langmuir equation assumed that molecules do not interact with each other. This is impossible as weak force of attraction exists even between molecules of same type.

5. The adsorbed molecules has to be localized i.e. decrease in randomness is zero (S=0). This cannot happen because on adsorption liquefaction of gases taking place, which results into decrease in randomness but the value, is not zero.

From above facts we can conclude that, Langmuir equation is valid under low pressure conditions.

Freundlich adsorption isotherm

Freundlich proposed another adsorption isotherm known as Freundlich adsorption isotherm or Freundlich adsorption equation or simple Freundlich isotherm.

The Freundlich adsorption equation (Freundlich, 1907) is perhaps the most widely used for the description of adsorption in aqueous systems. The Freundlich equation is of the form

$$q_e = K_F C_e^{1/n} \qquad \text{(Non –Linear form)} \qquad (3)$$

where q_e and C_e have definition as previously presented for the Langmuir isotherm. K_F is the so-called unit capacity factor that shows adsorption capacity and n is the empirical parameter that represents the heterogeneity of the site energies and also is indicative of the intensity of adsorption.

The logarithm of equation (4) given below is usually used to fit data as

$$\log q_e = \log K_F + \frac{1}{n} \log C_e \qquad \text{(Linear form)} \qquad (4)$$

The above equation is comparable with equation of straight line, y = mx + c where, m represents slope of the line and c represents intercept on y axis. Plotting a graph between log q_e and log C_e, we will get a straight line with value of slope equal to n and log K_F as y-axis intercept (Arivoli et al., 2009).

Limitation of Freundlich adsorption isotherm

Experimentally it was determined that extent of adsorption varies directly with pressure till saturation pressure P_s is reached. Beyond that point rate of adsorption saturates even applying higher pressure. Thus Freundlich adsorption isotherm failed at higher pressure.

1.2.8 Kinetic models of adsorption

Kinetic models of adsorption are the study of rates of adsorption processes. Adsorption kinetics includes investigations of how different experimental conditions can influence the speed of an adsorption and yield information about the reaction's mechanism and transition states, as well as the construction of mathematical models that can describe the characteristics of an adsorption process.

The rate equation shows the detailed dependence of the reaction rate on the concentrations of reactants and other species present. Different mathematical forms are possible depending on the reaction mechanism. The actual rate equation for a given reaction is determined experimentally and provides information about the reaction mechanism. The rate equation of adsorption kinetics was analyzed by the use of pseudo-first-order, pseudo-second-order kinetics models and an intraparticle diffusion model (Hui, et al. 2009).

Pseudo-First-Order model

The adsorption kinetic data were described by the Lagergren model which is the pseudo first-order model (Lagergren, 1898). The earliest known equation is describing the adsorption rate based on the adsorption capacity. The pseudo first-order equation is commonly expresses as follows:

$$\frac{dq}{dt} = k_1(q_e - q_t) \qquad (5)$$

By applying the boundary condition $q_t = 0$ at $t = 0$, integrating equation (5) to obtain equation (6) as follows

$$\ln(q_e - q_t) = \ln q_e - k_1 t \qquad (6)$$

where k_1 (min^{-1}) is the rate constant of the pseudo-first order model, where q_t (mg g^{-1}) and q_e (mg g^{-1}) denote the amount of adsorbent adsorbed at time t (min) and equilibrium, respectively. The slope of linear equation between ln (q_e - q_t) and t plot gives the pseudo-first-order rate constant, k_1.

Pseudo-Second-Order model

In addition, a pseudo-second-order (Ho, et al., 1999) can be written as in equation 7.

$$\frac{dq}{dt} = k_2(q_e - q_t)^2 \qquad (7)$$

Integrating equation (7) with the conditions of $q_t = 0$ at $t = 0$ and $q_t = q_t$ at time t and rearranging into a linear form gives an equation (8)

$$\frac{t}{q_t} = \frac{1}{k_2 q_e^{\,2}} + \frac{1}{q_e}t \qquad (8)$$

where k_2 is the rate constant of pseudo-second-order adsorption (g mg^{-1} min^{-1}), q_e is the amount of adsorbent adsorbed at equilibrium (mg g^{-1}) and q_t is the amount of adsorbent on the surface of the sorbent (mg g^{-1}) at any time t (min). The values of k_2 and q_e were calculated from the intercept and slope of the plots of t / q_t versus t, respectively.

Intraparticle diffusion model

The intra-particle diffusion model (IPD) proposed by Weber and Morris (Weber, et al. 1963) as shown in equation (9).

$$q_t = k_P t^{1/2} + C \qquad (9)$$

where q_e and q_t are the amount of adsorbent adsorbed (mg g^{-1}) at equilibrium and at any time t, respectively, k_P is the rate constant of intraparticle diffusion (mg g^{-1} $min^{-1/2}$).

The nature of the initial adsorption behavior can be explained with the initial factor based on the intraparticle diffusion model. In the first instance, equation (10) can be written as

$$q_{ref} = k_P t_{ref}^{1/2} + C \qquad (10)$$

where t_{ref} is the longest time of adsorption and q_{ref} is the amount of Rhodamine B adsorbed at t_{ref}. Subtracting equation (10) by equation (9), we have

$$q_{ref} - q_t = k_P\left(t_{ref}^{1/2} - t^{1/2}\right) \qquad (11)$$

Rearrangement of equation (11) yields

$$\left(\frac{q_t}{q_{ref}}\right) = 1 - R_i\left[1 - \left(\frac{t}{t_{ref}}\right)^{1/2}\right] \qquad (12)$$

The parameter R_i is defined as the initial factor based on the intraparticle diffusion model. R_i is expressed in equation (13)

$$R_i = \frac{q_{ref} - C}{q_{ref}} \qquad (13)$$

The R_i value is divided into four zones: $0.9 < R_i < 1.0$ is called weak initial adsorption (zone 1); $0.5 < R_i < 0.9$ is the intermediate initial adsorption (zone 2); $0.1 < R_i < 0.5$ is strong initial adsorption (zone 3); and $R_i < 0.1$ approaches complete initial adsorption (zone 4) (Wu, et al. 2009).

1.2.9 Thermodynamic studies

The van't Hoff equation provides information about the temperature dependence of the equilibrium constant in equation (14). The plot of ln K_c on the y-axis and 1/T on the x-axis will give the value of ΔH° from slope and ΔS° from intercept. The Gibb's free energy (ΔG°) is calculated in equation (15).

$$\ln K_c = \frac{\Delta S^\circ}{R} - \frac{\Delta H^\circ}{RT} \qquad (14)$$

$$\Delta G^\circ = -RT \ln K_c \qquad (15)$$

where K_c is the ratio of C_A, the solid-phase concentration of Rhodamine B at equilibrium (mg L^{-1}), to C_e, the equilibrium concentration of

Rhodamine B in solution (mg L^{-1}), *R* is the universal gas constant (8.314 J K^{-1} mol^{-1}), and *T* is the absolute temperature (K).

The thermodynamic parameters were estimated in order to understand the feasibility and nature of the adsorption process. For an endothermic reaction, heat is absorbed, making the net enthalpy change positive and for an exothermic reaction, heat is released, making the net enthalpy change negative. The positive value of entropy suggests that the degree of randomness at the solid-liquid interface is increased. Moreover, the negative value of Gibb's free energy confirms the thermodynamic feasibility and spontaneity (Umar, et al. 2015).

1.3 Review of Literatures

There have been many researches concerned in the adsorption of dye and heavy metal ions on carbon material surface. This interest is due to the importance of the following issues: surface chemistry, water chemistry, analytical chemistry, chemical engineering and environmental studies. Many researchers have studied preparation and characterization of powder activated carbon, granular activated carbon and adsorption of cationic dyes and metal ions on carbon materials such as:

Sirichote, et al. (2008), produced the activated carbons from agricultural wastes, such as bagasse (B), oil palm shell (OP), and pericarp of rubber fruit (PR) by chemical activation with zinc chloride. The obtained activated carbons were characterized and the results showed that iodine number of B, OP and PR were 939, 808 and 868 mg g^{-1}, respectively. The values of BET surface area were 1,076, 770 and 877 mg g^{-1} for B, OP and PR, respectively. The points of zero charge (pH_{pzc}) were 4.2(B), 6.1(OP), and 6.4(PR). Adsorption of phenol in aqueous solution at pH 2 and pH 12 were determined by UV-Visible spectrophotometer at 30^{o}C. The adsorption data were fitted to Freundrich isotherm.

Hayeeye, et al. (2014), performed the adsorption of Rhodamine B, on activated carbon obtained from pericarp of rubber fruit (PrAC) and commercial activated carbon (CAC). PrAC and CAC characterized by the scanning electron microscopy (SEM), the BET surface area, and the point of zero charge (pH_{pzc}). The effects of various experimental parameters such as contact time, dye concentration, amount of activated carbon, pH and temperature were analyzed. The adsorption isotherm fitted well to the Langmuir model. At pH 4.0, the maximum adsorption capacities were 0.2306, 0.2356, 0.2756, and 0.2981 mmol g^{-1} for PrAC and 0.8957, 0.9588, 0.9841, and 1.0263 mmol g^{-1} for CAC at 30, 40, 50, and 60°C, respectively. From the effect of temperature dependence of these adsorptions indicated that they were endothermic processes.

Madhavakrishnan, et al. (2009), studied the adsorption of crystal violet on *Ricinus Communis* activated carbon (RCPC) which was activated with sulfuric acid to increase the ability to adsorb crystal violet. The effect of crystal violet sorption as contact time, initial concentration of the dye solution, the amount of adsorbent and pH were studied. The equilibrium time was 60 min. The adsorption was in accordance with the Langmuir and Freundlich model. The maximum adsorption capacity of crystal violet on RCPC was 48.0 mg g^{-1} at initial pH 6.8 ± 0.2. Kinetic data was given by Lagergren model (pseudo-first-order model) and pseudo-second-order model. The results showed that RCPC could be used to adsorb crystal violet dye effectively instead of activated carbon.

Mohamed, et al. (2010), studied Cr (VI) adsorption on the two comparative activated carbons prepared from coconut palm without modification (virgin activated carbon) and activated carbon modified (modified activated carbon) through immersion in a solution of polyethylene which is low molecular weight polyethyleneimine; LMW PEI. The results showed that LMW PEI was adsorbed on the powder activated carbon about 228.2 mg g^{-1}. They studied various effective factors such as pH, concentration of Cr (VI), and the amount of PEI on activated carbon. The study on modified activated carbon adsorption, the researchers proposed

a model to absorb. It was found that the adsorption of modified activated carbon followed Freundlich model and effectively adsorb Cr (VI) higher than virgin activated carbon.

Ghaedi, et al. (2015), activated carbon was prepared from walnut wood which was non-toxic, locally available and cheap and was activated with $ZnCl_2$. This adsorbent was characterized using BET, FT-IR and SEM and it was used for removing of Pb^{2+} ions and methylene blue (MB) from aqueous solution. The equilibrium data obtained at optimum condition were fitted Langmuir model isotherm and the maximum adsorption capacities of Pb^{2+} ions and MB were 58.82 and 18.52 mg g^{-1}. From kinetic data was revealed that the adsorption rate follows pseudo-second order kinetic model and intraparticle diffusion model.

However, powder activated carbon was difficult for practical use. Therefore, there were many researchers used a synthetic polymer to adsorb instead of powder activated carbon.

Minghua, et al. (2012), prepared nano fiber membrane from polyethersulfone / polyethylene-eimine (PES / PEI) and used it as an absorbent for anionic dyes and heavy metals from solution. The various factors affecting the adsorption for example, the volume of the membrane, concentration, pH, adsorption time and temperature to absorb were studied. The results showed that the removal of metal ions and anionic dyes on nano PES / PEI fiber membrane depending on the pH of the process and the amount of absorption is highest at pH = 1 and 5-7 for anionic dyes and metal ions, respectively. Moreover, nano PES / PEI fiber membrane can also be recycled. From data of adsorption equilibrium, according to the Langmuir model by the maximum adsorption capacities are 1,000, 344.83, 454.44, 94.34, 161.29 and 357.14 mg g^{-1} for sunset yellow FCF, fast Green FCF, Amaranth, Pb (II), Cu (II) and Cd(II) ions, respectively. The kinetics for anionic dyes and heavy metal ions adsorptions obeyed pseudo-second-order kinetic model. The intra-particle diffusion explained the rate of adsorption and from thermodynamics data, the values of Gibb's

free energy, entropy and enthalpy of adsorption for the anionic dye and metal ions showed that adsorptions were spontaneous and exothermic process.

Nevertheless, the adsorption on synthetic polymer is not biodegradable. Therefore, other researches prepared biodegradable polymer as degradable adsorbent for more friendly environmental.

Rahchamani., et. al (2011), issue studied adsorption of methyl violet using polyacrylamide (PAA). The study factors that affected adsorption included the contact time, the amount of PAA, pH and temperature. The equilibrium adsorption study was evaluated by Langmuir adsorption model. The maximum adsorption capacity of methyl violet is 1,136 mg g^{-1} and the adsorption increase with increasing temperatures. From kinetic study found that the adsorption kinetics followed pseudo-second-order model and from the thermodynamics data such as enthalpy, Gibb's free energy and entropy suggested that adsorption of methyl violet on PAA is spontaneous and endothermic process.

Hongzhang., et al (2004), studied the adsorption of Cr (VI) on wheat flour which modified by immersion in a solution of $FeCl_3$ (Fe-modified steam exploded wheat straw; Fe-SEWS) and study the factors that affect the adsorption, such as initial concentration of Cr (VI), time and pH. The adsorption was fitted by Langmuir isotherm and Freundlich isotherm model. The Fe-SAWS adsorbent could absorb Cr (VI) up to 96% and the percentage desorption was 87-90% at initial concentration of soluble Cr (VI) 70 mg L^{-1}, pH 2 and Fe-SAWS adsorbent 3 g.

Senthilkumaar., et. al (2011), prepared adsorbent from lignocellulose, which is a natural polymer by immersion phosphoric acid for adsorb the anionic dyes which are direct blue (DB) and reactive blue (RB) and the effective factors of adsorption, such as initial concentration, temperature and pH. The model of adsorption followed Langmuir isotherm model and kinetics study found that the adsorption obeyed pseudo-second-order. The data of thermodynamics of DB and RB

adsorption revealed that the adsorption was endothermic process (the positive value of enthalpy).

Although, those biodegradable polymer adsorbents were easy to use and low cost but their adsorption capacities were less than activated carbon. Therefore, many researchers tried to modify adsorbents by mixing activated carbon with polymer to be more effective in adsorption and more easy to use.

Dong-Wan, et al. (2011), they modified granular activated carbon which was prepared by coating quaternary ammonium-containing polymer [3-(methacryloylamino)propyl]-trimethylammonium chloride, onto granular activated carbon (GAC) to remove nitrate and Cr(VI) from aqueous solution. The removal efficiencies for nitrate and Cr (VI) increased as the concentration of the cationic polymer used for modification increased to 0.25%, but those decreased slightly when the polymer concentration further increased to 2.5%. Kinetics experiments indicated the adsorption was a fast process, reaching equilibrium in 90 and 120 min for nitrate and Cr (VI) adsorption, and the maximum equilibrium uptake of nitrate and Cr (VI) were about 26 and 81 mg g^{-1}, respectively. The adsorptions of both anions were well described by pseudo-second-order kinetic model and Langmuir isotherm model. There was a linear relationship between the amounts of desorbed chloride and adsorbed nitrate and Cr(VI), suggesting the main effect of modification was enhancement of ion exchange capacity of GAC. The thermodynamic data showed that adsorption process would be thermodynamically favourable, spontaneous, and exothermic nature. The adsorption capacity for Cr(VI) decreased continuously with an increase in initial solution pH from 3 to 8 but such an effect was less significant for nitrate. The nitrate and Cr(VI) adsorption decreased the most in the presence of sulfate, followed by chloride and phosphate. The overall results demonstrated the potential utility of a cationic polymer for enhancement of performances of GAC-based materials for anions removal from aqueous solutions.

Eun-Ah, et al. (2012), investigated the depth profile of mercuric ion after the reaction with polysulfide–rubber-coated activated carbon (PSR-AC). Micro-

X-ray fluorescence (μ-XRF) imaging techniques and mathematical modelling were used. The μ-XRF results revealed that mercury was concentrated at 0–100 μm from the exterior of the particle after 3 months of treatment with PSR-AC in 10 ppm $HgCl_2$ aqueous solution. The μ-X-ray absorption near edge spectroscopic (μ-XANES) analyses indicated HgS as a major mercury species, and suggested that the intra-particle mercury transport involved a chemical reaction with PSR polymer. An intra-particle mass transfer model was developed based on either a Langmuir sorption isotherm with liquid phase diffusion (Langmuir model) or a kinetic sorption with surface diffusion (kinetic sorption model). The Langmuir model predicted the general trend of mercury diffusion, although at a slower rate than observed from the μ-XRF map. A kinetic sorption model suggested faster mercury transport, which overestimated the movement of mercuric ions through an exchange reaction between the fast and slow reaction sites. Both μ-XRF and mathematical modeling results suggest mercury removal occurs not only at the outer surface of the PSR-AC particle but also at some interior regions due to a large PSR surface area within an AC particle.

Mansooreh, et al. (2012**)**, concerned the increase in removal of platinum group metals even their low availability in nature and their environmental. In this research, the commercial activated carbon was used to optimize the palladium and platinum removal by applying the Taguchi approach. According to the results, the optimum operating conditions for palladium and platinum removal by activated carbon were pH 2, particle size of adsorbent 0.21 mm and adsorbent dose 10 g L^{-1}. Under these optimum operating conditions, more than 98% of palladium and platinum were removed by activated carbon in 3 h. The equilibrium adsorption data were well described by the Langmuir and Freundlich models. While the commercial activated carbon had the palladium and platinum adsorption capacities of 35.7 and 45.5 mg g^{-1}, respectively, the bio-polymer modified activated carbon was able to adsorb 43.5 and 52.6 mg g^{-1} of palladium and platinum, respectively. It was observed that the adsorption kinetics of palladium and platinum on these adsorbents could be well analyzed with pseudo-second-order model.

Hwang, et al. (2013), improved the filtration efficiency and permeability of polymer membranes simultaneously during water treatment, by adding different ratios of activated carbon (AC) and polyethylene glycol (PEG) into polyphenylsulfone (PPSU)/polyetherimide (PEI) polymers to prepare the novel composite polymer membranes. The results showed that the addition of AC significantly affected the membrane morphology, pore size distribution, porosity, and chemical properties. With this increase in AC concentration, the filtration flux and permeability of the AC/PPSU/PEI/PEG composite membrane improved. The addition of hydrophilic pore-formation agent PEG helped to increase the surface hydrophilicity and porosity of the AC/PPSU/PEI/PEG composite membranes. The intrinsic membrane resistances decreased with the rising concentration of PEG. The optimum component of the AC/PPSU/PEI/PEG composite membrane was 0.25/35/5/6 wt.%, and the corresponding membrane permeability and humic acids (HAs) removal efficiency were 184 L m^{-2} h^{-1} and 80%, respectively.

The results from many researchers showed that the adsorbent prepared by mixing activated carbon with polymer was easier to use than PAC. However, its adsorption capacity was still lower than PAC. In this work we developed a new adsorbent by compacting AC and poly(lactic) acid (PLA) in bead form which prepared by phase inversion method and used to adsorb dye (Rhodamine B) and heavy metal ion (Pb^{2+} ions). Rhodamine B and Pb^{2+} ions were selected as representative common cationic adsorbates in textile and food industries effluent, for their adsorption studies from wastewater. Evaluation and optimization of the experimental controlling conditions such as PLA/AC dose, contact time, pH, and temperature as well as the adsorption isotherm of Rhodamine B and heavy metal ion on PLA/AC composite bead form were explored and discussed in this study.

1.4 Objectives

1.4.1 To prepare a granular activated carbon material from PLA and AC using phase inversion method.

1.4.2. To characterize the obtained PLA/AC 5% wt. beads.

1.4.3. To evaluate and optimize of the experimental controlling conditions of dye (Rhodamine B) and heavy metal ions (Pb^{2+} ions) adsorption such as PLA/AC dose, contact time, and pH.

1.4.4. To investigate the kinetics model and adsorption isotherm of dye (Rhodamine B) and heavy metal ions (Pb^{2+} ions) on PLA/AC composite bead form.

1.4.5. To study thermodynamics of Rhodamine B sorption on PLA/AC composite bead form from the effect of temperature.

CHAPTER 2

METHOD OF STUDY

2.1 Chemicals and materials

1. Rhodamine B, $C_{28}H_{31}ClN_2O_3$; Laboratory reagent grade, Assay >97% ; Fluka.
2. Poly(lactic acid) (PLA), Natureworks, Department of Materials Science and Technology, PSU.
3. Lead (II) nitrate, $Pb(NO_3)_2$; Assay >98%, UNILAB; Griffith School of Engineering, Nathan Campus, Griffith University.
4. Activated carbon (AC), Assay 99%, Sigma – Aldrich.
5. N-methyl-2-pyrrolidone (NMP), C_5H_9NO; RCI Labscan limited, Department of Materials Science and Technology, PSU.
6. Sodium hydroxide, NaOH; A.R., RCI Labscan limited.
7. Hydrochloric acid, HCl; A.R., 37%, Merck.
8. Distilled water; Department of Chemistry, PSU.
9. Deionized water; Griffith School of Engineering, Nathan Campus, Griffith University.

2.2 Equipment and Instruments

2.2.1 Department of Chemistry, PSU

1. Analytical balance; Classic, Mettler-Toledo.
2. Thermostat shaker water bath; Memmert.
3. Hotplate and stirrer; IKA C-MAG HS7, Merck.
4. UV-Vis spectrophotometer; UV 2600, Shimadzu.
5. Oven; Memmert
6. The Benchtop pH meter; ST3100-F, Ohaus
7. Thermometer

2.2.2 Scientific Equipment Center, PSU

1. Scanning electron microscope, SEM; Quanta 400, FEI, Czech Republic.
2. Scanning electron microscopy with energy dispersive X-ray spectroscopy (SEM-EDX); Quanta 400, FEI, Czech Republic.
3. Elemental analysis (C, H, N, O), CE instruments Flash EA 1112 series, Thermo Quest, Italy.
4. Fourier-transform infrared spectrophotometer and diffuse reflectance accessory, FT-IR and ATR mode; Spectrum GX, Perkin Elmer, US.

2.2.3 Griffith School of Engineering, Nathan Campus, Griffith University

1. Atomic absorption spectrophotometer (GBC SDS-270), Australia.

2. Rotary shaker, Griffith University, Australia.

2.2.4 Science and Technology Service Center, Chiang Mai University (STSC-CMU)

1. Model Autosorb 1 MP, Quanta chrome, USA

2.3 Methods

2.3.1 Preparation of poly(lactic acid)/activated carbon composite beads form (PLA/AC beads)

The PLA/AC beads were prepared by phase inversion technique (Mulder et al. 2000) in the following steps. First, the AC was sieved to 200 – 270 mesh size (Bhatnagar, et al. 2005) and dried at 110 °C for 24 h before using. The homogeneous aqueous solution of PLA of 10 % wt. was prepared by dissolving in NMP then the given proper amount of AC of 1, 2, 3, 4, 5% wt. was added in the PLA solution, stirred at room temperature for 24 h. The mixture was then added dropwise into water. The PLA/AC beads were washed many times with double distilled water then dried at 60 °C.

2.3.2 Characterization of PLA/AC beads

2.3.2.1 Scanning electron microscopy (SEM)

Scanning electron microscope (Quanta 400) located at Scientific Equipment Center, PSU was used to analyze the morphology of the PLA/AC bead.

2.3.2.2 Elemental composition (C, H, N, O) analysis

Elemental composition (C, H, N and O) analysis was performed on the samples using a FLASH EA 112 Elemental Analyzer instrument at Scientific Equipment Center, PSU.

2.3.2.3 Surface area and the pore size distribution

Surface area and the pore size distribution measurements of the best of PLA/AC bead which was chosen for this study were obtained from nitrogen adsorption isotherms at 77 K using the Model Autosorb 1 MP, Quanta chrome at Science and Technology Service Center, Chiang Mai University (STSC-CMU). The Surface area was taken from adsorption isotherms using the Brunauer-Emmett-Teller (BET) equation (Brunauer, et al. 1938) and the pore size distribution was determined by the Barrett-Joyner-Halenda (BJH) model (Barrett, et al. 1951).

2.3.2.4 Fourier-transform infrared spectrophotometry (FT-IR)

The functional groups of PLA/AC beads were analyzed by Fourier-transform infrared spectrophotometer, FT-IR. The Transmission IR spectra of the carbon samples were obtained using ATR technique. It was located at Scientific Equipment Center, PSU.

2.3.2.5 Point of zero charge measurements (pH_{pzc})

The point of zero charge (pH_{pzc}) means the pH at which the total numbers of positive and negative charges on its surface become zero was estimated by using the pH drift method (Jia et al., 1998 and Jia et al., 2002). The Benchtop pH meter (ST3100-F, Ohaus) was used for adjustment of pH of the tested solutions. The procedure was described as follows: the pH of each of a series of 0.1 mol L^{-1} NaCl solutions was adjusted to successive initial values between 2 and 12, by adding either 0.1 mol L^{-1} HCl or NaOH. The PLA/AC 5% wt. beads were added into each of these NaCl solutions using a PLA/AC : NaCl solution ratio of 0.25 g : 50 mL. They were sealed and left overnight under stirring at ambient temperature. Then, the graph of final pH (pH_f) versus initial pH (pH_0) was plotted. The pH which the curve crossed the line $pH_f = pH_0$ was taken as the pH_{pzc} of the PLA/AC 5% wt. beads adsorbent.

2.3.3 Adsorption studies

2.3.3.1 Adsorbate (Rhodamine B and Pb^{2+} ions solution)

Rhodamine B and Pb^{2+} ions were chosen for this study. Molecular weight of Rhodamine B is 479.02 g mol^{-1} and atomic weight is 207.2 g mol^{-1} for Pb^{2+} ions. The stock solutions were diluted with distilled water to obtain standard solutions with concentration ranging from 50 – 600 mg L^{-1} for Rhodamine B and 100 - 4000 mg L^{-1} for Pb^{2+} ions for adsorption isotherm studies.

2.3.3.2 Adsorption isotherm studies of Rhodamine B and Pb^{2+} ions on the PLA/AC 5% wt. composite beads form

Adsorption isotherm studies of Rhodamine B and Pb^{2+} ions onto the PLA/AC 5% wt. beads were carried out by batch adsorption method (Rahchamani, et al., 2011). The procedure of the adsorption experiments was as follows: 0.25 g of PLA/AC 5% wt. beads were added to a series of 50 mL solutions of Rhodamine B at various concentrations (50 – 600 mg L^{-1}) and agitated in a thermostat shaker at 30, 40, 50 and 60 °C. The Rhodamine B adsorption was studied at pH 4.0 which is the natural pH of Rhodamine B. Isotherms were obtained from these solutions which were used to determine their thermodynamic parameters. The concentrations of Rhodamine B in solution before and after adsorption were analyzed using UV-Vis spectrophotometer (UV 2600, Shimadzu) at a wavelength of 554 nm. The concentrations were then quantitatively estimated using the linear regression equations obtained by plotting a calibration curve with a range of Rhodamine B concentrations from 0 – 5 mg L^{-1} and regression coefficient (R^2) was 0.9989.

For Pb^{2+} ions adsorption, 0.25 g of PLA/AC 5% wt. beads were added into 50 mL sample of 100 - 4000 mg L^{-1} of Pb^{2+} ions solution, and the mixture was agitated in a rotary shaker at 23±2 °C and at pH 3, 4 and 5. The Pb^{2+} ions concentrations, before and after adsorption, were determined by atomic absorption spectrophotometer.

Moreover, all of the experiments were repeated three times to check the reproducibility of the data and the average values were taken. The adsorption capacity, q_e (mg g^{-1}), and the percentages of Rhodamine B and Pb^{2+} ions adsorbed by PLA/AC 5% wt. beads were calculated from the equations (16) and (17) (Hayeeye, et al., 2104 and Hayeeye, et al.,2015), respectively as follows:

$$q_e = \frac{V(C_0 - C_e)}{W} \qquad (16)$$

$$\%\ dye\ adsorbed\ = \frac{C_0 - C_e}{C_e} \times 100 \qquad (17)$$

where q_e is the adsorption capacity (mg g^{-1}), V is the volume of the solution (L), W is the mass of the adsorbent (g) and C_0 and C_e are the initial concentration and the equilibrium concentration of Rhodamine B and Pb^{2+} ions (mg L^{-1}), respectively.

The effects of various parameters, namely contact time (0 – 54 h for Rhodamine B and 0 – 180 min for Pb^{2+} ions), pH (2 – 12 for Rhodamine B and 1.5 – 5.5 for Pb^{2+} ions) and amount of PLA/AC 5% wt. beads (0.10 - 0.50 g for Rhodamine B and Pb^{2+} ions) were experimentally explored. To determine the effect of pH, the values of initial pH of the Rhodamine B and Pb^{2+} ions were adjusted by using HCl or NaOH solution.

2.3.3.3 Adsorption kinetic studies of Rhodamine B and Pb^{2+} ions on the PLA/AC 5% wt. composite beads form

The equilibrium data were used to evaluate kinetic adsorption isotherm. Kinetic experiments were conducted for different initial concentrations of Rhodamine B (50, 100 and 200 mg L^{-1}) and Pb^{2+} ions (50, 300 and 500 mg L^{-1}). The values of initial pH of the Rhodamine B and Pb^{2+} ions solution were 4.0 and 5.0, respectively. 0.25 g of the PLA/AC 5% wt. beads were added into 50 mL of Rhodamine B and Pb^{2+} ions solution. They were then continuously shaken. Solution samples of 1 mL were withdrawn at pre-determined time intervals using a syringe and analyzed for residual Rhodamine B and Pb^{2+} ions solutions by UV-Vis spectrophotometer at a wavelength of 554 nm and atomic absorption spectrophotometer, respectively. All experiments were carried out in triplicate to ensure statistical quality control and the values given are mean of these experimental results. The adsorption kinetic models of Rhodamine B and Pb^{2+} ions such as pseudo-first-order and pseudo-second-order kinetic models were fitted the kinetic data.

CHAPTER 3

RESULTS AND DISCUSSION

3.1 Preparation of PLA/AC beads

The optimum ratio of PLA and AC-powder for preparation the PLA/AC beads were studied. The composition of PLA and AC were listed in Table 1. In this research, the optimal weight ratio of PLA: AC is 19 : 1 for forming PLA/AC beads by phase inversion technique as shown in Table 2 and their photos are illustrated in Figure 7. The obtained PLA/AC beads were dried at 60 °C for 24 h. Their characterizations were investigated by scanning electron microscopy (SEM), surface area and pore size distribution (BET analysis), fourier-transform infrared spectrophotometry (FT-IR), elemental composition (C, H, N, O) analysis, energy dispersive x-ray spectroscopy (EDX) and point of zero charge measurements.

Table 1 Effect of the PLA concentration for PLA/AC beads form

PLA Solution (% wt./wt.)	AC (g)	The PLA/AC beads form
5	0.2	×
7	0.2	×
10	0.2	✓

Table 2 The effect of ratio of PLA solution and AC-powder for PLA/AC beads forming

PLA Solution (% wt./wt.)	PLA solution (g)	AC powder (g)	% wt. of AC	The PLA/AC bead form
10	19.8	0.2	1%	✓
	19.6	0.4	2%	✓
	19.4	0.6	3%	✓
	19.2	0.8	4%	✓
	19.0	1.0	5%	✓

Figure 7 The digital photo of PLA/AC beads

3.2 Characterization of PLA/AC beads

The different techniques that were used to characterize of PLA/AC bead were scanning electron microscopy (SEM), elemental composition (C, H, N, O) analysis, surface area and pore size distribution (BET analysis), fourier-transform infrared spectrophotometry (FT-IR) and point of zero charge measurements (pH_{pzc}).

3.2.1 Morphology of PLA/AC bead adsorbent from scanning electron microscopy (SEM technique)

SEM technique was employed to study the surface morphology of the PLA, PLA/AC 2% wt. and PLA/AC 5% wt. beads and the SEM images were displayed in Figure 8. It can be observed that SEM analysis presents differences in the surface morphology between PLA, PLA/AC 2% wt. and PLA/AC 5% wt. beads.

In this study, porous of PLA/AC beads were prepared by phase inversion technique from a solution mixture of PLA, AC and NMP. The exchange of NMP and water (non-solvent) evoked the formation of pores within the PLA beads. The results from SEM images that the spherical beads were formed with a diameter about 3 mm in all studied cases. Figure 8(a), (c) and (e) displayed the external surfaces and Figure 8(b), (d) and (f) showed the cross-sectional forms of PLA, PLA/AC 2% wt. and PLA/AC 5% wt. beads. All the adsorbent beads show numerous pores on the surface and therefore the pores present a highly inter-connected structure in the cross-sectional images. Moreover, an increased AC content in the PLA solution increased the porosity of the PLA/AC bead. This offered an advantageous condition for adsorption of Rhodamine B and Pb^{2+} ions from aqueous solution.

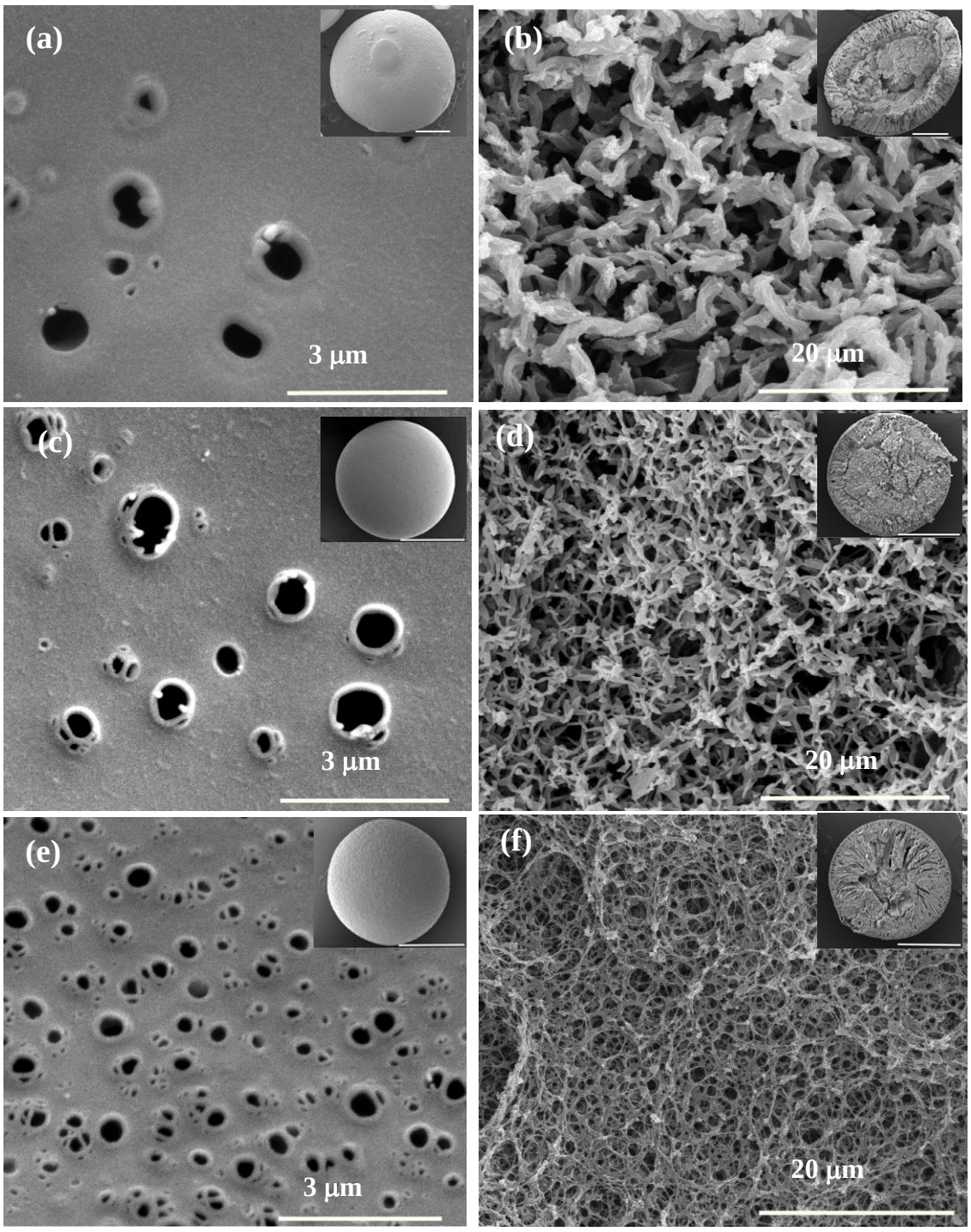

Figure 8 SEM images of external surface and cross-section of (a, b) PLA, (c, d) PLA/AC 2% wt. bead and (e, f) PLA/AC 5 % wt. bead.

3.2.2 Surface area and pore size distribution of PLA/AC bead

A comparison of characteristics of PLA/AC 2% wt. bead and PLA/AC 5% wt. bead was summarized in Table 3. The BET surface area of PLA/AC 5% wt. bead was 95.98 $m^2 g^{-1}$ and higher than PLA/AC 2% wt. bead (9.62 $m^2 g^{-1}$) as a result of the PLA/AC 5% wt. bead has the highest amount of AC, which is the optimum amount for bead formation.

By the construction of nitrogen adsorption isotherm, an understanding of the surface area and porosity of an adsorbent can be achieved. The adsorption volume of adsorbent was measured over a wide range of relative pressures at 77 K.

The PLA/AC 5% wt. bead had the highest adsorption capacity. Therefore, this adsorbent bead was chosen for structural analysis through the Brunauer-Emmett-Teller (BET) equation. Nitrogen adsorption isotherms measured for PLA/AC 5% wt. beads were shown in Figure 9. It is evident that all isotherms can be classified into six types. It can be seen that the adsorption-desorption isotherm of PLA/AC 5% wt. bead was classified according to IUPAC classification (Sing, et al., 1985) as a type IV adsorption isotherm. Moreover, type IV isotherms are assigned by several mesoporous industrial adsorbents (Kuila, et al., 2013).

It is well-known that the pores of adsorbents are usually classified into three groups, micropore (2 nm), mesopore (2 - 50 nm), and macropore (> 50 nm) (Juang, et al., 2002) using the Barrett, Joyner and Halenda (BJH) model, as shown in Figure 10, the pore diameter of the PLA/AC 5% wt. bead is in the range of 2 - 28 nm identified as mesopore and it has a comparatively narrow pore size distribution, with a mean pore diameter of 3.34 nm. Therefore, the mesoporous character of the PLA/AC 5% wt. bead adsorbent is confirmed by its IUPAC classification and also the BJH model.

Table 3 The surface characteristics of PLA/AC 2% wt. and PLA/AC 5% wt. beads

Sample	BET surface area (m^2 g^{-1})	Total pore volume (cm^3 g^{-1})	Average pore diameter (nm)
PLA/AC 2% wt. bead	9.62	0.02	6.89
PLA/AC 5% wt. bead	95.98	0.16	3.34

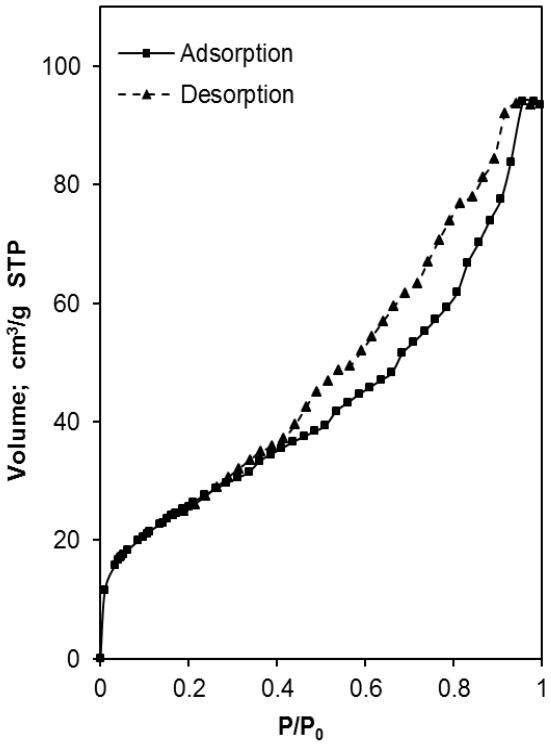

Figure 9 The adsorption – desorption isotherms of N_2 at 77 K for the PLA/AC 5% wt. bead.

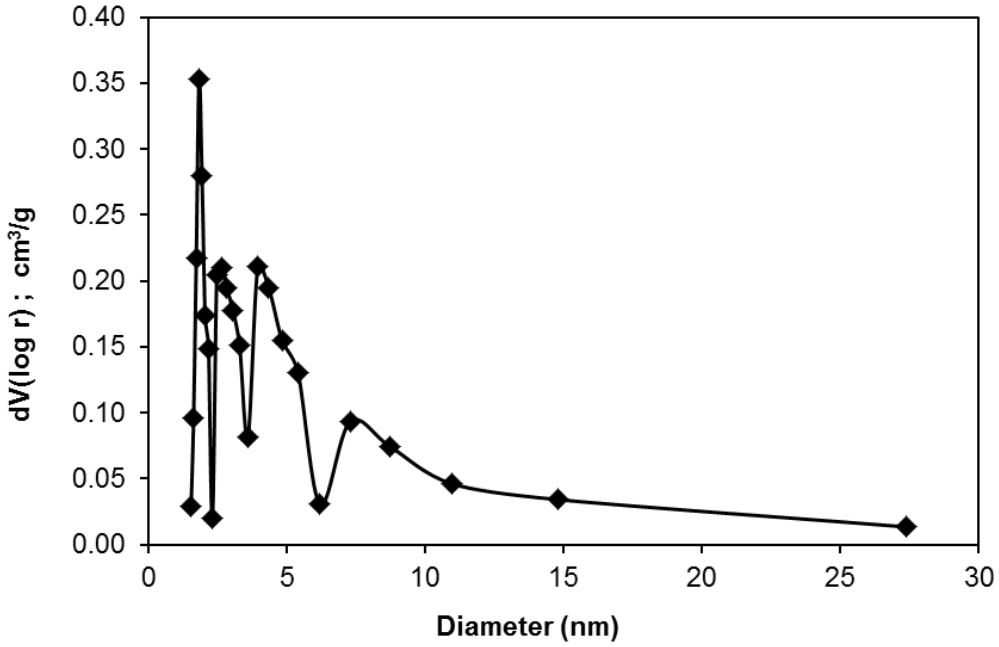

Figure 10 BJH pore size distribution of PLA/AC 5% wt. bead.

3.2.3 Elemental composition (C, H, N, O) analysis

The characteristic of PLA/AC 5% wt. was investigated to verify the elemental composition. Table 4 presents the element composition of the PLA/AC 5% wt. bead compared with that of the PLA bead. It is seen that PLA/AC leads to an increase in the carbon content of PLA bead. The carbon contents are found to be 48.93 % wt. and 57.96 % wt. for PLA and PLA/AC 5 % wt. bead, respectively.

Table 4 Elemental compositions of PLA and PLA/AC 5% wt. bead.

Sample	Elemental composition, wt%				
	C	H	N	O	Ash
PLA	48.93	4.63	0.02	41.70	4.72
PLA/AC 5% wt.	57.96	4.80	0.04	31.91	5.29

3.2.4 Fourier-transform infrared spectrophotometry (FT-IR)

The assignment of a specific wave number to given functional group is not possible although numerous FT-IR spectroscopic studies are conducted on numerous forms of carbon as a result of the characteristic bands of various functional groups overlap and shift, depending on their molecular structures and environments (Fuente, et al., 2003). All the same, a consensus in the assignment of band frequencies to different functional groups is possible to a certain extent.

Figure 11 shows the FT-IR spectrum of AC, PLA and PLA/AC 5% wt. bead. The FT-IR spectra of AC are shown in FT-IR spectrum, which resident functionalities including the band at about of 3,300 cm^{-1} is attributed to the hydrogen bonded O-H stretching vibration. The band at 1,700 cm^{-1} is associated with C=O stretching vibration of keto-carbonyl groups. The cellulose in AC can be characterized by the highest intensity band at 600 cm^{-1} which is attributed to C-O stretching vibration.

The specific functional groups of PLA were assigned as follows: at about the band at about of 3,200 cm^{-1} is attributed to the hydrogen bonded O-H stretching vibration and the C=O peaks in the 1,700 cm^{-1}. While aliphatic CH_3 and CH_2 deformation are present in the 1,500 - 1,100 cm^{-1} region, a high intensity broad band forms in the 1300 - 1000 cm^{-1} region which is attributed to C-O stretching vibrations. The peaks becoming apparent in the 900 - 750 cm^{-1} region relate to CH vibration (Stuart, 2004). Moreover, the FT-IR spectra of PLA and PLA/AC 5% wt. bead are very similar. It shows that the addition of AC to have a little blue shifted on the change of functional groups of PLA.

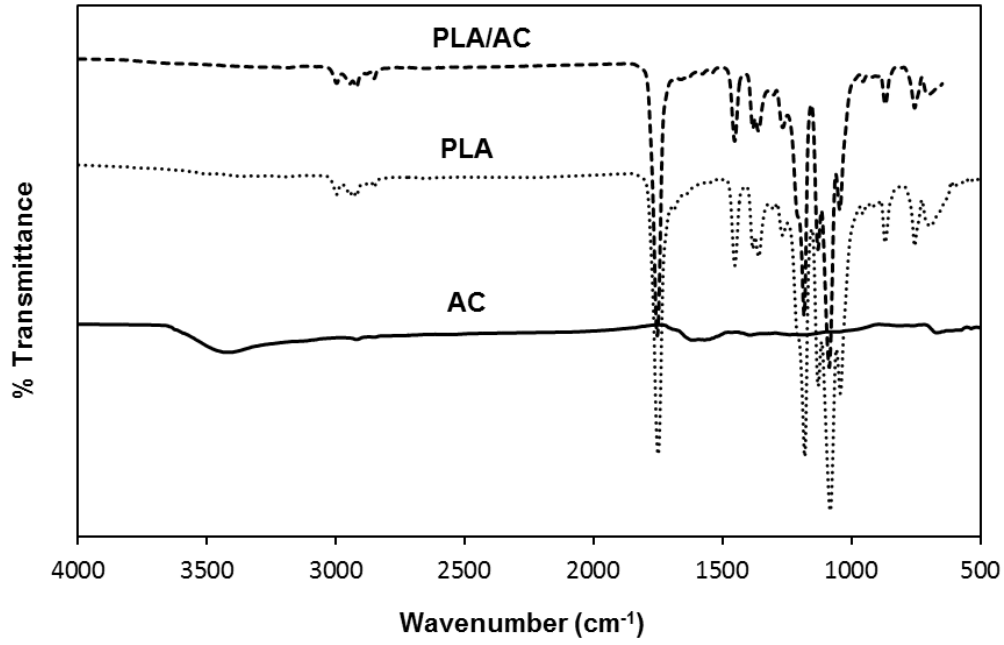

Figure 11 FT-IR spectra of PLA, AC and PLA/AC 5% wt. bead.

3.2.5 Point of zero charge measurements (pH_{pzc})

In Figure 12, the graph of final versus initial pH obtained by using pH drift method (Jia, et al., 2002) for PLA/AC 5% wt. beads. The results show that pH_{pzc} of PLA/AC 5% wt. bead is 3.5 indicating the PLA/AC 5% wt. bead has acidic surface in nature. The graph of final pH (pH_f) versus initial pH (pH_0) is employed to determine the point at that initial pH and final pH values are equal. This point is taken as the pH_{pzc} of the beads.

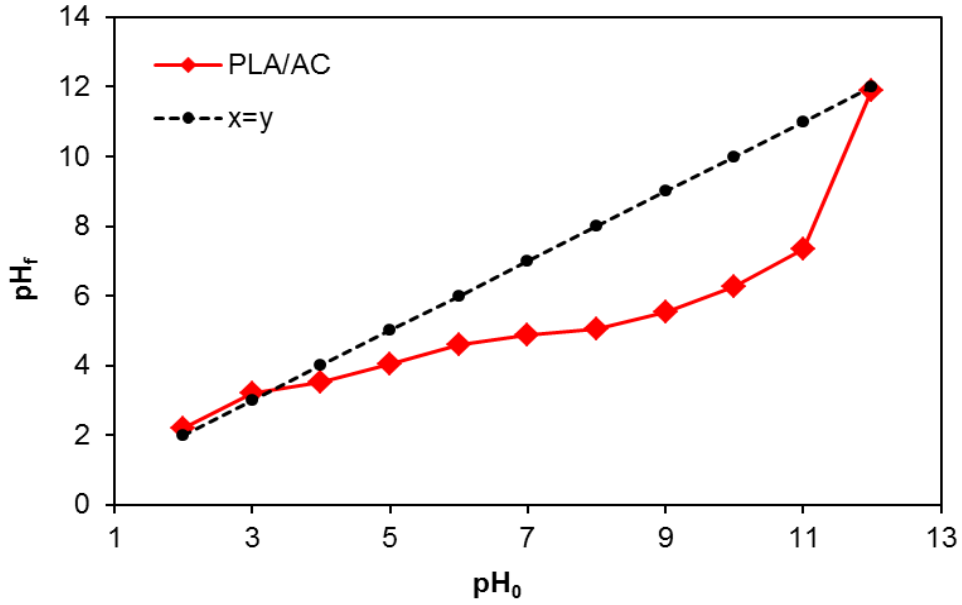

Figure 12 Graphs of final pH versus initial pH for determination the point of zero charge (pH_{pzc}) of PLA/AC 5% wt. beads.

The amphoteric character of surface oxides S-CO_2 where S represents the carbon surface can be explained as follows (Kadirtvalu, et al., 2000).

For pH < pH_{pzc}, the dominant reaction is:

$$S\text{-}CO_2 + 2H_2O \longleftrightarrow S\text{-}C\,(OH^+)_2 + 2OH^-$$

The release of hydroxyl ions induces an increase of pH and a protonated surface of the carbon materials.

For pH > pH_{pzc}, the following reaction takes place:

$$S\text{-}CO_2 + 2H_2O \longleftrightarrow S\text{-}C(O^-)_2 + 2H_3O^+$$

The carbon surface is deprotonated and the release of protons induces a decrease in pH.

The pH and acid-base values of the carbon materials provide good indication of the surface oxygen complexes and the electrical surface changes which

were undergone by them. These surface changes arise from the interaction between the carbon surface and the aqueous solution. The complexes on the carbon surfaces are generally classified as acidic, basic, and neutral groups.

3.3 Adsorption studies

3.3.1 Rhodamine B adsorption on PLA/AC 5% wt. beads

3.3.1.1 The effect of AC content in PLA solution in forming beads for Rhodamine B sorption

The different dosages of AC content in the 0, 1, 2, 3, 4 and 5 % wt. were studied in the presence of 100 mg L^{-1} of Rhodamine B at pH 4 as shown in Figure 13. The results indicated that the percentage of adsorbed dye increased with increasing AC content owing to the availability of more adsorption sites and also the increment of surface area of AC. When the PLA solution contained AC 5 % wt., the highest percentage sorption and Rhodamine B adsorbed per gram of PLA/AC beads at equilibrium were 88.99 % and 35.69 mg g^{-1}, respectively. This indicated that an increment of q_e value may be due to the adsorbent having a very large surface area and plenty of adsorption sites; thus a small increase in the quantity of adsorbent provided much greater surface areas to adsorb large numbers of Rhodamine B molecules (Senthilkumaar, et al., 2011). The number of adsorption sites relied on the dose of AC in PLA/AC beads. However, 5% wt. of AC was highest AC content employed in the preparation of PLA/AC beads; any further increase in the weight percent of AC content more than 5% wt. could not make the bead form.

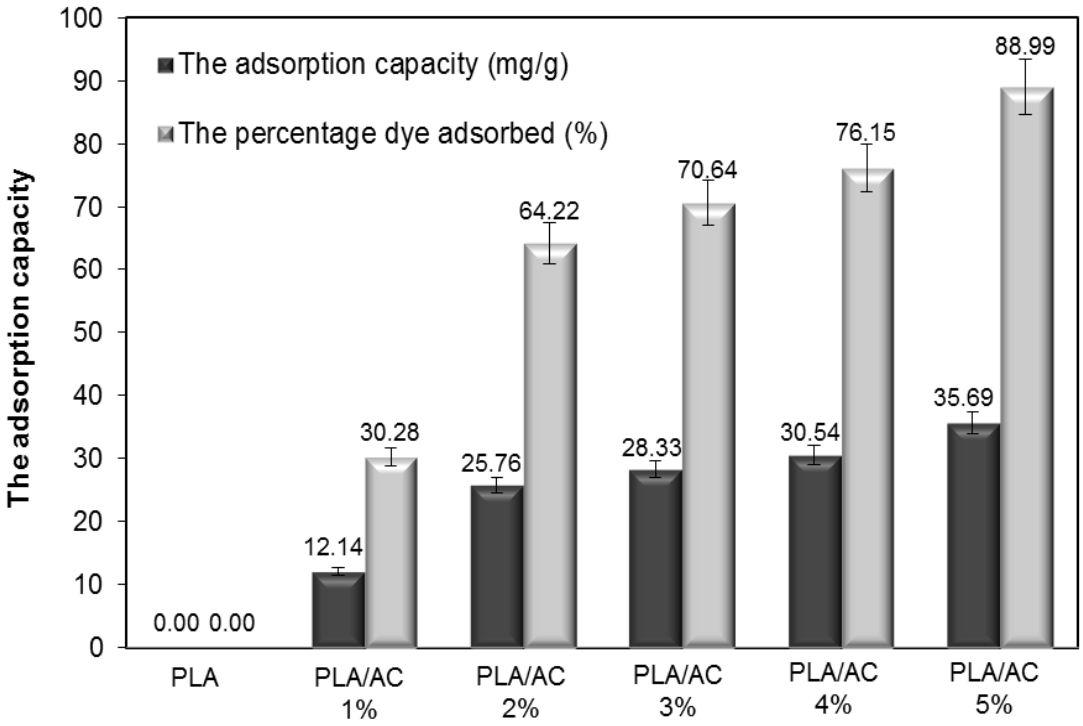

Figure 13 Effect of AC content (0, 1, 2, 3, 4 and 5% wt.) added into PLA solution in forming beads for 100 mg L^{-1} of Rhodamine B adsorption at equilibrium.

The amount of Rhodamine B adsorbed by the PLA/AC beads was calculated after these beads were successfully prepared via phase inversion technique and also a corresponding variation of factors such as contact time, pH, temperature and PLA/AC dose was noted. The total amount of Rhodamine B adsorbed in each of these factors was recorded.

3.3.1.2 Effects of contact time and initial Rhodamine B concentration

The effects of contact time and initial Rhodamine B concentration were studied at three different initial concentrations of 50, 100 and 200 mg L^{-1} for Rhodamine B are shown in Figure 14. The results showed that the rate of uptake of Rhodamine B was quite fast in the first period and 50% of the entire uptake occurred in 3 h as a result within the first period the PLA/AC 5% wt. beads were exposed to high concentrations of molecules of Rhodamine B at the greatest number of

adsorption sites of AC. A slower rate of uptake was observed after 3 h until 39 h that no more significant adsorption was observed because the AC in the PLA/AC 5% wt. beads had no more available adsorption sites for Rhodamine B molecules. Thus, the equilibrium time for Rhodamine B sorption was around 39 h, which is not too long a time, at 30°C, pH 4 and a bead dosage of 0.25 g. Furthermore, Figure 14 also shows the effect of Rhodamine B concentration on adsorption and the results show an increment in the amount adsorbed because the initial concentration of Rhodamine B is increased. It was found that the adsorption capacity, q_e increase with an increase the initial Rhodamine B concentration due to the increase in initial dye concentration enhanced the interaction between Rhodamine B and PLA/AC 5% wt. beads (Thakur, et al., 2017).

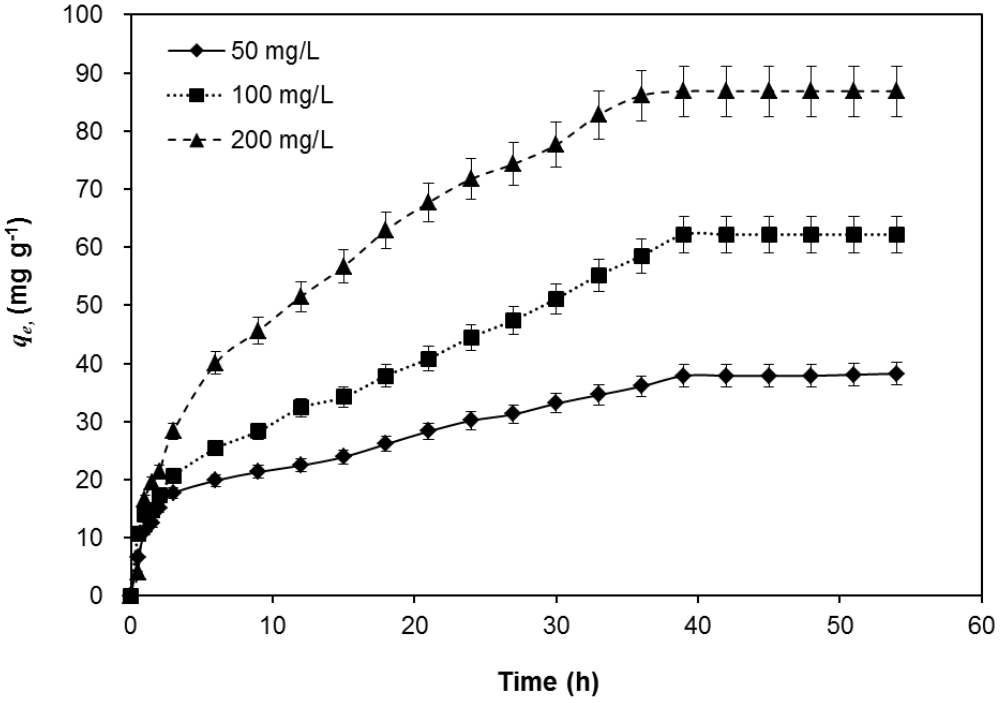

Figure 14 Effect of equilibrium time and initial Rhodamine B concentration (50, 100 and 200 mg L^{-1}) adsorbed on PLA/AC 5% wt. beads (0.25 g) at 30°C and pH = 4.

3.3.1.3 Kinetics of adsorption

The experiments of kinetics of adsorption were studied at three different initial concentrations of 50, 100 and 200 mgL^{-1} for Rhodamine B. The non-linearity of kinetic models were plotted by the Origin Pro 8.1 program. The pseudo-second-order model yielded better than the plot of pseudo-first-order model due to the greater values of the correlation coefficients, R^2. Figure 15 presents the pseudo-second-order kinetic model for the adsorption of Rhodamine B on PLA/AC 5% wt. beads. All the kinetic parameters of pseudo-first-order, pseudo-second-order models including the correlation coefficients, R^2, are presented in Table 5. The pseudo-second-order rate constant values, k_2, were 1.48, 1.89 and 7.34 g mg^{-1} min^{-1} for 50, 100 and 200 mg L^{-1}, respectively.

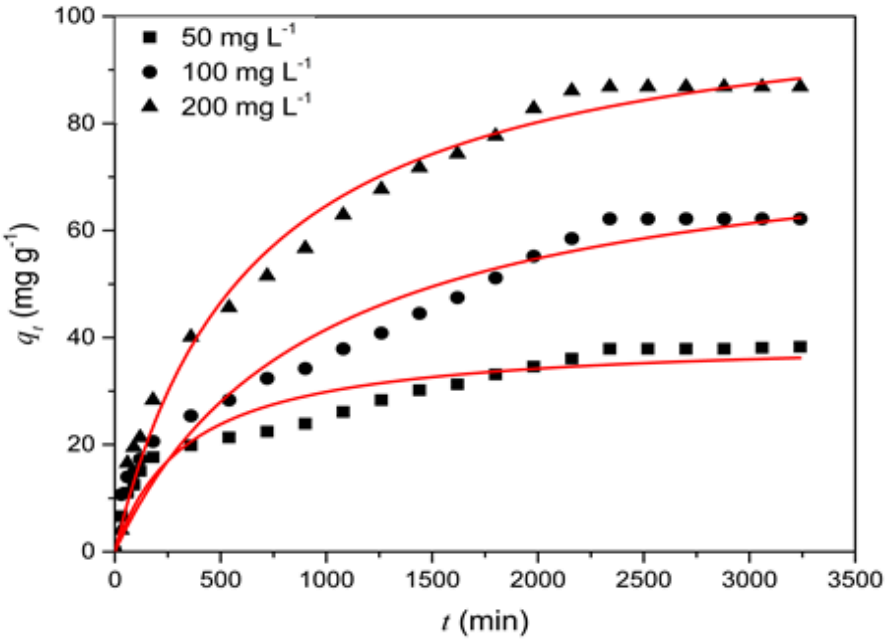

Figure 15 The pseudo-second-order adsorption kinetic model for the adsorption of Rhodamine B (50, 100 and 200 mg L^{-1}) on PLA/AC 5% wt. beads (0.25 g) at 30°C and pH = 4.

Table 5 Kinetic parameters for the pseudo-first-order, the pseudo-second-order models with various initial concentrations of Rhodamine B (50, 100 and 200 mg L^{-1}) at 30 ºC, PLA/AC 5% wt. beads dose 0.25 g, pH = 4.0.

C_0 (mg L^{-1})	q_e (exp) (mg g^{-1})	Pseudo-first-order			Pseudo-second-order		
		q_e (mg g^{-1})	k_1 ($\times 10^{-3}$) (min^{-1})	R^2	q_e (mg g^{-1})	k_2 (g mg^{-1} min^{-1})	R^2
50	37.90	47.89	1.40	0.921	40.02	7.34	0.981
100	62.19	56.37	1.10	0.913	70.47	1.89	0.982
200	86.85	77.81	1.30	0.959	105.77	1.48	0.999

It is known that the adsorption process for porous materials can be separated into three stages: (1) the external surface adsorption, (2) the gradual adsorption stage wherever the intraparticle diffusion is rate controlled onto sites, and (3) the interior surface adsorption that is the final equilibrium stage (Wu, et al., 2009, Cheung, et al., 2007). The possibility of intraparticle diffusion was explored by using the intraparticle diffusion model (equation 9) and the intraparticle diffusion rate constant value, k_P which can be evaluated from the slope of the linear plot between q_t and $t^{1/2}$as shown in Figure 16 and Table 6.

The intraparticle diffusion model gave the best fit because the values of the correlation coefficient, R^2 were closest to one. The intraparticle diffusion rate constants, k_P, were 1.00, 1.09 and 1.61 mg g^{-1} $min^{-1/2}$ for 50, 100 and 200 mg L^{-1} of Rhodamine B concentration, respectively. In addition, the R_i values from the intraparticle diffusion model of PLA/AC 5% wt. beads were 0.82, 0.94 and 0.98 for Rhodamine B concentration 50, 100 and 200 mg L^{-1}, respectively. The R_i values $0.9 < R_i < 1.0$ for 100 and 200 mg L^{-1} of Rhodamine B were known as zone 1 indicated the weak initial adsorption which is the high initial result in low external mass transfer and low initial uptake rates. For 50 mg L^{-1} of Rhodamine B, the R_i value $0.5 < R_i <$

0.9 was called zone 2 intermediate initial adsorption that is the high initial result in high external mass transfer and high initial uptake rates.

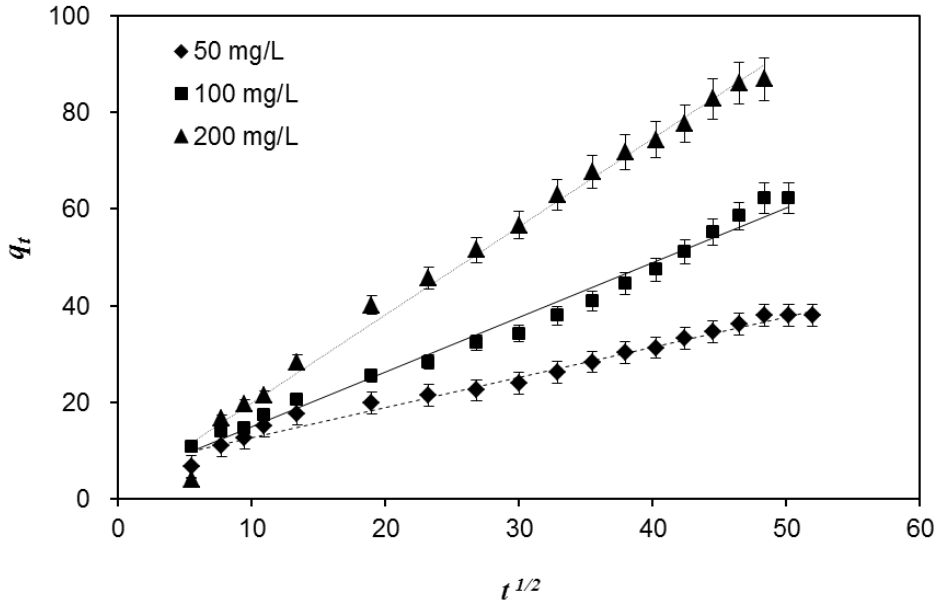

Figure 16 The intraparticle diffusion model for the adsorption of Rhodamine B on PLA/AC 5% wt. beads (0.25 g) at 30°C and pH = 4.

Table 6 The intraparticle diffusion parameters of Rhodamine B adsorption on PLA/AC 5% wt. beads at different initial concentrations at 30 ºC, PLA/AC 5% wt. bead dose 0.25 g, and pH = 4.

C_0 (mg L^{-1})	q_e (exp) (mg g^{-1})	Intraparticle diffusion		
		k_p (mg g^{-1} $min^{-1/2}$)	R^2	R_i
50	37.90	1.00	1.000	0.82
100	62.19	1.09	0.985	0.94
200	86.85	1.61	0.967	0.98

3.3.1.4 Effect of pH on Rhodamine B uptake by PLA/AC 5% wt. bead

The pH value of Rhodamine B solution is necessary when considering the ionic states of the surface of the PLA/AC 5% wt. beads. The experiments were conducted at varied final pH values in the range 2.05 – 11.04 of the PLA/AC 5% wt. beads. It can be seen from Figure 17, that the adsorption capacity, q_e of adsorbent increases with increased pH of the solution. The sharpest increase in q_e is observed between pH 4 and 5. These results indicate the suitability for using the PLA/AC 5% wt. beads in treatment of acidic wastewater. At lower pH values than pH_{pzc} (3.5), the high concentration of H^+ ions promotes the protonation of the functional groups of AC in the PLA/AC 5% wt. beads. The higher overall positive charge results in repulsion of the positive charge of Rhodamine B. At low pH values, the H^+ ions compete with Rhodamine B for the adsorption sites (Kobya, et al., 2005). However, at pH value less than pK_a of Rhodamine B (pK_a = 4.2) assisted the binding process of Rhodamine B to PLA/AC 5% wt. beads was promoted as a results of the generation of hydrogen bond between carboxylic group of Rhodamine B and PLA/AC 5% wt. beads (Zhang, et al., 2011). At pH of Rhodamine B exceeding 4 that is higher than pH_{pzc}(3.5), the PLA/AC 5% wt. beads surfaces tend to become negatively charged, thus as Rhodamine B is a cationic dye, the adsorption was improved by electrostatic attraction (Rais, et al., 2010). Moreover, the results showed that pH_{pzc} was additional affected than pK_a for Rhodamine B adsorption on PLA/AC 5% wt. beads.

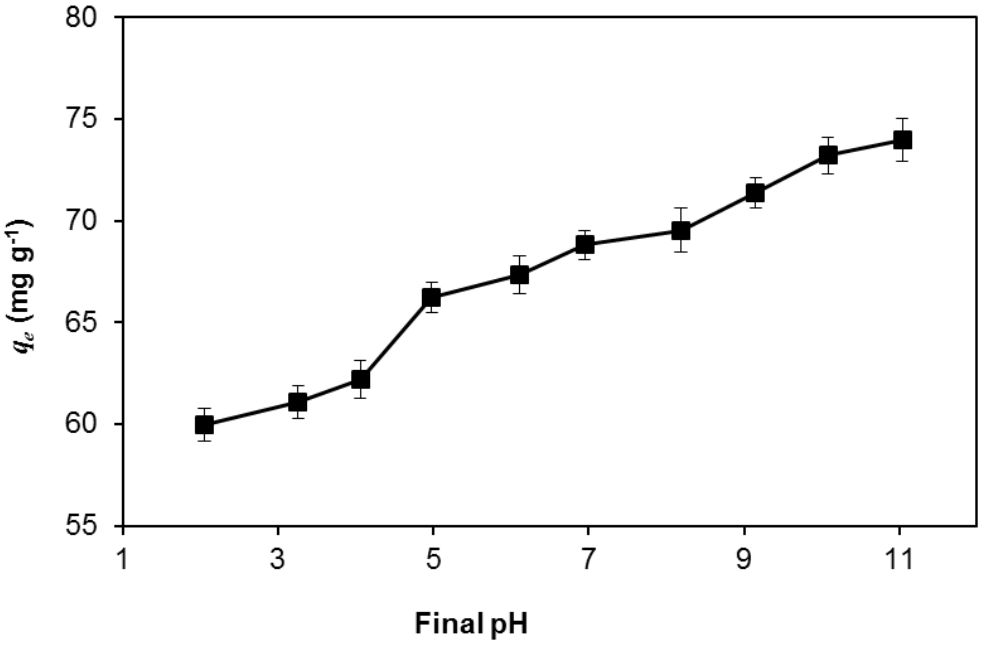

Figure 17 Adsorption of Rhodamine B (100 mg L^{-1}) on PLA/AC 5% wt. beads with pH range 2.05 – 11.04.

3.3.1.5 Effect of PLA/AC 5% wt. bead dosage on equilibrium Rhodamine B adsorption

To study the effect of PLA/AC 5% wt. beads dosage on the removal of 100 mg L^{-1} Rhodamine B, we used dosages of PLA/AC 5% wt. beads from 0.10 g to 0.50 g. The results in Figure 18 showed that the percentage sorption of Rhodamine B at equilibrium increases with increased dosages of PLA/AC 5% wt. beads. After 0.25 g of PLA/AC 5% wt. beads, the percentage of Rhodamine B adsorption slightly increases. This result may be due to after the certain dose of PLA/AC 5% wt. beads, the maximum adsorption capacity was reached and the amount of Rhodamine B molecule bound to the adsorbent and the amount of free dye molecule remains constant even with further addition of the dose of beads (Hayeeye, et al.,2017). The percentage of Rhodamine B adsorption and the highest adsorption capacity, q_e at equilibrium were 77.52% and 62.19 mg g^{-1}, respectively obtained from 0.25 g of PLA/AC 5% wt. beads. This dosage was here considered to be the optimum level as

also the time to reach equilibrium was short, which was desirable in industrial applications (Jamal, et al., 2013).

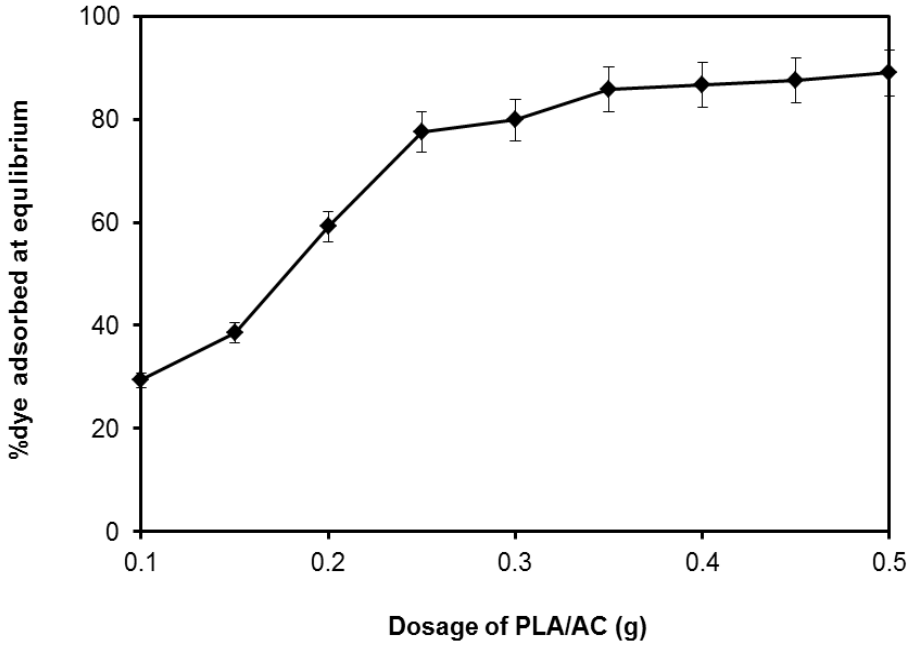

Figure 18 Effect of PLA/AC 5% wt. beads dosage, 0.1– 0.5 g/50 mL for Rhodamine B sorption at 30°C, pH = 4 and 100 mg L^{-1} of initial dye concentration.

3.3.1.6 Adsorption isotherms of Rhodamine B on PLA/AC 5% wt. beads

Figure 19 shows the best fit of non-linear adsorption isotherms of PLA/AC 5% wt. beads for Rhodamine B in the aqueous phase under the conditions at equilibrium time of 39 h, 30°C, pH 4.0, and PLA/AC 5% wt. beads dosage of 0.25 g. The adsorption isotherm plots have a typical shape of L isotherms (Limousin, et al., 2005), indicating a reduction in the number of active sites on the beads at a high residual Rhodamine B concentration in the solution phase. In addition, it shows the effect of temperature (30 - 60 °C) on the adsorption capacity of PLA/AC 5% wt. beads which increases with a rise in the temperature of adsorption as results of the Rhodamine B molecules have high kinetic energy at high temperatures. Thus, Rhodamine B molecules were speedily adsorbed onto the PLA/AC 5% wt. beads.

This result recommended that Rhodamine B adsorption on the PLA/AC 5% wt. beads was an endothermic adsorption process.

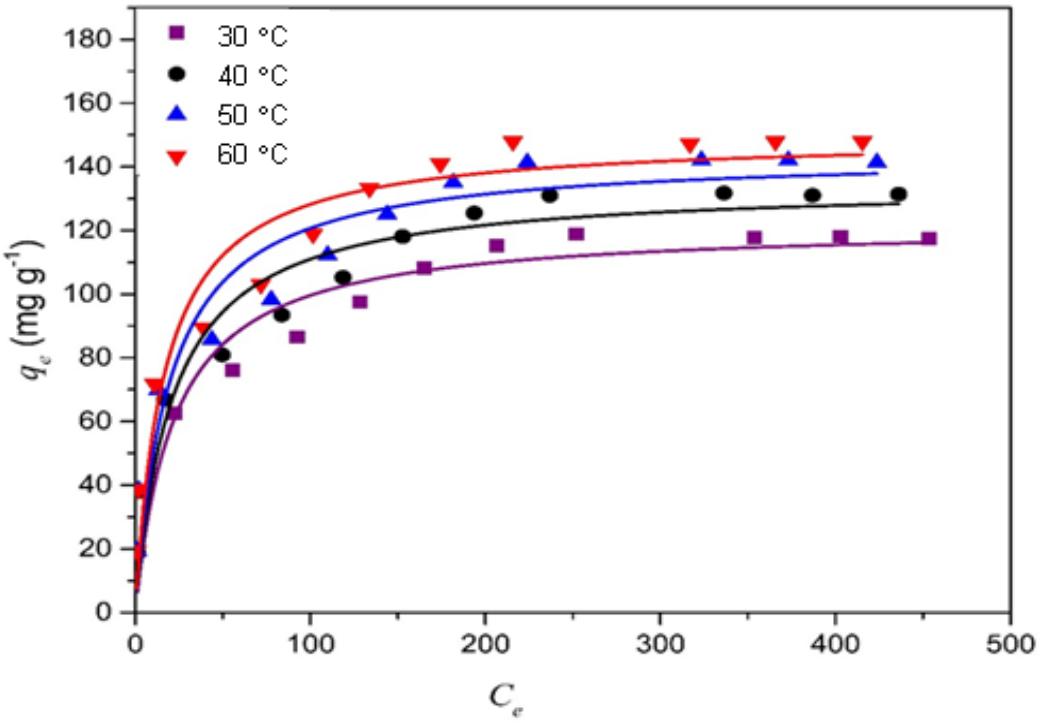

Figure 19 The non-linear plot of Langmuir adsorption isotherm of Rhodamine B on PLA/AC 5% wt. beads at different temperatures, dye concentrations 50 – 600 mg L^{-1}, pH = 4.

Two well-known phenomenological equations could be applied Langmuir and Freundlich equations. Figure 20 are displayed the non-linearity of Langmuir adsorption isotherms of Rhodamine B on PLA/AC 5% wt. beads at 30, 40, 50 and 60°C and pH 4. The best fit is obtained by the Langmuir model which has the greater values of correlation coefficient, R^2 than Freundlich model. The parameters of Langmuir and Freundlich adsorption isotherms are displayed in Tables 7.

Table 7 Parameters of the Langmuir and the Freundlich models for Rhodamine B adsorption by PLA/AC 5% wt. beads (0.25 g) at various temperatures, pH = 4.

Temp (°C)	Langmuir			Freundlich		
	q_m (mg g^{-1})	b (L mg^{-1})	R^2	K_F (mg g^{-1})	n	R^2
30	121.93	0.04	0.995	22.88	3.40	0.958
40	134.64	0.05	0.995	23.80	3.24	0.958
50	144.20	0.05	0.992	25.69	3.22	0.956
60	149.57	0.06	0.996	27.31	3.29	0.953

The maximum adsorption capacity (q_m) by PLA/AC 5% wt. beads for Rhodamine B, as determined from the Langmuir model fit to the data, was 149.57 mg g^{-1}, that is better than that various reported adsorbents as shown in Table 8.

Even, some adsorbents such as gelatin/activated carbon composite bead (GE/AC 10% wt. beads) (Hayeeye, et al., 2017) and activated carbon (LSAC) and pyruvic acid (PA)-modified activated carbons (PA-LSAC and LSAC-PA) (Namasivayam, et al., 2016) have the maximum adsorption capacity higher than PLA/AC 5% wt. beads but the method of preparation of PLA/AC beads were easier than GE/AC beads. GE/AC beads were prepared under controlling temperature while PLA/AC beads were prepared at ambient temperature. Moreover, the preparation of PLA/AC 5% wt. beads forming was easier and faster than that of GE/AC 10% wt. beads and the amount of AC content in GE/AC 10% wt. beads was higher than PLA/AC 5% wt. beads. For LSAC, PA-LSAC and LSAC-PA are AC-powder which shows usually higher adsorption capacity than granular AC such as PLA/AC 5% wt. beads. However, the aim of this work is to resolve the difficulty of usages of AC-powder.

Table 8 Maximum Rhodamine B adsorption capacities compared with other adsorbents reported in the literature. ,

No	Adsorbent	*pH*	q_m (mg g^{-1})	*Ref.*
1.	Anaerobic sludge biosorbent	7.0	19.52	Wang, et al., 2006
2.	Sodium montmorillonite	7.0	42.12	Selvama, et al., 2008
3.	Natural adsorbent perlite	7.0	55.31	Vijayakumar, et al., 2012
4.	Activated carbon prepared from pericarp of rubber fruit	4.0	110.46	Hayeeye, et al. 2014
5.	Waste of seeds of *Aleurites Moluccana*	6.0	117.01	Postai, et al., 2016
6.	Granular activated carbon from black tea leaves	2.0	53.2	Mohammad, et al., 2012
7.	Oil palm empty fruit brunch granular activated carbon	9.0	69.86	Manase, et al., 2012
8	Gelatin/activated carbon composite (GE/AC 10% wt.)	4.0	256.41	Hayeeye, et al., 2017
9.	Activated carbon prepared from walnut shell	9.0	18.70	Sumanjit, et al. 2008
10.	Activated carbon (LSAC) and pyruvic acid (PA)-modified activated carbons (PA-LSAC and LSAC-PA)	3.8	370.37, 384.62, 333.33 (LSAC, PA-LSAC, LSAC-PA)	Namasivayam, et al., 2016
11.	Acid activated mango (*Magnifera indica*) leaf powder	7.0	3.31	Khan, et al., 2011
12.	Activated carbon prepared from the steel and fertilizer industries	5.5	91.1	Bhatnagar, et al., 2005
13.	*Thespusia populinia* bark	7.0	77.18	Hema, et al., 2009
14.	Activated carbon prepared from Acacia nilotica leaves	6.0	33.00	Prasad, et al., 2012
15.	Zinc oxide loaded activated carbon (ZnO-AC)	7.0	128.21	Saini, et al., 2017
16.	Baryte	7.0	137.17	Vijayakumar, et al., 2010

17.	Formaldehyde treated parthenium carbon(WC) and phosphoric acid treated parthenium carbon(PWC)	7.0	28.82, 59.17 (WC, PWC)	Hem, et al., 2009
18.	Jute stick powder	7.0	87.70	Panda, et al., 2009
19.	Polysulfone/activated carbon composite (PSF/AC 2% wt.)	4.0	25.71	Sattar, et al., 2014
20.	Polylacic acid/activated carbon composite bead (PLA/AC 5% wt.)	4.0	149.57	**This study**

3.3.1.7 Thermodynamic studies

The van't Hoff plot for adsorption of Rhodamine B on PLA/AC 5% wt. beads at different temperatures (30, 40, 50 and 60 ºC), 100 mg L^{-1} of Rhodamine B concentrations and pH = 4.0 is shown in Figure 20. The graph was plotted between ln K_c and 1/T that K_c was the ratio of C_A and C_e. The enthalpy change ($\Delta H°$) and entropy change (ΔS°) were calculated from slope and intercept. Moreover, the Gibb's free energy ($\Delta G°$) resolves from equation (15). These thermodynamic parameters will be used for explanation of the practicalities and nature of the adsorption process. The results given in Table 9 indicate that the negative value of ΔG° at all temperatures confirms the thermodynamic feasibility and spontaneity of the Rhodamine B adsorption process onto the PLA/AC 5% wt. beads. The endothermic adsorption process is verified by the positive value of ΔH° (23.92 kJ mol^{-1}). The positive value of ΔS° was 0.089 kJ $mol^{-1}K^{-1}$ which suggests that the degree of randomness at the solid-liquid interface increases throughout adsorption of Rhodamine B onto the PLA/AC 5% wt. beads (Umar, et al., 2015).

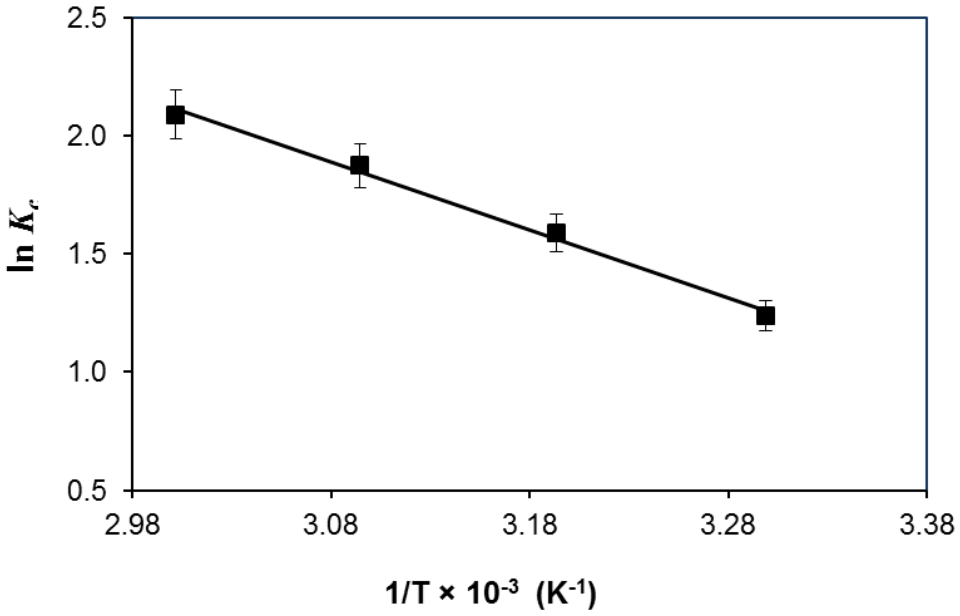

Figure 20 The van't Hoff plot for adsorption of Rhodamine B on PLA/AC 5% wt. beads at 30 ºC, 40 ºC, 50 ºC and 60 ºC, dye concentration 100 mg L^{-1} and pH = 4.

Table 9 The thermodynamic parameters for Rhodamine B sorption by PLA/AC 5% wt. beads (0.25 g), from initial dye concentration 100 mg L^{-1} at pH = 4.

T(K)	$-\Delta G^\circ$ (kJ mol^{-1})	ΔS° (kJ $mol^{-1}K^{-1}$)	ΔH° (kJ mol^{-1})
303	3.12	0.089	23.92
313	4.13		
323	5.04		
333	5.79		

3.3.1.8 Characterizations of PLA/AC 5% wt. beads after Rhodamine B adsorption

Elemental composition (C, H, N and O) analysis

The elemental composition (C, H, N and O) analyses of PLA/AC 5% wt. bead before and after adsorption of Rhodamine B (PLA/AC RB) were investigated as shown in Table 10. It can be seen that the percentage of nitrogen in PLA/AC RB had increased from 0.04 % for PLA/AC 5%wt. beads to 1.36% for PLA/AC RB. This results were confirmed the Rhodamine B sorption on PLA/AC 5% wt. beads.

Table 10 Elemental compositions of PLA/AC 5% wt. bead and PLA/AC RB.

The adsorbent	Elemental composition, wt%			
	C	H	N	O
PLA/AC 5% wt. bead	57.96	4.80	0.04	31.91
PLA/AC RB	56.31	4.95	1.36	31.18

Fourier-transform infrared spectrophotometry (FT-IR)

The PLA/AC 5% wt. bead, Rhodamine B and PLA/AC RB were characterized by FT-IR spectroscopy to obtain the evidence of Rhodamine B adsorption on PLA/AC as shown in Figure 21. The PLA/AC 5% wt. bead absorbed at 1,758.94 cm^{-1} (C=O stretching in esters), 1,461.93 cm^{-1}, 1,390.57 cm^{-1} (-CH stretching in CH_3), 1,188.06 cm^{-1}, 1,095.48 cm^{-1} (C-O stretching) and 881.40 cm^{-1}, 767.61 cm^{-1} (-CH stretching in CH_2). The particular functional groups of Rhodamine B were assigned as follows: the band at about 3,483.26 cm^{-1} (-OH stretching), 2991.44 cm^{-1} (C-H stretching), 2,347.24 cm^{-1} - 1,487.04 cm^{-1} (-CH stretching in aromatic) 1,710.77 cm^{-1}(C=O stretching in carboxylic acid), 1,600.83 cm^{-1} (C=C stretching in aromatic) 1278.73 cm^{-1}(C-C stretching in aromatic), 1055.01 cm^{-1} (C-N stretching), 690.48 cm^{-1} (-OH stretching) (Stuart, 2004). After Rhodamine B adsorption, the band at 690.48 cm^{-1} shifted to 709.75 cm^{-1} which attributed to the

hydrogen bonding between the –COOH group of Rhodamine B and the PLA/AC 5% wt. bead. This result provided a proof of Rhodamine B adsorption on PLA/AC 5% wt. bead.

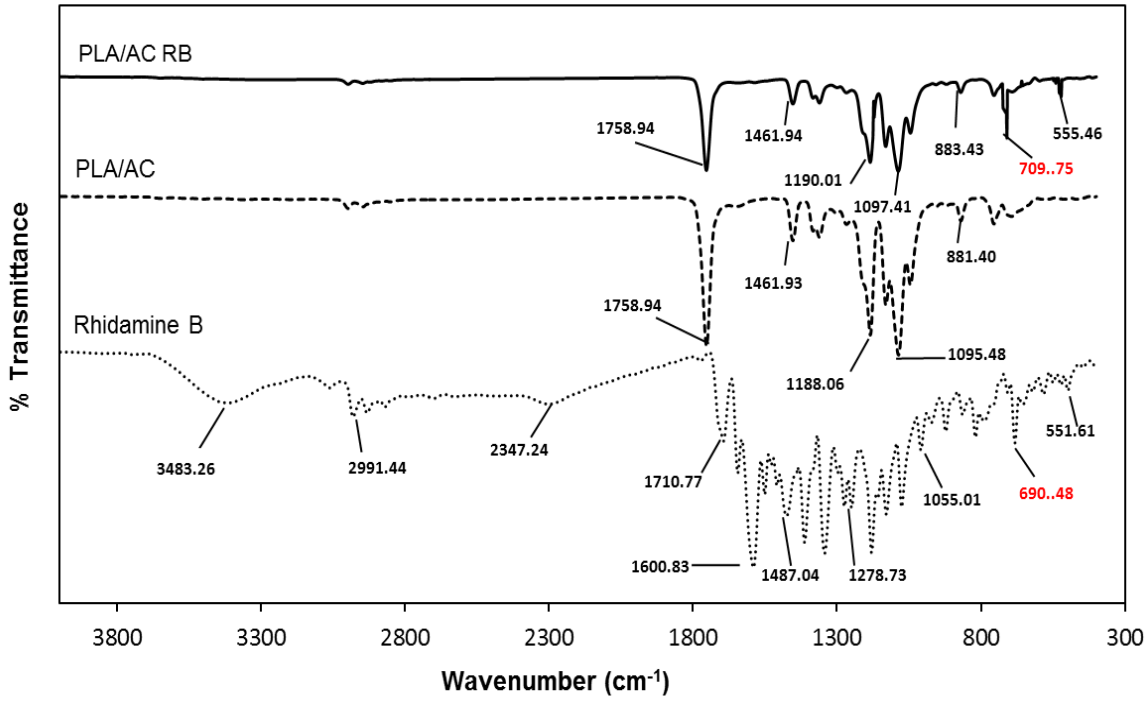

Figure 21 FT-IR spectra of PLA/AC 5% wt. bead, Rhodamine B and PLA/AC RB.

3.3.1.9 Desorption studies

The percentage of desorbed Rhodamine B solution decreased from 46.81 to 26.27 with increase in pH from 1.93 to 10.98 as shown in Figure 22. The trend in the desorption process at pH 1.93 – 10.98 was just opposite to the adsorption process as a result of the effect of pH (Figure 17). This indicates that the dye adsorption is mainly as a result of physical adsorption and our adsorbent can be recovered which may make the treatment process economically (Namasivayam, et al., 2001).

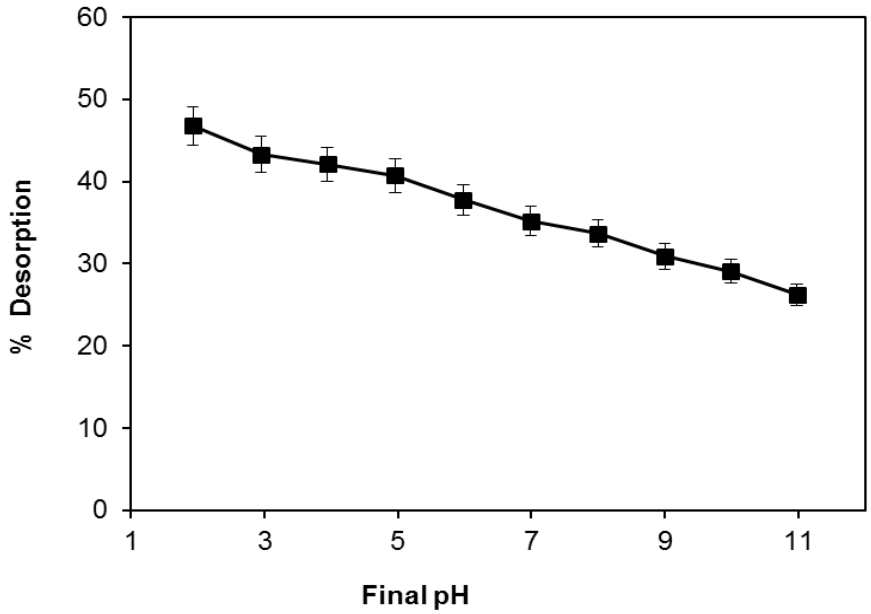

Figure 22 The desorption of Rhodamine B on PLA/AC 5% wt. beads with various pH (1.93– 10.98) at 30 ºC, dye concentrations 100 mg L^{-1} and PLA/AC 5% wt. dose 0.25 g.

3.3.2 Pb^{2+} ions adsorption on PLA/AC 5% wt. beads

3.3.2.1 Effects of contact time and initial Pb^{2+} ions concentration

The time to reach the equilibrium is necessary to know about kinetic adsorption study (Yi, et al., 2003). The adsorbed amount at time, *t* (q_t) was used to verify the kinetic models. The graph plotted on q_t and *t* for all the three different initial Pb^{2+} ions concentrations (50, 300, and 500 mg L^{-1}) at 23±2 °C, pH 5.0 and dosage of 0.25 g of PLA/AC 5% wt. beads are illustrated in Figure 23. The result showed that Pb^{2+} ions sorption capacity increased by increasing Pb^{2+} ions concentration. However, the various initial concentrations were not effect to equilibrium time. It was found that the uptake equilibrium of Pb^{2+} ions on PLA/AC beads was achieved after 60 min and no remarkable changes appeared for longer time. As expected, the adsorbed amount increased with initial Pb^{2+} ions concentration. The

shapes of the curves representing Pb^{2+} ions uptake versus time suggested two adsorption steps. The first step occurring throughout the first 30 min indicated a fast adsorption after which equilibrium was slowly achieved. The maximum percentages of Pb^{2+} ions removal for 50, 300 and 500 mg $L^{-1}$of initial Pb^{2+} concentrations were 83.85, 78.79 and 71.77 % at 60 min intervals, respectively. Consequently, 180 min was chosen to ensure the equilibrium in the kinetic studies and determine of the adsorption isotherms.

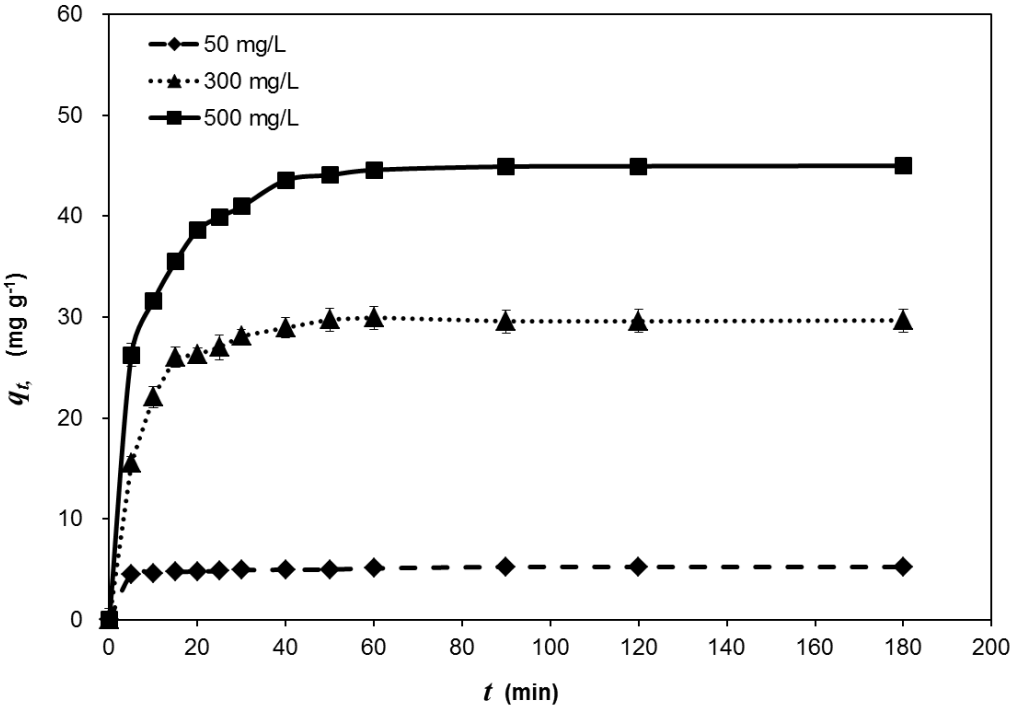

Figure 23 Effect of contact time of Pb^{2+} ions adsorption onto PLA/AC 5% wt. beads at 50, 300 and 500 mg L^{-1} of Pb^{2+} ions concentration. PLA/AC dose 0.25 g/ 50 mL, temperature 23±2°C and pH = 5.

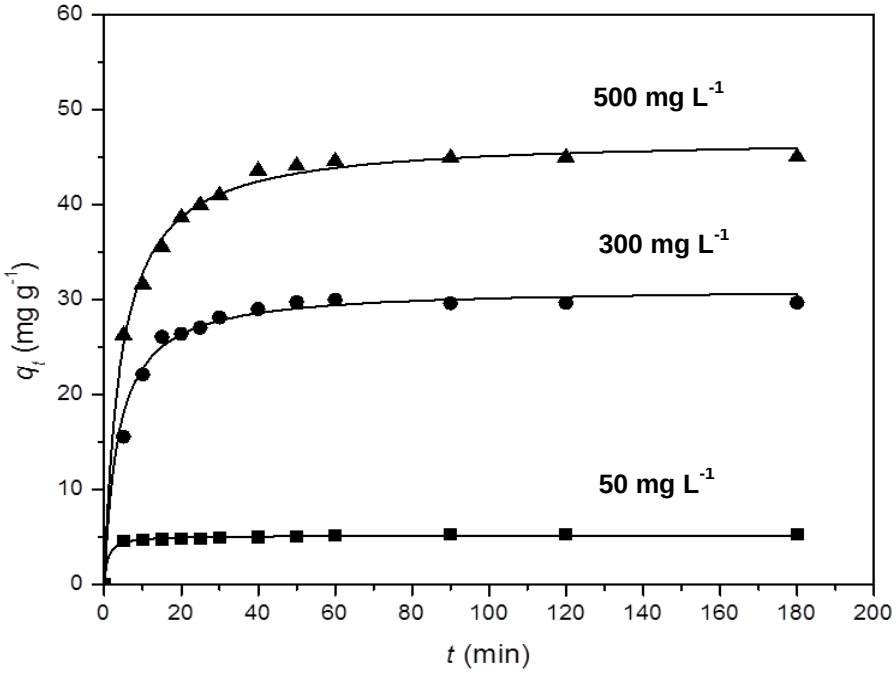

Figure 24 The non-linear plots of pseudo-second-order model for Pb^{2+} ions adsorption onto PLA/AC 5% wt. beads. PLA/AC dose 0.25 g/ 50 mL, temperature 23±2°C and pH = 5.

The plot in Figure 24 shows a good agreement of dynamical data corresponding to pseudo-second-order kinetic model. As shown in Table 11, the value of correlation coefficient (R^2) of pseudo second order kinetic model for Pb^{2+} ions on PLA/AC 5% wt. beads were extremely high ($R^2 > 0.99$). Moreover, the equilibrium sorption capacities for pseudo-second-order were much closer to the experimental results than those of the pseudo-first-order system.

Table 11 Parameters of kinetic studies for the non-linearity of the pseudo-first-order and the pseudo-second-order models with various initial concentrations of Pb^{2+} ions (50, 300 and 500 mg L^{-1}) at 23±2°C, PLA/AC dose 0.25 g, and pH = 5.

C_0 (mg L^{-1})	q_e (exp) (mg g^{-1})	Pseudo-first-order			Pseudo-second-order		
		q_e (mg g^{-1})	k_1 ($\times 10^{-1}$) (min^{-1})	R^2	q_e (mg g^{-1})	k_2 ($\times 10^{-3}$) (g mg^{-1} min^{-1})	R^2
50	5.25	4.89	4.38	0.991	5.15	2.13	0.995
300	29.57	29.11	1.32	0.987	31.20	8.61	0.999
500	44.90	43.27	1.11	0.981	45.01	4.89	0.998

3.3.2.2 Effect of pH

It is well known that the pH of the system is a very important variable parameter in the adsorption process as a result of the surface charge of the adsorbent typically depends on the pH of the solution. Figure 25 depicts the effect of pH on Pb^{2+} ions adsorption by PLA/AC beads in the pH range of 1.5 – 5.5. The results showed that the pH increased from 1.5 to 5.0, the Pb^{2+} ions adsorption capacity increased. These can be explained that at lower pH values, the high concentration of H^+ ions promotes the protonation of functional groups such as carboxylic groups within the adsorbent to become positive charges and repel the positive charges of the cationic ions leading to reduction of Pb^{2+} ions adsorption. An alternative view is that at such low pH values the H^+ ions compete with Pb^{2+} ions for the adsorption sites (Kobya, et al., 2005).

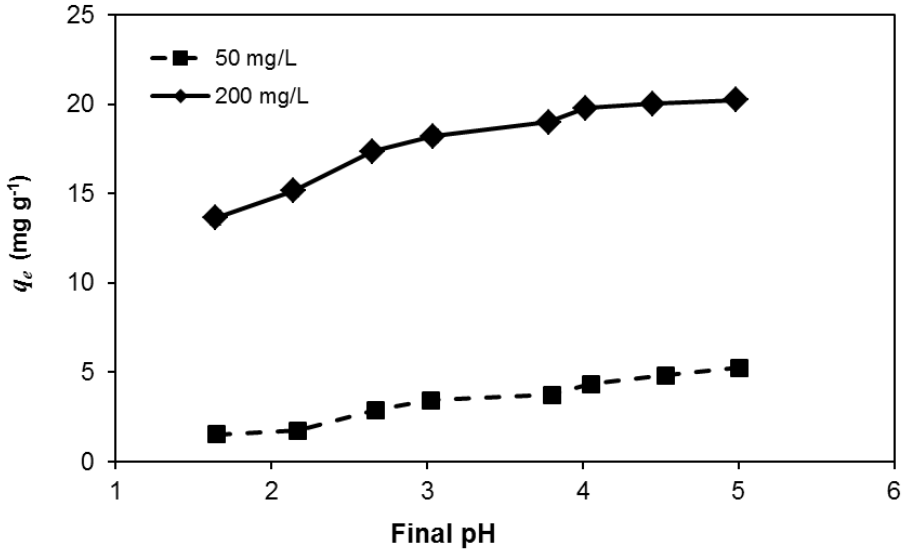

Figure 25 Effect of pH on PLA/AC 5% wt. beads for Pb^{2+} ions adsorption. PLA/AC dose 0.25 g /50 mL, temperature 23±2°C, Pb^{2+} concentration of (a) 50 mg L^{-1} and (b) 200 mg L^{-1}.

3.3.2.3 Effect of PLA/AC 5% wt. beads dosage

Figure 26 shows the adsorption of Pb^{2+} ions by the variation on PLA/AC 5% wt. beads dosage. It had been determined that percent adsorption of Pb^{2+} ions increased from 41 – 80%, 44 – 84 % and 55 – 85 % with increasing adsorbent dosage from 0.1 - 0.4 g/50 mL for Pb^{2+} ions initial concentrations of 100, 200 and 300 mg L^{-1}, respectively. This was due to a large number of binding sites for complexation of Pb^{2+} ions. Thus, the PLA/AC beads dosage is one of the very important parameters which influence the extent of Pb^{2+} ions uptake from the solution. The percentage of adsorbed Pb^{2+} ions adsorbed reached a maximum value when the load of PLA/AC beads was 0.4 g. However, after 0.25 g of beads, the adsorption capacity slightly increased with the increasing of PLA/AC beads. This PLA/AC beads dosage (0.25 g) is here considered to be the optimum level. Additionally, the time to achieve equilibrium was short and worthy which is appropriate to industrial applications (Namasivayam, et al., 1999).

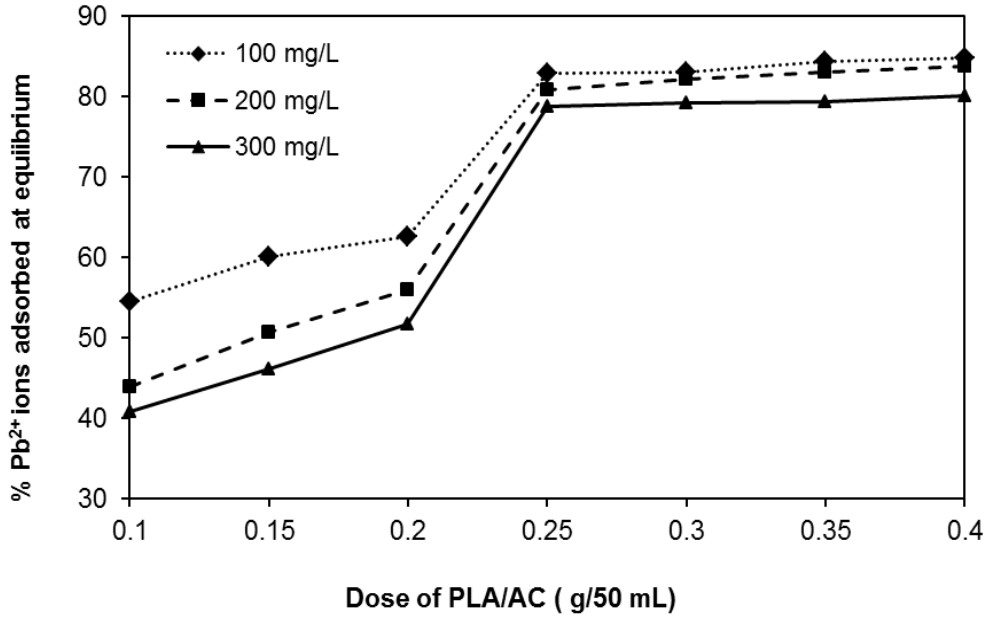

Figure 26 Effect of PLA/AC 5% wt. beads dosage for Pb^{2+} ions adsorption. PLA/AC dose 0.1 – 0.4 g / 50 mL, temperature 23±2°C and pH = 5.

3.3.2.4 Adsorption isotherm of Pb^{2+} ions on PLA/AC 5% wt. beads

Mathematical fittings using non-linear regression of equilibrium data of Pb^{2+} ions on PLA/AC beads sorption are shown in Figure 27 and correspond to be the L-2 type isotherm. This type represents the ratio between the concentrations of Pb^{2+} ions remaining in solution and adsorbed on the PLA/AC beads decreasing as increase in Pb^{2+} ions concentration which providing a concave curve (Limousin, et al., 2005). This indicated that there was a reduction in the number of active sites on the adsorbent surface at a higher Pb^{2+} ions concentration in the solution phase.

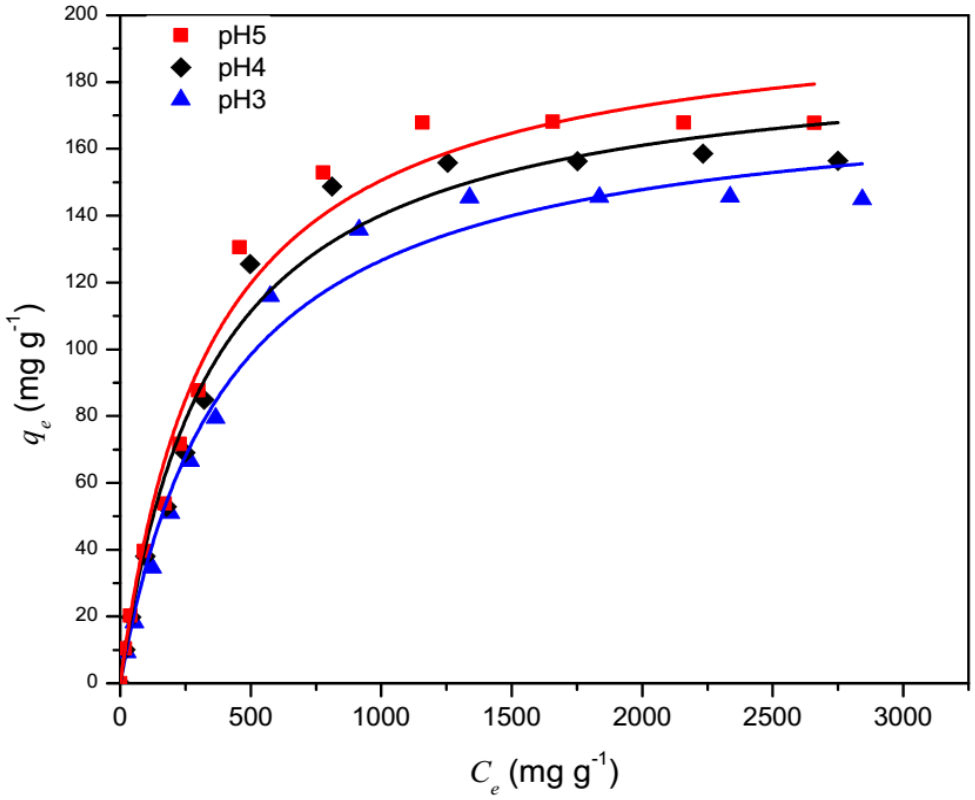

Figure 27 The non-linear plots of Langmuir adsorption isotherm for Pb^{2+} ions adsorption on PLA/AC 5% wt. beads at pH 3, 4 and 5.

Table 12 Parameters of the Langmuir and the Freundlich models for Pb^{2+} ions adsorption on PLA/AC 5% wt. beads at 23±2°C and pH 3, 4 and 5.

pH	Langmuir			Freundlich		
	q_m (mg g^{-1})	b (L mg^{-1})	R^2	K_F (mg g^{-1})	n	R^2
3	177.55	0.0024	0.99	2.00	1.71	0.93
4	189.25	0.0028	0.99	2.91	1.78	0.94
5	202.81	0.0029	0.99	2.71	1.79	0.93

Figure 27 shows the best fit of adsorption isotherms of Langmuir model for Pb^{2+} ions adsorption onto PLA/AC beads at 23±2 ºC, from initial concentrations of 100 – 4000 mg L^{-1} and pH range 3 - 5. Moreover, all of the fitted parameters are summarized in Table 12. It is well known that the favorability of adsorption was indicated by the dimensionless separation factor (R_L) which calculated from the data in Table 12, the R_L values were 0.07 – 0.80 at pH 3, 4 and 5 within the initial Pb^{2+} ions concentration of 100 – 4000 mg L^{-1} which recommended that Langmuir isotherm is favorable. The obtain results revealed that the equilibrium data of Pb^{2+} ions sorption on PLA/AC beads were well represented by the Langmuir and the Freundlich models. Of these two models, the Langmuir model gave better fit with higher correlation coefficient, R^2 (Table 12), indicating monolayer adsorption mechanism.

A comparison of the maximum Pb^{2+} ions uptake capacities (q_m, mg g^{-1}) by PLA/AC 5% wt. beads to those of other adsorbents reported in the literature is given in Table 13. It can be concluded that the maximum adsorption capacity of PLA/AC 5% wt. beads for Pb^{2+} ions sorption was higher than others in these literatures.

Table 13 The maximum adsorption capacities of Pb^{2+} ions compared with other adsorbents reported in the literature.

No	Adsorbent	*pH*	q_m (mg g^{-1})	*Ref.*
1.	Apricot stone activated carbon	5.0	22.84	Kobya, et al., 2005
2.	Palm shell activated carbon with chelating polymer	5.0	20.00	Aroua, et al., 2012
3.	Walnut wood activated carbon	5.0	47.62	Ghaedi, et al., 2015
4.	Coconut shell-based granulated modified activated carbon	5.0	29.44	Jyotsna , et al., 2004
5.	Nano hydroxyapatite (HAp) and hydroxyapatite granular activated carbon nanocomposite (C-HAp)	6.0	HAp = 83.83 C-HAp = 9.31	Fernando, et al., 2015
5.	Pure chitosan (PC) and goethite/chitosan nanocomposite (GC)	6.0	PC = 36.61 GC = 61.51	Rahimi, et al., 2015
6.	Chitin nanofibers (CNFs) and chitosan nanoparticles (CNPs)	5.0	CNFs = 60.24 CNPs = 94.34	Siahkamari, et al., 2017
8.	Magnetic ATP/FA/Poly(AA-co-AM) ternary nanocomposite microgel	5.0	40.0	Peng, et al., 2014
9.	Magnetic Fe_3O_4@ silica–xanthan gum composites	6.0	20.32	Jianga, et al., 2015
10.	Magnetic chitosan (MC) , graphene oxide (GO) and magnetic chitosan/graphene oxide imprinted Pb^{2+} (Pb-MCGO)	6.0	MC = 47.91 GO = 45.23 Pb-MCGO = 79.80	Wang, et al., 2016
11.	Lanthanide metal–organic frameworks	6.5	5.07	Jamali, et al., 2016
12.	Natural adsorbent perlite	6.0	31.25	Atakl, et al., 2013
13.	Polylacic acid/activated carbon composite bead (PLA/AC 5% wt.)	5.0	202.81	**This study**

3.3.2.5 Characterization of PLA/AC 5% wt. beads after Pb^{2+} ions adsorption

Figure 28 presents the EDX spectra and dot mapping of PLA/AC bead before and after adsorption of Pb^{2+} ions by the energy dispersive x-ray spectrometer system SEM/EDX employing a standard less qualitative EDX analytical technique. The qualitative spectra for PLA/AC bead before adsorption are shown in Figure 28(a), indicated that C, O are the main elements. The single of the element in PLA/AC 5% wt. bead was pictured by the bright points in dot mapping. After Pb^{2+} ions adsorption as illustrated in Figure 28(b), it was found that the EDX spectrum of PLA/AC bead showed the main components consisting of C, O, and Pb. The presence of Pb^{2+} ions in the spectrum confirmed the adsorption of Pb^{2+} ions on the PLA/AC 5% wt. bead. Moreover, the elemental distribution mapping of EDX for PLA/AC bead adsorbed Pb^{2+} ions by dot mapping was illustrated that the dot map for Pb in Figure 28(b) clearly presented the distribution of Pb^{2+} on the surface of PLA/AC 5% wt. bead.

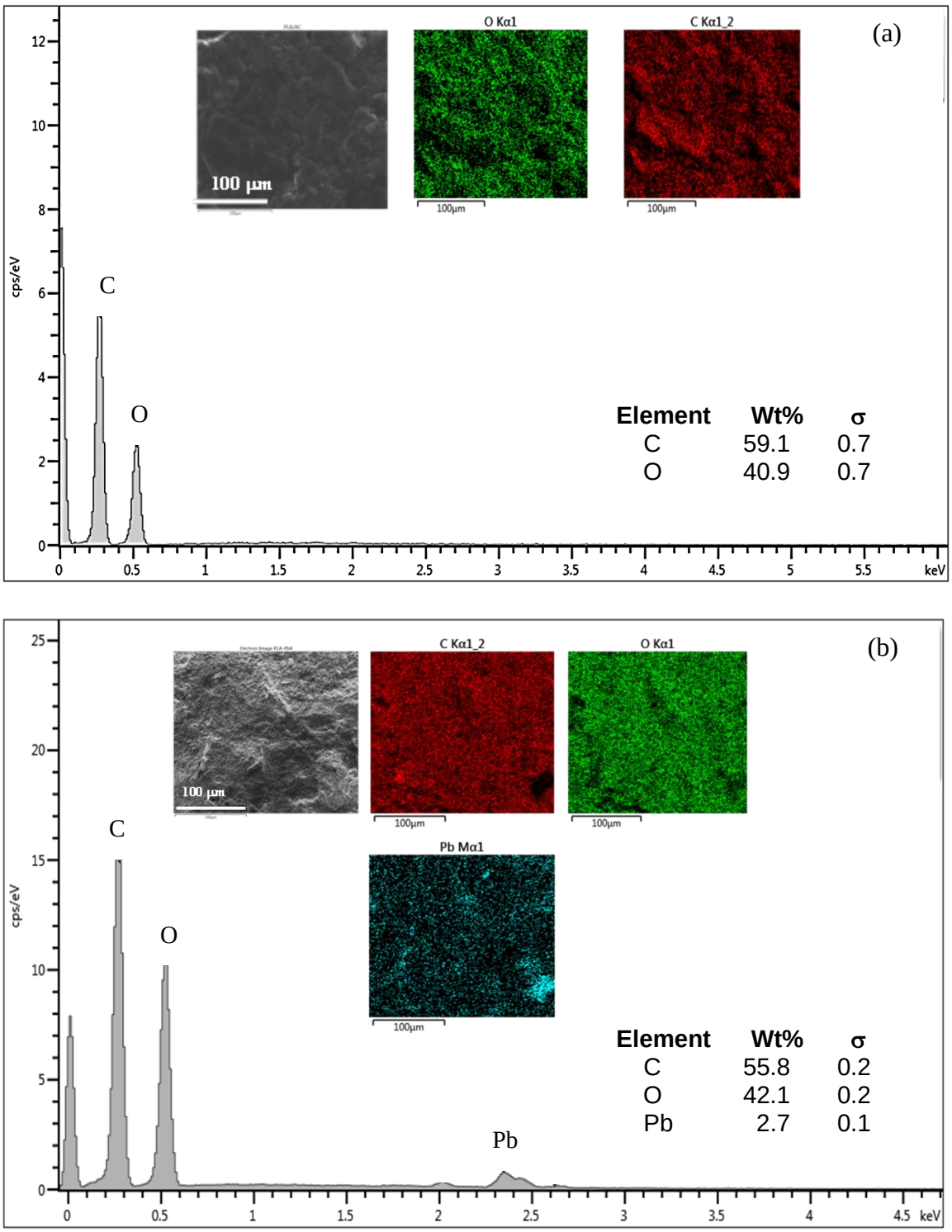

Figure 28 EDX spectra and dot mapping of PLA/AC 5% wt. bead (a) before and (b) after Pb^{2+} ions adsorption.

CHAPTER 4

CONCLUSION

The PLA/AC 5% wt. bead was successfully prepared in a facile method by a solution mixture of PLA/AC/NMP via a phase inversion technique as potential adsorbent. The obtained PLA/AC 5% wt. beads which are highly porous, non-toxic, efficient, cheap, handy and eco-friendly was used for the adsorption Rhodamine B and Pb^{2+} ions from aqueous solutions.

The PLA/AC 5% wt. bead was characterized for some physical properties. The results from SEM images showed that the spherical bead was formed with a diameter about 3 mm. The bead showed numerous pores on the surface and therefore the pores presented a highly inter-connected structure in the cross-sectional images. Moreover, an increased AC content in the PLA solution increased the porosity of the PLA/AC bead. This offered an advantageous condition for adsorption of Rhodamine B and Pb^{2+} ions from aqueous solution.

The BET surface area of PLA/AC 5% wt. bead was 95.98 $m^2 g^{-1}$. The adsorption-desorption isotherm of PLA/AC 5% wt. beads were classified according to IUPAC classification as a type IV adsorption isotherm which was pointed out to be a purely mesoporous material.

The PLA/AC 5% wt. bead was investigated to verify the elemental composition. The carbon content was found to be increased in PLA/AC bead (57.96 % wt.) compared with PLA bead that had no AC (48.93 % wt.).

The point of zero charge (pH_{pzc}) of PLA/AC 5% wt. bead was 3.5 indicating the PLA/AC 5% wt. bead has an acidic surface in nature.

The kinetic adsorption studies of Rhodamine B and Pb^{2+} ions can be successfully described by the pseudo-second-order kinetic model. Moreover, the intraparticle diffusion model of Rhodamine B uptake by the PLA/AC 5% wt. beads can be fitted. In addition, the R_i values from the intraparticle diffusion model of

PLA/AC 5% wt. beads were 0.82, 0.94 and 0.98 which are respectively values of intermediate initial adsorption (zone 2) for 50 mg L^{-1} and weak initial adsorption (zone 1) for 100 and 200 mg L^{-1} of Rhodamine B.

The adsorptions of Rhodamine B and Pb^{2+} ions onto the PLA/AC 5% wt. beads were found to obey the Langmuir isotherm model and the maximum adsorption capacity (q_m) values were found to be 149.57 mg g^{-1} and 202.81 mg g^{-1}, respectively.

The thermodynamic studies had revealed that the adsorption of Rhodamine B on PLA/AC 5% wt. beads was a spontaneous and the endothermic process.

The elemental composition (C, H, N and O) analyses of PLA/AC 5% wt. beads before and after sorption of Rhodamine B (PLA/AC RB) were investigated to verify the elemental composition. They were found that that the percentage of nitrogen of PLA/AC RB was increased from 0.04 % and 1.36 % for PLA/AC 5% wt. beads and PLA/AC RB, respectively. Moreover, from FT-IR spectra of Rhodamine B adsorption on PLA/AC 5% wt., the band at 690.48 cm^{-1} shifted to 709.75 cm^{-1} which was assigned to the hydrogen bonding between the –COOH group of Rhodamine B and PLA/AC 5% wt. beads. This result provided a proof of Rhodamine B adsorption on PLA/AC 5% wt. beads.

For Pb^{2+} ions adsorption on PLA/AC 5% wt. beads, the EDX spectrum of PLA/AC 5% wt. beads after Pb^{2+} ions adsorption showed the main components consisting of C, O, and Pb which confirmed the adsorption of Pb^{2+} ions on PLA/AC 5% wt. beads.

From all of these results, it can be concluded that the beads of PLA/AC 5% wt. are not only more convenient to use than the the powder activated carbon, but also have higher adsorption capacity for removal of Rhodamine B and Pb^{2+} ions. Therefore, the PLA/AC 5% wt. beads are remarkably effective adsorbent for removal of dyes and heavy metals in wastewater.

REFERENCE

Activated Carbon from Wikipedia, the free encyclopedia. http://en.wikipedia.org/wiki/activated carbon (accessed 16/08/16)

Amy, L.L., Guangquan, L. and John T.Y. (1995). Photocatalysis on TiO_2 surfaces: principles, mechanisms, and selected results. *Chemical Review*, 95(3): 735–758.

Anirudhan, T.S. and Ramachandran, M. (2015). "Adsorptive removal of basic dyes from aqueous solutions by surfactant modified bentonite clay (organoclay): Kinetic and competitive adsorption isotherm" *Process Safety and Envir. Protect*., 95: 215-225.

Arivoli, S. and Thenkuzhali, M. (2008). "Kinetic, mechanistic, thermodynamic and equilibrium studies on the adsorption of rhodamine B by acid activated low cost carbon". *E-Journal of Chemistry*, 5: 187-200.

Arivoli, S., Thenkuzhali, M. and Martin Deva Prasath, P. (2009). Adsorption of Rhodamine B by Acid Activated Carbon – Kinetic, Thermodynamic and Equilibrium Studies. *Orbital the Electronic Journal of Chemistry*. 1(2) : 138-155.

Aroua, M.K., Yin, C.Y., Lima, F.N., Kana, W.L. and Ashri, W.M. (2009). "Effect of impregnation of activated carbon with chelating polymer on adsorption kinetics of Pb^{2+}". *Journal of Hazardous Materials*, 166: 1526–1529.

Ashly, S., Prasad, L. and Manonmani, S. (2014)."A comparative study of microwave and chemically treated Acacia nilotica leaf an eco-friendly adsorbent for the removal of Rhodamine B dye from aqueous solution". *Arabian Journal of Chemistry*, 7: 494-503.

Atakl, Z.Ö.K and Yürüm, Y. (2013). "Synthesis and characterization of anatase nanoadsorbent and application in removal of lead, copper and arsenic from water". *Chemical Engineering Journal*, 225: 625–635.

Barakat, M.A. (2011). "New trends in removing heavy metals from industrial wastewater". *Arabian Journal of Chemistry*, 4(4): 361–377.

Bansode, R.R., Losso, J.N., Marshall, W.E., Rao, R.M. and Portier, R.J. (2003). "Adsorption of metal ions by pecan shell-based granular activated carbons". *Bioresource Technol.*, 89 :115–119.

Barrett, E. P.; Joyner, L. G. and Halenda, P. P., (1951). "Pore Size Distribution for Porous Materials". *Journal of the American Chemical Society*, 73: 373-380.

Bhatnagar, A. and Jain, A.K. (2005). "A comparative adsorption study with different industrial wastes as adsorbents for the removal of cationic dyes from water". *Journal of Colloid and Interface Science*, 281: 49 -55.

Brathwaite, R.L. and Rabone, S.D. (1985). "Heavy Metal Sulphide Deposits and Geochemical Surveys for Heavy Metals in New Zealand". *Journal of the Royal Society of New Zealand*. 15 (4): 363–370.

Brunauer, S., Emmett P. and Teller, E. (1938). "Adsorption of gases multimolecular layers". *Journal of the American Chemical Society*, 60 : 309–319.

Bánfalvi, G (2011). "CHAPTER 1 Heavy Metals, Trace Elements and their Cellular Effects". *Cellular Effects of Heavy Metals*: 3–28.

Cheung, W.H., Szeto, Y.S. and McKay, G. (2007). "Intrapaticle diffusion process during acid dye adsorption onto chitosan". *Bioresource Technology*, 98: 2897–2904.

Chuah, T.G., Jumasiah, A., Azni, I., Katayon, S. and Choong, TSY. (2005). "Rice husk as a potentially low-cost biosorbent for metal and dye removal: an overview". *Desalination,* 175: 305–316.

Chuenchom, L. (2004). "Adsorption of cadmium (II) and lead (II) ions on activated carbons obtained from bagasse and pericarp of rubber fruit". Master of Science Thesis in Physical Chemistry, Prince of Songkla University.

Cram 101 Textbook reviews, General, Organic and Biochemistry, 8th edition, pp. 45.

Crini, G. (2006). "Non-conventional low-cost adsorbents for dye removal: a review". *Bioresource Technology,* 97 106-185.

Czepirski, L., Balys, M.R. and Komorowska-Czepirska, E. (2000). "Some generalization of Langmuir adsorption isotherm". *Internet Journal of Chemistry.* 3(14): 1099-8292.

Dind, Ph. and Schmid, H. (1978). "Application of solar evaporation to waste water treatment in galvanoplasty". *Solar Energy*, 20(3) : 205-211.

Dobrevsky, I., Dimova-Todorova, M. and Panayotova, T. (1997). "Electroplating rinse waste water treatment by ion exchange". *Desalination*, 108(1–3): 277 – 280.

Dogan, M., Ozdemir, Y. and Alkan, M. (2007). "Adsorption kinetics and mechanism of cationic methyl violet and methylene blue dyes onto sepiolite". *Dyes and Pigm*ent, 75 : 701–713.

Dong-Wan, C., Chul-Min, C., Yongje, K., Byong-Hun, J., Frank, W.S., Eung-Seok, L. and Hocheol, S. (2011). "Adsorption of nitrate and Cr(VI) by cationic

polymer-modified granular activated carbon". *Chemical Engineering Journal*, 175: 298-305.

Dye from Wikipedia, the free encyclopedia. http://en.wikipedia.org/wiki/dye (accessed 1/08/16)

Edwin, V.A. (2008). "Studies on the Removal of rhodamine B and malachite green from aqueous solutions by activated carbon*".* *E-Journal of Chemistry.*,5(4): 844-852.

Eun-Ah, K., Angelia, L.S., Scott, F. and Richard, G.L. (2011). " Immobilization of Hg(II) in water with polysulfide-rubber (PSR) polymer – coated activated carbon". *Water research,* 45, 453- 460.

Fabíola, V., Danielle, M., Antônio, Augusto, U.S., Vítor, J.P., Selene, M.A. and Guelli U.S. (2016). "Removal of hexavalent chromium from electroplating wastewaters using marine macroalga Pelvetia canaliculata as natural electron donor". *Chemical Engineering Journal*, 290: 477 - 489.

Fernando, M.S., Silva, R.M. and Nalin de Silva, K.M. (2015). Synthesis, characterization, and application of nano hydroxyapatiten and nanocomposite of hydroxyapatite with granular activated carbon for the removal of Pb2+from aqueous solutions". *Applied Surface Science*, 351: 95–103.

Ferris, L.M. (1959). "Lead nitrate—Nitric acid—Water system". *Journal of Chemicals and Engineering Date*, 5 (3): 242–242.

Ferrari, L., Kaufmann, J., Winnefeld, F. and Plank, J. (2010). "Interaction of cement model systems with superplasticizers investigated by atomic force microscopy, zeta potential, and adsorption measurements". *Journal of Colloid Interface Science*, 347 (1): 15–24.

Foo, K.Y. and Hameed, B.H. (2010). “Insights into the modeling of adsorption isotherm systems”. *Chemical Engineering Journal*. 156 (1): 2–10.

Fuente, E., Menendez, J. A., Dyez, M. A., Sau’rez, D. and Montes-Moran, M.A. (2003). “Infared Spectroscopy of Carbon Materials: A Quantum Chemical Study of Model Compounds”. *Journal Physical Chemistry B*, 107: 6350-6359.

Garg, V.K., Kumar, R. and Gupta, R. (2004). “Removal of malachite green dye from aqueous solution by adsorption using agro-industry waste: a case study of *Prosopis cineraria*”. *Dyes and Pigments*, 62: 1–10.

Garlotta, D. (2001). A literature review of poly(lactic acid). *Journal of Polymers and the Environment*, 9(2): 63-84.

Ghaedi, M., Mazaheri, H., Khodadoust, S, Hajati, S. and Purkait, MK. (2015). “Application of central composite design for simultaneous removal of methylene blue and Pb^{2+} ions by walnut wood activated carbon.” *Spectrochim Acta A Mol Biomol Spectrosc.*, 135: 479-490.

Hamdi, M.H. and Ashraf, E.S. (2008) “Activated carbon from agricultural by-products for the removal of rhodamine B from aqueous solution” *Journal of Hazardous Materials*, 168(2-3): 1070–1081.

Hayeeye, F., Sattar, M., Tekasakul, S. and Sirichote, O. (2014). “Adsorption of rhodamine B on activated carbon obtained from pericarp of rubber fruit in comparison with the commercial activated carbon”. *Songklanakarin Journal of Science and Technology*, 36 (2): 177-187.

Hayeeye, F., Sattar, M., Chinpa, W. and Sirichote, O. (2015). “Preparation and adsorption study of gelatin/activated carbon composite bead form”. *Advanced Materials Research*, 1077 : 18 - 22.

Hayeeye, F., Sattar, M., Chinpa, W. and Sirichote, O. (2017). "Kinetics and thermodynamics of Rhodamine B adsorption by gelatin/activated carbon composite beads". *Colloids Surface. A: Physicochemical and Engineering Aspects*, 513 : 259–266.

Hem, L., Suman, M., Garg, V.K. and Gupta, R.K. (2009). "Removal of a dye from wastewater by adsorption using treated parthenium biomass." *Journal of Hazardous Materials*, 153(1–2): 213–220.

Hema, M. and Arivoli, S. (2009). "Rhodamine B adsorption by activated carbon: kinetic and equilibrium studies" *Indian Journal of Chemical Technology*, 16: 38 – 45.

Ho, Y.S. and McKay, G. (1999). "Pseudo-second-order model for sorption processes". *Process Biochemistry*, 34 : 451–465.

Hongzhang, C., Zuohu, L. and Chun, L. (2004). "Adsorptive removal of Cr(VI) by Fe-modified steam exploded wheat straw". *Process Biochemistry*, 39: 541 – 545.

Hu, Q., Meng, Y., Sun, T., Mahmood, Q., Wu, D., Zhu, J. and Lu, G. (2011). "Kinetics and equilibrium adsorption studies of dimethylamine (DMA) onto ion-exchange resin". *Journal of Hazardous Materials*, 185 (2-3): 677–681.

Hui, Q., Lu, L., Bing-cai, P., Qing-jian, Z., Wei-ming, Z.and Quan-xing, Z. (2009). "Review, Critical review in adsorption kinetic models". *Journal of Zhejiang University SCIENCE A*, 10(5):716-724.

Hwang, L., Jyh-Cherng, C. and Ming-Yen, W. (2013). "The properties and filtration efficiency of activated carbon polymer composite membranes for the removal of humic acid." *Desalination*, 313: 166 – 175.

Jamal, A.A., Sulyman, M.O., Elazaby, K.Y. and Salah, M.A. (2013). "Adsorption of Pb(II) and Cu (II) from aqueous solution onto activated carbon prepared from dates stones". *International Journal of Environmental Science*s *and Development*, 4(2) : 191 – 195.

Jamali, A., Tehrani, A. Shemirani, F. and Morsali, A. (2016). Lannthanide metal–organic frameworks as selective microporous materials for adsorption of heavy metal ions, *Dalton Transactions*, 45(22) : 9193–9200.

Jaramillo, J., Gómez-Serrano, V. and Alvarez, PM. (2009) "Enhanced adsorption of metal ions onto functionalized granular activated carbons prepared from cherry stones." *Journal of Hazardous Materials*, 161(2-3): 670-676.

Jia, Y.F., Xiao, B. and Thomas, K.M. (2002). "Adsorption of metal ions on nitrogen surface functional groups in activated carbons". *Langmuir*, 18: 470 – 478.

Jianga, L., Liua, P. and Zhaoc, S. (2015). "Magnetic ATP/FA/Poly(AA-co-AM) ternary nanocomposite microgel as selective adsorbent for removal of heavy metals from wastewater". *Colloids Surface. A: Physicochemical and Engineering Aspects*, 470 : 31–38.

Jose, T. and Qiming, Y. (1999). "Biosorption of lead(II) and copper(II) from aqueous solutions by pre-treated biomass of Australian marine algae." *Bioresource Technology*, 69: 223-229.

Juang, R., Wu, F. and Tseng, R. (2002)."Characterization and use of activated carbons prepared from bagasses for liquid-phase adsorption". *Colloids and Surfaces A: Physicochemical and Engineering Aspects*, 201: 191-199.

Jyotsna, G., Kadirvelu, K. and Rajagopal, C. (2004). "Competitive sorption of Cu(II), Pb(II) and Hg(II) ions from aqueous solution using coconut shell-based activated carbon." *Adsorption Science and Technology*., 22(3) : 257- 273.

Jyotsna, G., Kadirvelu, K. Rajagopal, C. and Garg, V.K. (2005).“Removal of lead(II) by adsorption using treated granular activated carbon: Batch and column studies.” *Journal of Hazardous Materials B*, 125: 211–220.

Kant, R. (2012) “Textile dyeing industry an environmental hazard”. *Natural Science*, 4 : 22-26.

Khan, T.A., Sharma, S. and Ali, I. (2011). “Adsorption of rhodamine B dye from aqueous solution onto acid activated mango (*Magnifera indica*) leaf powder: equilibrium, kinetic and thermodynamic studies”. *Journal of Toxicology and Environmental Health Sciences*, 3(10) : 286-297.

Kima, J., Sohna, M., Kima, D., Sohn, S. and Kwon, Y. (2001). “Production of granular activated carbon from waste walnut shell and its adsorption characteristics for Cu^{2+} ion.” *Journal of Hazardous Materials*. 85(3) :301 – 315.

Kobya, M., Demirbas, E., Senturk, E. and Ince, M. (2005). “Adsorption of heavy metal ions from aqueous solutions by activated carbon prepared from apricot stone”. *Bioresource Technology*, 96 : 1518–1521.

Kuila, U. and Prasad, M. (2013). “Specific surface area and pore-size distribution in clays and Shales”. *Geophysical Prospecting*, 62(2): 341-362.

Li, J.R., Wanga, X., Baoling, Y. and Ming-Lai, F. (2014). “Layered chalcogenide for Cu^{2+} removal by ion-exchange from wastewater”. *Journal of Molecular Liquids*, 200(B) : 205 -212.

Liao, P.H., Gao, Y. and Lo, K.V. (1993). “Chemical precipitation of phosphate and ammonia from swine wastewater”. *Biomass and Bioenergy*, 4(5): 365-371.

Limousin, G., Gaudet,, J.P., Charlet, L., Szenknect, S., Barthe`s, V. and Krimissa, M. (2005). "Sorption isotherms: A review on physical bases, modeling and measurement". *Applied Geochemistry*, 22 : 249 - 275.

Lin, X., Bo, W., Guang, Y. and Mario, G. (2012). Poly(lactic acid)-based biomaterials: synthesis, modification and applications, biomedical science,engineering and technology, *InTech open science* : 249.

Lina, M., Rémi Lebrunb, O., Jean-François, B. and Hausler, R. (2007)."Treatment of an acidic leachate containing metal ions by nanofiltration membranes" *Separation and Purification Technology* , 54(3) : 306 – 314.

Madhavakrishnan, S., Manickavasagam, K., Vasanthakumar, R., Rasappan, K., Mohanraj, R. and Pattabhi, S. (2009). "Adsorption of crystal violet dye from aqueous solution using Ricinus Communis pericarp carbon as an adsorbent." *E-journal of Chemistry*, 6(4): 1109 – 1116.

Majewska-Nowak , K. (1989). " Effect of flow conditions on ultra-filtration efficiency of dye solutions and textile effluents". *Desalination* ,71: 127–132.

Manase, A. (2012). "Fixed bed adsorption studies of rhodamine B dye using oil plam empty fruits bunch activated carbon." *Journal Engineering Research and Studies*., 3(3): 1 – 4.

Mansooreh, S., Hakimeh, S. and Farzin, Z.A. (2012)."Evaluation of activated carbon and bio-polymer modified activated carbon performance for palladium and platinum removal". *Journal of the Taiwan Institute of Chemical Engineers*, 43(5): 696–703.

Martin, O. and Avérous, L. (2001). "Poly(lactic acid): plasticization and properties of biodegradable multiphase systems". *Polymer*, 42 (14): 6209–6219.

Milan, K. (2014). " REVIEW, Adsorption, chemisorption, and catalysis ". *Chemical Papers*, 68 (12): 1625–1638.

Minghua, M., Lingdi, S., Guishan, H., Meifang, Z., Yu, Z., Xuefen, W., Yanmo, C. and Benjamin, S.H. (2012). "Micro-nano structure poly (ether sulfones)/ poly(ethyleneimine) nanofibrous affinity membranes for adsorption of anionic dyes and heavy metal ions in aqueous solution". *Chemical Engineering Journal*, 197: 88 – 100.

Mohamed, K.A., Mojdeh, O. and Wan Mohd Ashri, W. D. (2010). "Hexavalent chromium adsorption on impregnated palm shell activated carbon with polyethyleneimine." *Biology Technology*, 101: 5098 – 5103.

Mohammad, A.H. and Md Shah, A. (2012). "Adsorption kinetics of rhodamine B on used black tea leaves." *Journal of Environmental Health Science and Engineering*., 9(2):1 – 7.

Mulder, M. (2000), MEMBRANE PREPARATION/ Phase inversion membranes, University of Twente, Enschede, The Netherlands :3331 – 3345.

Namasivayam, C. and Kadirvelu, K. (1999). "Uptake of Mercury (II) from wastewater by activated carbon from an unwanted agricultural solid by-product: coirpith". *Carbon*, 37: 79 – 84.

Namasivayam, C. Radhika, R. and Suba, S. (2001). "Uptake of dyes by a promising locally available agricultural solid waste: coir pith". *Waste Management*, 21 : 381 - 387.

Namasivayam, C., Muniasamy, N., Gayatri, K., Rani M. and Ranganathan, K. (2016). Enhancement of rhodamine B removal by modifying activated carbon developed from Lythrum salicaria L. with pyruvic acid, *Colloids Surface. A: Physicochemical and Engineering Aspects*, 489: 154 - 162.

National Organization for Rare Disorders. (2015). “Heavy Metal Poisoning”. Retrieved 11/02/16.

Ninan, N., Grohens, Y., Elain, A., Kalarikkal, N. and Thomas, S. (2014).“Synthesis and characterization of gelatin/zeolite porous scaffold”. *European Polymer Journal*, 49: 2433-2445.

Panda, G.C., Das, S.K. and Guha, A.K. (2009). “Jute sticks powder as a potential biomass for the removal of congo red and rhodamine B from their aqueous solution”. *Journal of Hazardous Materials*, 164(1): 374 – 379.

Peng, X., Xu, F., Zhang, W., Wang, J., Zeng, C., Niu, M. and Chmielewská, E. (2014). “Magnetic Fe_3O_4@silica–xanthan gum composites for aqueous removal and recovery of Pb^{2+}”. *Colloids Surface. A: Physicochemical and Engineering Aspects.* 443: 27– 36.

Postai, D.L., Demarchi, C.A., Zanatta, F., Melo, D.C. and. Rodrigues, C.A. (2016). “Adsorption of rhodamine B and methylene blue dyes using waste of seeds of *Aleurites Moluccana*, a low cost adsorbent”. *Alexandria Engineering Journal*, 55 : 1713–1723.

Prasad, A.L. and Santhi, T. (2012). “Adsorption of hazardous cationic dyes from aqueous solution onto Acacia nilotica leaves as an eco-friendly adsorbent”. *Sustainable Environment Research*, 22(2): 113 - 122.

Prashant, M. (2012). “ Treating textile effluents by coagulation - flocculation method using different dosing compositions”. *Advances in Applied Science Research*, 3(4): 2514-2517.

Rahchamani, J., Zavvar, M.H. and Behzad, M. (2011).“Adsorption of methyl violet from aqueous solution by polyacrylamide as an adsorbent: isotherm and kinetic studies”. *Desalination*, 267: 256-260.

Rahimi, S., Moattari, R.M., Rajabi, L. and Derakhshan, A.A. (2015). "Optimization of lead removal from aqueous solution using goethite/chitosan nanocomposite by response surface methodology". *Colloids Surface. A: Physicochemical and Engineering Aspects*, 484: 216–225.

Rais, A. and Rajeev, K. (2010). "Adsorption of amaranth dye onto alumina reinforced polystyrene". *CLEAN – Soil, Air, Water*, 39 (1): 74 - 82.

Ramalho, R.S. (1983) "CHAPTER 3 – Pretreatment and Primary Treatment". Introduction to Wastewater Treatment Processes (Second Edition): 79–165.

Ramalho, R.S. (1983). "CHAPTER 5 – Secondary Treatment: The Activated Sludge Process". Introduction to Wastewater Treatment Processes (Second Edition): 211–339.

Ramalho, R.S. (1983). "CHAPTER 8 – Tertiary Treatment of Wastewaters". Introduction to Wastewater Treatment Processes (Second Edition): 485–571.

Rao, C.S. (1992). " Environmental Pollution Control Engineering". Wiley,

Rengaraj S., Yeon, J.W, Kim, Y., Yung, Y., Ha, Y.K and Kim, W.H. (2007). "Adsorption characteristics of Cu(II) onto ion exchange resins 252H and 1500H: kinetics, isotherms and error analysis". *Journal of Hazardous Materials*, 143: 469 – 477.

Rhim, J.W., Mohanty, A.K., Singh, S.P. and Perry, K.W. (2006). "Effect of the processing methods on the performance of polylactide films: Thermocompression versus solvent casting". *Journal of Applied Polymer Science*, 101(6): 3736-3742.

Saini, J., Garg, V.K., Gupta, R.K. and Kataria, N. (2017). "Removal of Orange G and Rhodamine B dyes from aqueous system using hydrothermally synthesized zinc oxide loaded activated carbon (ZnO-AC)". *Journal of Environmental Chemical Engineering*, 5 : 884 - 892.

Sattar, M., Hayeeye, F., Chinpa, W. and Sirichote, O. (2014). "Preparation and adsorption study of polysulfone/activated carbon composite bead form". *Applied Mechanics and Materials*, 625: 106 - 109.

Selvama, P.P., Preethi, S., Basakaralingam, P., Thinakaran, N., Sivasamy, A. and Sivanesan, S. (2008). "Removal of rhodamine B from aqueous solution by adsorption onto sodium montmorillonite". *Journal of Hazardous Materials*, 155: 39–44.

Semerjian, L. and Ayoub, G.M. (2003). "High-pH–magnesium coagulation–flocculation in wastewater treatment". *Advances in Environmental Research*, 7(2): 389-403.

Senthilkumaar, S., Kalaamani, P., Subburamaan, C.V., Subramaniam, N.G. and Kang, T.W. (2011). "Adsorption behavior of organic dyes in biopolymers impregnated with H_3PO_4: thermodynamic and equilibrium studies". *Chemical Engineering Technology*, 34 (9): 1459-1467.

Sharaf El-Deen, G.E. and Sharaf El-Deen, S.E.A. (2016). "Kinetic and isotherm studies for adsorption of Pb(II) from aqueous solution onto coconut shell activated carbon". *Desalination and Water Treatment*, 57(59) : 28910-28931.

Shi, L., Zhang, G., Wei, D., Yan, T., Xue, X., Shi, S. and Wei, Q. (2014). "Preparation and utilization of anaerobic granular sludge-based biochar for the adsorption of methylene blue from aqueous solutions". *Journal of Molecular Liquids*, 198: 334-340.

Siahkamari, M., Jamali, A. Sabzevari, A. and Shakeria, A. (2017). "Removal of lead(II) ions from aqueous solutions using biocompatible polymeric nano-adsorbents: A comparative study". *Carbohydrate Polymers*, 157: 1180–1189.

Sing, K.S., Everett, D.H., Haul, R.A., Moscou, L., Peirotti, R.A, Siemieniewska, T. and Rouquerol, J. (1985). "Reporting physisorption data for gas/solid systems with special reference to the determination of surface area and porosity". *Pure and Applied Chemistry*, 57(4): 603-619.

Sirichote, O., Innajitara, W., Chuenchom, L., Panumati, S., Chudecha, K., Vankhaew, P.and Choolert, V. (2008). "Adsorption of phenol from diluted aqueous solutions by activated carbons obtained from bagasse, oil plam shell and pericarp of rubber fruit". *Songklanakarin Journal of Science and Technology*, 30(2): 185 – 189.

Sivakumar, A. and Isaac, C.P.J. (2013). "Removal of lead and cadmium ions from water using *Annona squamosa* shell: kinetic and equilibrium studies". *Desalination and Water Treatment*, 51: 7700–7709.

Snare, M. (1982). "The photophysics of rhodamine B". *Journal of Photochemistry.* 18(4) : 335 – 346.

Srivastava, S. and Goyal, P. (2010). "Novel Biomaterials: Decontamination of Toxic Metals from Wastewater". Springer-Verlag.: pp. 2.

Stuart, B.(2004). "Infrared Spectroscopy: Fundamentals and Applications". John Wiley & Sons, Ltd. ISBNs: 0-470-85427-8.

Sumanjit, P., Tejinder, S.W. and Ishu, I.K. (2008). "Removal of rhodamine B by adsorption on walnut shell charcoal". *Journal of Surface Science and Technology*, 24 : 179 - 193.

Suna, D., Zhang, X., Wu, Y. and Liu, X. (2010). "Adsorption of anionic dyes from aqueous solution on fly ash". *Journal of Hazardous Materials,* 181: 335–342.

Sutton, P.M. (1994) "Combining biological and physical processes for complete treatment of oily wastewaters". *International Biodeterioration & Biodegradation*, 33(1) : 3-21.

Thakur, A. and Kaur, H. (2017). "Response surface optimization of Rhodamine B dye removal using paper industry waste as adsorbent". *International Journal of Industrial Chemistry*, First online (2017) 1 - 12.

Tiwari, S., Tripathi, I.P. and Tiwari, H.L. (2013). " Effects of lead on environment ". *International Journal of Emerging Research in Management &Technology*, 2(6): 1-5.

Umar, I.A., Abdulraheem, G., Bala, S. Muhammad, S.and Abdullahi, M. (2015). "Kinetics, equilibrium and thermodynamics studies of C.I. Reactive Blue 19 dye adsorption on coconut shell based activated carbon". *International Biodeterioration & Biodegradation*, 102: 265 – 273.

Velmurugan, P., Rathina,V. and Dhinakaran, G. (2011). "Dye removal from aqueous solution using low cost adsorbent". *International Journal of Environmental Sciences*, 1(7): 1492 - 1503.

Vijaraghavan, N.S. (1999) . "Environmental unit in textile industry". Director BIS, bhopal science tech. *Entrepreneur*, 7: 3-9.

Vijayakumar, G., Yoo, C.K. Elango, K.G.P. and Dharmendirakumar, M. (2010). "Adsorption characteristics of rhodamine B from aqueous solution onto barite". *Clean*, 38 (2): 202 – 209.

Vijayakumar, G., Tamilarasan, R. and Dharmendirakuma, M. (2012). "Adsorption, kinetic, equilibrium and thermodynamic studies on the removal of basic dye Rhodamine B from aqueous solution by the use of natural adsorbent perlite". *Journal of Materials and Environmental Science*, 3(1): 157-170.

Wang, Y., Mu, Y., Zhao, Q.B. and Yu, H.Q. (2006). "Isotherms, kinetics and thermodynamics of dye biosorption by anaerobic sludge". *Separation and Purification Technology*, 50 : 1–7.

Wang, Y., Li, L.L., Luo, C., Wang, X. and Duan, H. (2016). "Removal of Pb^{2+} from water environment using a novel magnetic chitosan/graphene oxide imprinted Pb^{2+}". *International Journal of Biological Macromolecules,* 86: 505–511.

Wasif, A.I. and Kone, C.D. (1996) . "Textile processing and environmental consequences". *Textile and Engineering In-stitute,* : 1 - 15.

Wilson, K., Yang, H., Seo, C.W. and Marshall, W.E. (2006)."Select metal adsorption by activated carbon made from peanut shells". *Bioresource Technology* ,97 : 2266–2270.

World Health Organization, International Agency for Research on Cancer. (2006). "Inorganic and Organic Lead Compounds". IARC Monographs on the Evaluation of Carcinogenic Risks to Humans. International Agency for Research on Cancer. 87.

Wu, F.C., Tseng, R.L. and Juang, R.S. (2009). "Initial behavior of intraparticle diffusion model used in the description of adsorption kinetics". *Chemical Engineering Journal*, 153: 1–8.

Yi, Z., An, Z., Cui, G. and Li, J. (2003). "Stabilized complex film formed by co-adsorption of b-lactoglobulin and phospholipids at liquid/liquid interface, *Colloids Surface. A: Physicochemical and Engineering Aspects*, 223 : 11-16.

Yüzera, H., Karaa, M., Eyüp, S. and Mehmet, S.Ç. (2008). "Contribution of cobalt ion precipitation to adsorption in ion exchange dominant systems". *Journal of Hazardous Materials*, 151(1): 33-37.

Zeng ,Y., Wang, K., Jianfeng, Y. and Wang, H. (2008). "Hollow carbon beads for significant water evaporation enhancement". *Chemical Engineering Science*, 116: 704-709.

Zhang, K., Cheung, W.H. and Valix, M. (2005). "Role of physical and chemical properties of activated carbon in the adsorption of lead ions". *Chemosphere*, 60 : 1129-1140.

Zhang, R. Hummelgard, M., Lv, G. and Olin, H. (2011). "Real time monitoring of the drug release of rhodamine B on graphene oxide". *Carbon*, 49 : 1126 – 1132.

Zhua, C., Luana, Z., Wang, Y. and Shan, X. (2007). "Removal of cadmium from aqueous solutions by adsorption on granular red mud (GRM)". *Separation and Purification Technology*, 57: 161–169.

APPENDIX

List of Publications

Paper I Memoon Sattar, Fareeda Hayeeye, Watchanida Chinpa and Orawan Sirichote, "Preparation and characterization of poly (lactic acid) /activated carbon composite bead via phase inversion method and its use as adsorbent for Rhodamine B in aqueous solution".(2017). *Journal of Environmental Chemical Engineering*, Available online 6 July 2017, In Press, Accepted Manuscript.

Paper II Maimoon Sattar, Fareeda Hayeeye, Watchanida Chinpa, and Orawan Sirichote. "Preparation and characterization of polysulfone/activated carbon composite bead form". (2014). *Applied Mechanics and Materials*, 625, 106 – 109.

Accepted Manuscript

Title: Preparation and Characterization of Poly (lactic acid)/Activated Carbon Composite Bead via Phase InversionMethod and Its Use as Adsorbent for Rhodamine B in Aqueous Solution

Authors: Memoon Sattar, Fareeda Hayeeye, Watchanida Chinpa, Orawan Sirichote

PII: S2213-3437(17)30311-1
DOI: http://dx.doi.org/doi:10.1016/j.jece.2017.07.007
Reference: JECE 1722

To appear in:

Received date: 2-3-2017
Revised date: 29-6-2017
Accepted date: 3-7-2017

Please cite this article as: Memoon Sattar, Fareeda Hayeeye, Watchanida Chinpa, Orawan Sirichote, Preparation and Characterization of Poly (lactic acid)/Activated Carbon Composite Bead via Phase InversionMethod and Its Use as Adsorbent for Rhodamine B in Aqueous Solution, Journal of Environmental Chemical Engineeringhttp://dx.doi.org/10.1016/j.jece.2017.07.007

Preparation and Characterization of Poly (lactic acid)/ Activated Carbon Composite Bead via Phase Inversion Method and Its Use as Adsorbent for Rhodamine B in Aqueous Solution

Memoon Sattar[1], Fareeda Hayeeye[1], Watchanida Chinpa[2] and Orawan Sirichote[1,*]

[1]Department of Chemistry, Faculty of Science, Prince of Songkla University, Songkhla 90112, Thailand

[2]Department of Materials Science and Technology, Faculty of Science, Prince of Songkla University, Songkhla 90112, Thailand

[*] Corresponding author: Orawan Sirichote

Telephone: (+66) 0896577950

Email address: orawan.si@psu.ac.th

Highlights

- The PLA/AC 5% wt. beads were prepared by compacting AC and poly(lactic acid) via phase inversion method.
- The practical potential of PLA/AC beads can remove carcinogenic dye Rhodamine B from an aqueous solution.
- The kinetic and adsorption isotherm of Rhodamine B by PLA/AC were well fit by the intraparticle diffusion model and Langmuir adsorption isotherm, respectively.
- The adsorption process on PLA/AC was an endothermic process.

Abstract

The preparation of porous materials using biodegradable materials has attracted much attention in the field of environmental pollution control. A non-toxic, user-friendly and inexpensive adsorbent bead was prepared from poly (lactic acid) (PLA) and activated carbon (AC) using a phase inversion technique. The porous structure of the PLA/AC bead was characterized by scanning electron microscopy and nitrogen adsorption−desorption methods. The removal of the carcinogenic dye Rhodamine B was studied by batch equilibration method and it was found that the monolayer maximum adsorption capacity was 149.57mg g^{-1} at 60 °C, pH 4. A study of kinetics adsorption revealed that the Rhodamine B molecules diffused very rapidly into the interconnected pores of the PLA/AC 5% wt. beads and agreed very well with the intraparticle diffusion model. The negative value of Gibb's free energy indicated a spontaneous adsorption process, and the enthalpy change (23.92 kJ mol^{-1}) implied an endothermic adsorption process. Desorption studies showed that the percentage of desorbed Rhodamine B solution increased with a decrease in pH. The results indicated that the PLA/AC bead will provide a new alternative granular adsorbent for the removal of pollutant cationic dyes from water.

Key words: activated carbon; poly(lactic acid); phase inversion method; adsorption isotherm

1. Introduction

Dye is one of the major constituents of the wastewater discharge of many manufacturing processes including the dyeing, textile, leather, paint and plastics industries. Most of the dyes are resistant to light, heat, and oxidizing agents, and are usually non-biodegradable. One of the most basic dyes used in industry is Rhodamine B. It is frequently

Applied Mechanics and Materials Vol. 625 (2014) pp 106-109
© (2014) Trans Tech Publications, Switzerland
doi:10.4028/www.scientific.net/AMM.625.106

Preparation and Characterization of Polysulfone/Activated Carbon Composite Bead Form

Maimoon Sattar[1, a *], Fareeda Hayeeye[1, b], Watchanida Chinpa[2, c] and Orawan Sirichote[1, d]

[1]Department of Chemistry, Faculty of Science, Prince of Songkla University, Songkhla 90112, Thailand

[2]Department of Materials Science and Technology, Faculty of Science, Prince of Songkla University, Songkhla 90112, Thailand

[a *]maimoon_sattar@hotmail.com , [b]hin_999@hotmail.com, [c]watchanida.c@psu.ac.th , [d]orawan.si@psu.ac.th

* corresponding author : maimoon_sattar@hotmail.com

Keywords: Activated Carbon, Polysulfone, Adsorption

Abstract

Polysulfone/Activated Carbon (PSF/AC) composites in bead form were prepared for Rhodamine B sorption. The scanning electron microscope (SEM) shows that pure PSF bead is smooth surface while PSF/AC bead presents the pore distribution. FT-IR spectra indicate the existence of AC on the PSF/AC bead surface. Under adsorption test of Rhodamine B, it was found that an increase in the AC content in PSF solution results in an increase in the percentages of dye adsorption from 1.38 % to 71.56% for pure PSF bead and PSF/AC added with 4 wt% of AC, respectively.

Introduction

In the present, adsorption onto different adsorbents is widely used for removal of pollutants from wastewater treatment. Activated carbon (AC) is the most effective adsorbent for adsorption process due to very high surface area, porous sorbent, high capacity and high rate of adsorption and versatility [1]. However, a fine powder form of AC is not easy to use. Polysulfone (PSF), as shown in Fig 1(a), is a thermoplastic polymer and has been widely used in various fields involving food processing, biotechnology, and water treatment [2] due to its mechanical properties, and thermal and chemical stability. The aim of this work is to prepare the PSF/AC composite into bead form. The Rhodamine B (Fig.1 (b)) was selected for the adsorption experiment because this dye presents in the wastewater of several industries such as textile, leather, jute and food industries. The effect of AC added into the PSF solution on the morphology and the adsorption of Rhodamine B by PSF/AC adsorbent was studied.

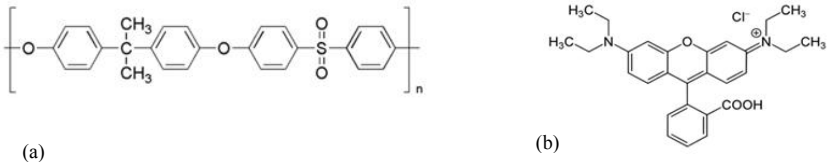

(a) (b)

Fig. 1 Structure of (a) Polysulfone and (b) Rhodamine B

VITAE

Name Miss Memoon Sattar

Student ID 5510230041

Educational Attainment

Degree	Name of Institution	Year of Graduation
Bachelor of Science (Chemistry)	Prince of Songkla University	2007
Master of Science (Physical Chemistry)	Prince of Songkla University	2010

Scholarship Awards during Enrolment

PSU Ph.D. Scholarship from the Graduate School, Prince of Songkla University**.**

List of Publication and Proceeding

1. Memoon Sattar, Fareeda Hayeeye, Watchanida Chinpa, and Orawan Sirichote, "Preparation and characterization of poly (lactic acid)/activated carbon composite bead via phase inversion method and its use as adsorbent for Rhodamine B in aqueous solution".(2017). *Journal of Environmental Chemical Engineering.* Available online 6 July 2017 In Press, Accepted Manuscript.

2. Fareeda Hayeeye, Memoon Sattar, Watchanida Chinpa, and Orawan Sirichote, "Kinetics and thermodynamics of Rhodamine B adsorption by gelatin/activated carbon composite beads". (2017). *Colloids and Surfaces A: Physicochemical and Engineering Aspects*. 513, 259–266.

3. Fareeda Hayeeye, Qiming Jimmy Yu, Memoon Sattar, Watchanida Chinpa, and Orawan Sirichote, "Adsorption of Pb^{2+} ions from aqueous solutions by gelatin/activated carbon composite bead form". (2017). *Adsorption Science & Technology*. 0(0), 1–17 (First online: 1 Jan 2017).

4. Fareeda Hayeeye, Maimoon Sattar, Watchanida Chinpa, and Orawan Sirichote, "Preparation and adsorption study of gelatin/activated carbon composite bead form". (2015). *Advanced Materials Research*. 1077, 18 - 22.

5. Fareeda Hayeeye, Maimoon Sattar, Surajit Tekasakul and Orawan Sirichote. "Adsorption of Rhodamine B on activated carbon obtained from pericarp of rubber fruit in comparison with the commercial activated carbon". (2014). *Songklanakarin Journal of Science and Technology*, 36 (2), 177-187.

6. Maimoon Sattar, Fareeda Hayeeye, Watchanida Chinpa, and Orawan Sirichote. "Preparation and characterization of polysulfone/activated carbon composite bead form". (2014). *Applied Mechanics and Materials*, 625, 106 – 109.

Oral presentation

Memoon Sattar, Fareeda Hayeeye, Watchanida Chinpa, and Orawan Sirichote, "Study of Rhodamine B sorption on the new adsorbent" Advance Composite Innovation Conference 2016, April 13 – 14, 2016, Melbourne, Australia.

Maimoon Sattar, Fareeda Hayeeye, Watchanida Chinpa, and Orawan Sirichote, "Preparation and characterization of polysulfone/activated carbon composite bead form" The 3rd International Conference on Process Engineering and Advanced Materials (ICPEAM2014) June 3 – 5, 2013, Malaysia.

.